ngineering
rary

UNITED STATES DEPARTMENT OF COMMERCE

Journal of Research

of the

National Bureau of Standards

Vol. 16, No. 4 April 1936

CONTENTS

RP	TITLE AND AUTHOR	Page
874.	Radio field-intensity and distance characteristics of a high, vertical broadcast antenna. Samuel S. Kirby....[Price 5c]	289
875.	Oxidation of wool: Effect of hydrogen peroxide on wool. Arthur L. Smith and Milton Harris....[Price 5c]	301
876.	Oxidation of wool: The lead acetate test for hydrogen peroxide bleached wool. Arthur L. Smith and Milton Harris....[Price 5c]	309
877.	Evaluation of ultraviolet solar radiation of short wave lengths. W. W. Coblentz and R. Stair....[Price 10c]	315
878.	Simplified apparatus for technical sugar colorimetry. Joseph F. Brewster....[Price 5c]	349
879.	Gloss investigations using reflected images of a target pattern. Richard S. Hunter....[Price 5c]	359
880.	An improved method for preparing cast-iron transverse test bars. A. I. Krynitsky and C. M. Saeger, Jr....[Price 5c]	367

The articles listed above may be purchased separately (see cover page II) at the prices indicated in the table of contents

A monthly periodical of pure and applied science published by our National Government

Journal of Research

of the

National Bureau of Standards

The January 1936 issue of the Journal of Research of the National Bureau of Standards began the sixteenth semiannual volume of this periodical. Fundamental researches in progress in the Bureau's laboratories are reported in this JOURNAL. If you are interested in new developments in science and technology, you should receive the JOURNAL. If you are not already a subscriber you are invited to send in your subscription.

Technical News Bulletin

This is a monthly publication containing short articles reporting progress of work in the Bureau laboratories, abstracts of papers which appear in the Journal of Research, accounts of scientific and technical meetings in which the Bureau has taken part, a list of all publications by members of the staff, and other items within the Bureau's fields. The BULLETIN is designed primarily to give a general and timely review of the activities of the Bureau in brief form. It is a prompt and reliable source of official information. If you have not already subscribed for the BULLETIN, you are invited to do so.

ANNUAL SUBSCRIPTION	Prices	
	United States, Canada, Cuba, Mexico, Newfoundland, Republic of Panama	Other countries
Journal of Research of the National Bureau of Standards:		
12 monthly issues (2 volumes), paper covers	$2.50	$3.25
Bound volume (½ year, 1 volume), blue buckram . . .	3.00	3.50
Technical News Bulletin, 12 monthly issues	.50	.70

Research Papers, reprinted individual articles appearing in the Journal of Research, are available from the Superintendent of Documents shortly after appearance of monthly issue of the JOURNAL.

Address orders only to
Superintendent of Documents, U. S. Government Printing Office,
Washington, D. C.

UNITED STATES DEPARTMENT OF COMMERCE
DANIEL C. ROPER, Secretary
NATIONAL BUREAU OF STANDARDS
LYMAN J. BRIGGS, Director

✦

Journal of Research

of the

National Bureau of Standards

✦

Volume 16, Number 4
April 1936

UNITED STATES
GOVERNMENT PRINTING OFFICE
WASHINGTON : 1936

For sale by the Superintendent of Documents, Washington, D. C. - - - - - Price 25 cents
$2.50 per year on subscription

The prices of the separate Research Papers appearing in this JOURNAL are given on the front cover page. If 100 or more copies of any separate are ordered, a discount of 25 percent is allowed. Those who desire copies of separate Research Papers should send their orders and remittances without delay to the Superintendent of Documents, U. S. Government Printing Office, Washington, D. C. This will aid him to determine the number of copies to be printed for sale. Research Papers are not printed from electrotypes, and usually no more reprints can be had when the first and only printing is exhausted.

U. S. DEPARTMENT OF COMMERCE NATIONAL BUREAU OF STANDARDS

RESEARCH PAPER RP874

Part of Journal of Research of the National Bureau of Standards, Volume 16, April 1936

RADIO FIELD-INTENSITY AND DISTANCE CHARACTERISTICS OF A HIGH, VERTICAL BROADCAST ANTENNA [1]

By Samuel S. Kirby

ABSTRACT

During December 1934, field-intensity records of emissions from radio station WBT, Charlotte, N. C., were made at seven different distances from the transmitting station before and after the construction and use of a high-mast antenna. In addition, field-intensity measurements were made at eight points on a circle at a distance of 1 mile from the transmitting station. The results showed that the substitution of the mast antenna for the older T and L antennas produced much greater ground-wave field intensities near the transmitter and somewhat greater total field intensities at greater distances. At the same time the amplitude of the fading was reduced at the first three recording stations at distances 69 to 142 kilometers. The fading at these first three stations was of a more-rapid type than at the more-distant stations. The antenna change did not appreciably affect the frequency of the fading. Wires were added to the mast antenna to increase its top capacity and thus make the current distribution in this antenna more nearly sinusoidal. This change seemed to reduce the fading amplitude at the first three recording stations by the suppression of certain high-angle radiation rather than by an increase of the intensity of the ground wave.

With all conditions of the transmitting antennas used greater values of the averages of the 10-minute peak field intensities were recorded at the receiving station at Meadows, Md., 552 kilometers, than at any other station from 69 to 879 kilometers.

CONTENTS

		Page
I.	Introduction	289
II.	Experimental data	291
III.	Analysis of records	293
IV.	Conclusions	299

I. INTRODUCTION

In December 1934 the antenna system of radio station WBT, 1080 kc/s, at Charlotte, N. C., was changed from a T antenna with a height of about 175 feet and a flat top with a length of 200 feet, to a vertical, guyed cantilever mast 429 feet or 0.47 wave length high. A short time before this, plans for a cooperative investigation of the effects of such a change were made by the Columbia Broadcasting System and the National Bureau of Standards. In accordance with these plans seven automatic field-intensity recorders [2] were set up at

[1] Presented at the Tenth Annual Convention of the Institute of Radio Engineers, Detroit, Mich., July 1, 2, and 3, 1935.

[2] K. A. Norton and S. E. Reymer. *A continuous recorder of radio field intensities.* BS J. Research 11, 373 (1933) RP597.

various distances from the transmitting station, as shown by the map in figure 1. These recorder locations were Salisbury, Lexington, Greensboro, and Durham, N. C., Charlottesville, Va., Meadows, Md., and Boonton, N. J. It was intended to have the recording stations as nearly as possible on the same great-circle path. This condition was approximately satisfied, although Durham, N. C., was somewhat out of line. The recorders were set up during the latter part of November 1934 and ran for about 6 weeks with calibrations about twice per week.

FIGURE 1.—*Locations of radio station WBT and seven recording stations.*

Unfortunately, the T antenna was in the way of the mast construction and had to be taken down about the middle of November. An unsatisfactory temporary antenna was used until December 4, after which time an inverted L antenna, 110 feet high with a flat top 200 feet long, was used. With this antenna the field intensity at 1 mile was about 0.88 that of the T. Otherwise it was believed that the characteristics of the L antenna were similar to those of the T.

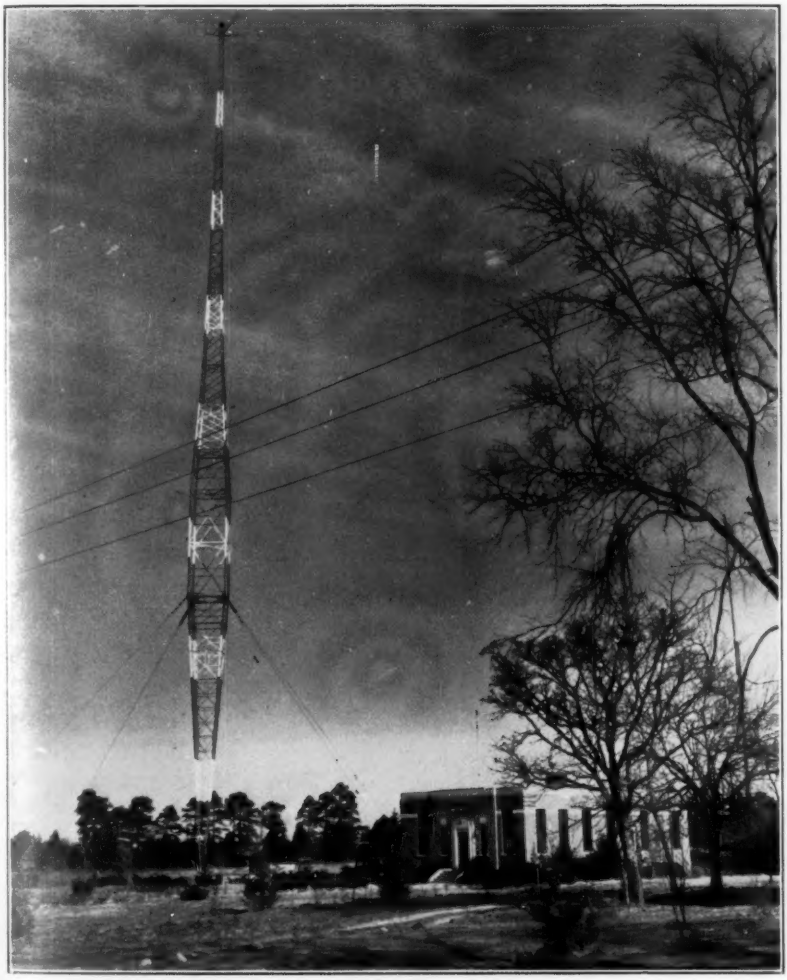

FIGURE 2.—*Radio Station WBT high-mast antenna.*

Until December 17 the sloping down lead of the L was between 50 and 100 feet from the mast, the construction of which was completed about December 13. On December 17, after the L antenna and the old towers supporting it were removed, a decrease of fading of the emissions from the mast was observed at Salisbury and Lexington. This was an indication that the proximity of the L affected the mast, so it might be expected that the proximity of the mast affected the L. The effect of any coupling between these two antennas, however, should have reduced the differences between their performances. In other words, the differences found would have been greater if each antenna had been operated without the presence of the other. Emissions from the mast were recorded only 2 days before the L was removed.

II. EXPERIMENTAL DATA

The WBT mast antenna is shown in Figure 2. The ground system consisted of 120 radials of no. 10 hard-drawn copper wire, each radial being 300 feet in length. The remote end of each radial was attached to a 0.5-inch ground rod driven to a depth of 4 feet.

Records of emissions from the L antenna were made from about December 5 to 15 and from the mast from about December 16 to 31. The mast was used both alone and with 4 wires added to increase its top capacity. These wires were stretched from crossarms at the top downward to the waist of the tower below the center and later nearly to the ground.

The field intensities at a distance of 1 mile are shown for the old T and the new mast in figure 3. These measurements were made by W. B. Lodge of the Columbia Broadcasting System. They show that the ground wave was increased about 1.75 times by the use of the mast instead of the T. The average field intensity at 1 mile from the L antenna was 760 mv/m, this being one-half the field intensity at 1 mile from the mast.

Figure 4 shows some night records from each of the seven recording stations and from each of the two antennas. The power input to the antenna in each case was 50 kw. The only changes at the transmitting station were the changes of antenna indicated in figure 4. At all of the receiving stations, excepting Durham, the night records shown in this figure were made simultaneously. Day records of emissions from the mast are also shown in this figure, M and L representing the mast and L, respectively.

An inspection of figure 4 will indicate the general characteristics of fading and field intensity as the distance from the transmitting station was increased. However, this inspection will also indicate that it is difficult and unsafe to judge the respective merits of the two antennas from a few short records taken with successive antenna changes.

Consider the records taken at Salisbury. The first three one-hour records of transmissions from the mast, the L, and the mast in turn indicate that the field intensity was increased and the fading decreased by the substitution of the mast for the L. This is the conclusion which will be drawn later from a consideration of all of the records from December 5 to 30. The last hour's record of transmissions from the L taken between 0210 and 0300 EST, however, would indicate that there was less fading of emissions from the L. It is

believed that this change was brought about by a change of the ionosphere and that the first three one-hour records indicated the relative performance of the mast and the L antennas as observed at Salisbury. Whatever the change in the ionosphere after 0200 EST may have

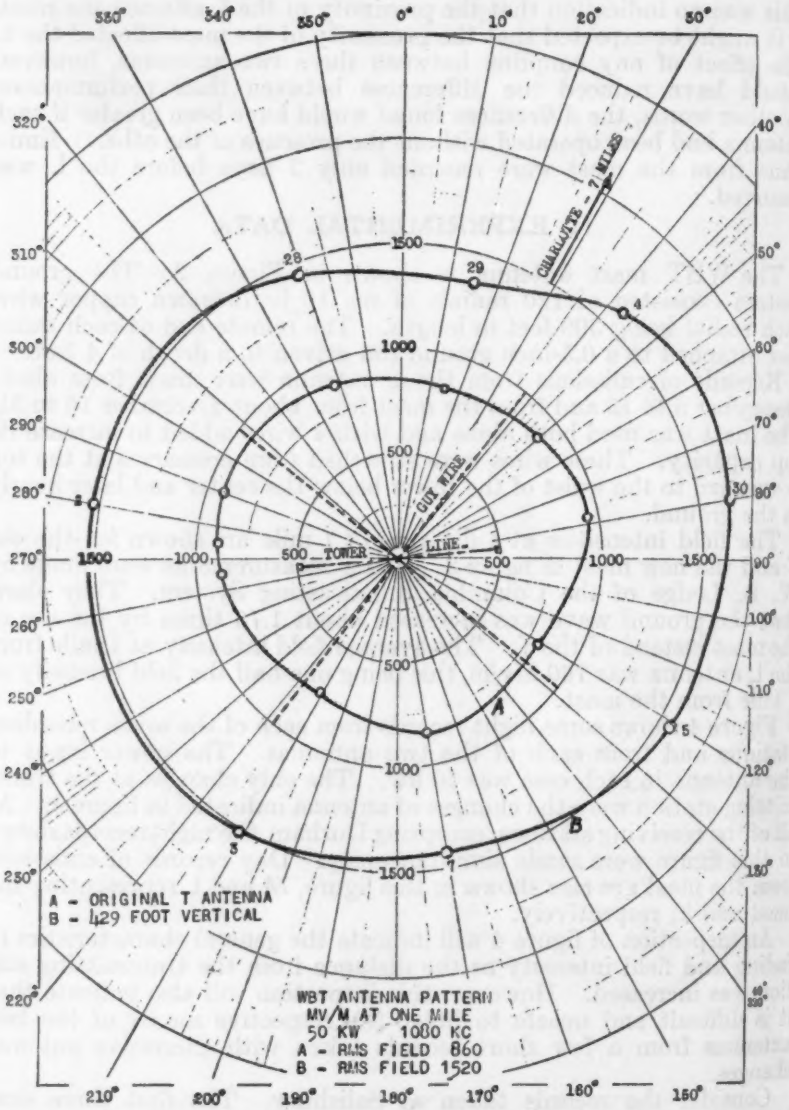

FIGURE 3.—*Field intensities at a distance of 1 mile.*

A indicates T antenna; B mast antenna.

been, its effect did not depend critically on the angle of incidence of the wave on the ionosphere, as the same effect was indicated at nearly all of the recording stations simultaneously.

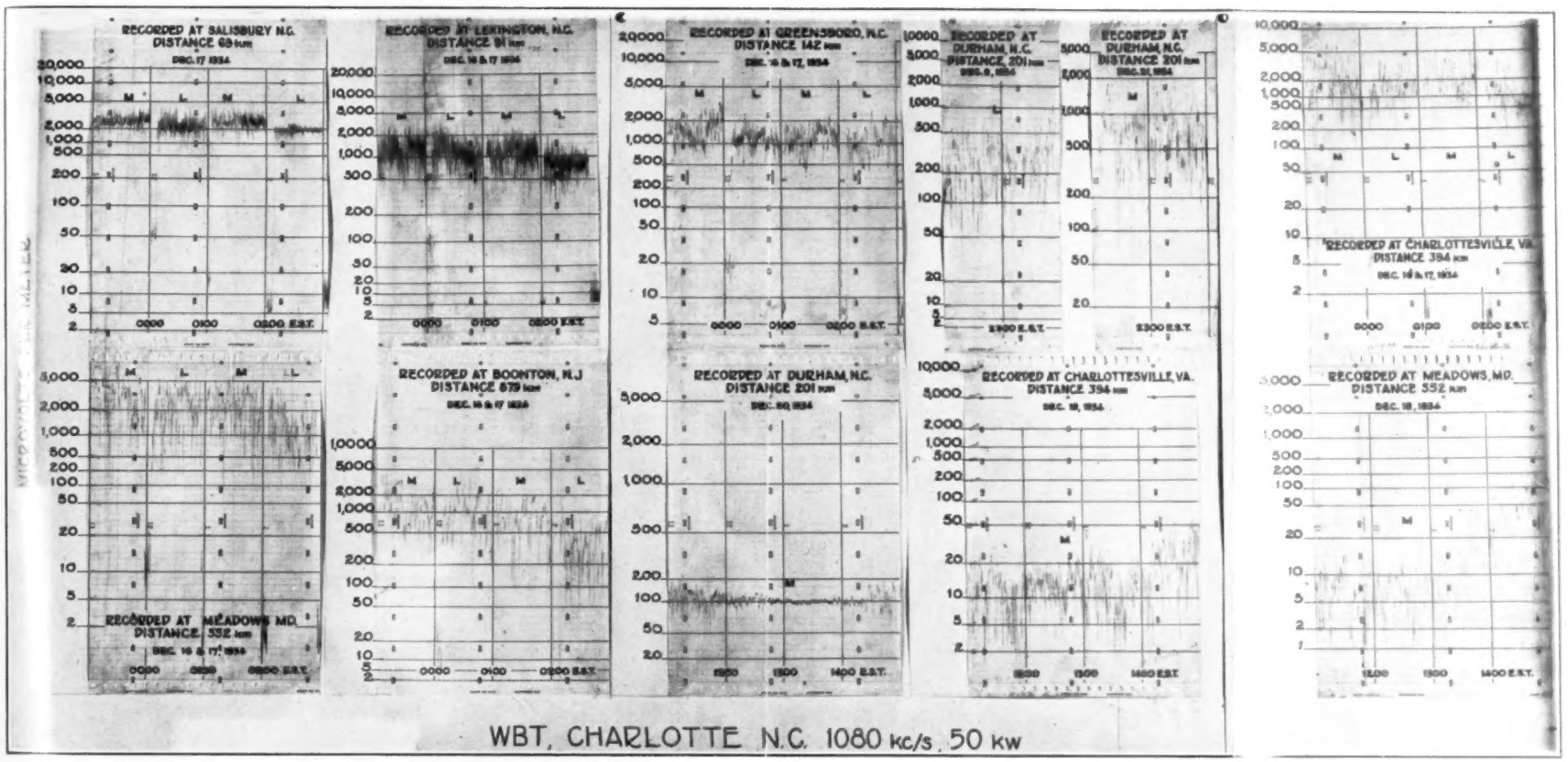

FIGURE 4.—*Field-intensity records of emissions from the* L *and mast* (M) *at night, and from the mast during day.*

The records from 2300 December 16 to 0200 December 17 present, qualitatively, very well the relative performance of the two antennas as observed from different distances. Points to be noted are the field intensity, the amplitude of the fading, and the rapidity of the fading. It might be pointed out that on this night the peak values of field intensity were greater at Meadows, Md., than at any other recording station. Although the amplitude of the fading increased with the distance for some distance from the transmitting station, the fading at moderate distances was much more rapid and therefore more destructive. The fading at Lexington was an example of this.

Some day-records are included in this figure to show the distances at which sky wave became appreciable during the daytime. Considerable sky wave was found at Durham during most of the day, and at the more distant receiving points sky wave was predominant during the day was well as the night. By comparing the peak values of the day and night field intensities it will be seen that the night field intensities were about 250 and 350 times the day field intensities at Charlottesville and Meadows, respectively. This indicates that even when the daytime sky wave at this frequency is strongest as it is in midwinter that it is even then very highly absorbed in the ionosphere. Waves of this frequency could not pass through the E region of the ionosphere during the day.

III. ANALYSIS OF RECORDS

From the records given here it may be seen that it is difficult to draw satisfactory conclusions by simple inspection of the records or from records taken over short periods. These records have been analyzed by measuring the maxima and minima for each 10-minute period and averaging the day values and the night values separately for daily averages. The hours from 0800 to 1600 EST were arbitrarily used as day hours and 1800 to 0000 EST as night hours. The daily averages were again averaged over the period during which a particular antenna was used.

Figure 5 shows the averaged night field intensities for both the L and the mast plotted together for comparison. It should be noted that with the exception of the Lexington records the 10-minute maximum field intensities at all distances were greater in the case of the mast than in the case of the L. Part of this increase of field intensity was caused by an increase in the ratio of low-angle to high-angle radiation and part probably was caused by the increased radiation efficiency of the high-mast antenna. Similarly the minimum values in the case of the mast were greater than those in the case of the L at all recording stations. In this figure the graph labeled "Inverse distance, power 25 kw, radiated" indicates the inverse distance values of field intensity as given for the ground wave with no absorption, by the formula for a vertical infinitesimal doublet,

$$F=\frac{C\sqrt{P_r}}{D},$$

where F is the field intensity, in microvolts per meter, C is the velocity of light, in kilometers per second; P_r is the power radiated, in kilowatts; and D is the distance, in kilometers. The use of 25 kw

for the radiated power is based on the assumption that the radiation efficiency of the antenna was 50 percent, and the distribution of energy the same as for the vertical infinitesimal doublet, which were the conditions assumed by Norton, Kirby, and Lester [3] for a large number of miscellaneous antennas. The graph labeled "Inverse distance-mast" was based on the average value of field intensity at 1 mile from the mast antenna. Similar graphs based on the average field intensity at 1 mile for the old T and L antennas are not shown but would have fallen below both of those plotted. The average

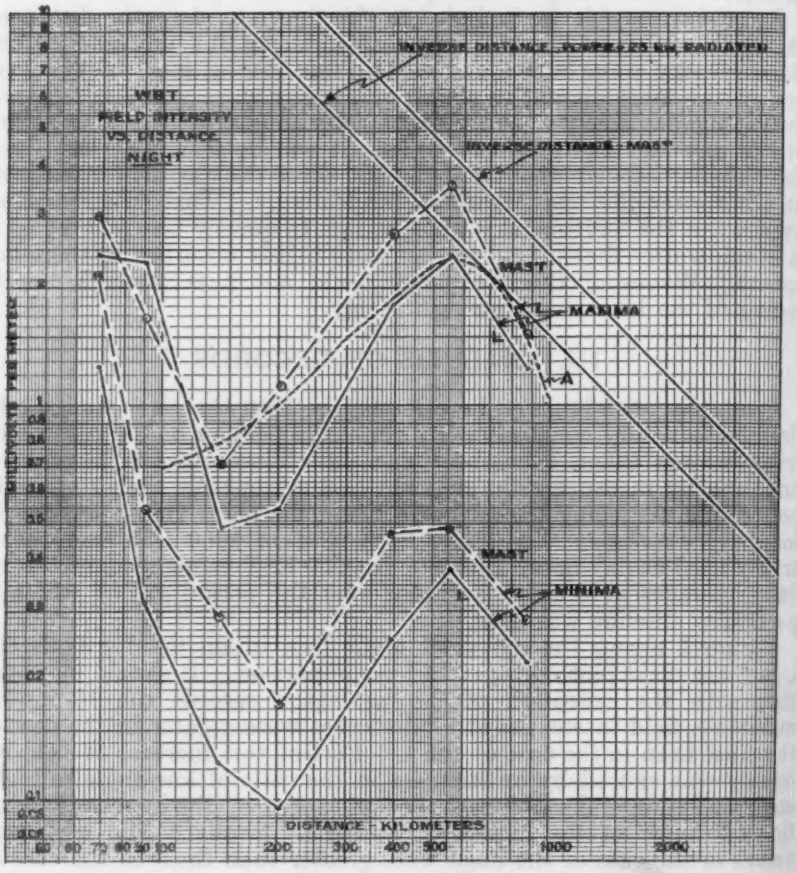

FIGURE 5.—*Average of 10-minute maximum and minimum field intensities of emissions from* L *and mast antennas.*

values of the 10-minute peak field intensities from the L antenna did not reach the inverse distance graph for 25 kw radiated at any of the receiving stations. However, many of the individual peaks did exceed the inverse distance values. In a similar manner the average 10-minute peak field intensities from the mast did not exceed the inverse distance values as calculated from the field intensities at 1 mile, but

[3] K. A. Norton, S. S. Kirby, and G. H. Lester. *An analysis of continuous records of field intensity at broadcast frequencies.* BS J. Research 11, 807 (1934) RP752; Proc. Inst. Radio Eng. 23, 1183 (1935).

many of the individual peak values did exceed the inverse distance values. The smooth dashed curve shown in this figure represents the empirical formula for 25 kw radiated, for sky-wave field intensities as given by Norton, Kirby, and Lester.[4] The sky-wave field intensities received at Meadows, 552 km, exceeded those recorded at any other station. The latter result corroborates the result found by Norton, Kirby, and Lester (see reference 3) that for a large number of miscellaneous broadcasting stations, the maximum sky-wave field intensities were produced at a distance of about 600 km.

Figure 6 shows the ratios of the amplitudes of night fading from the mast and the L antennas. The mast had a decided advantage over the three shortest paths and this result may reasonably be ascribed to an increase in the ratio of ground wave to sky wave.

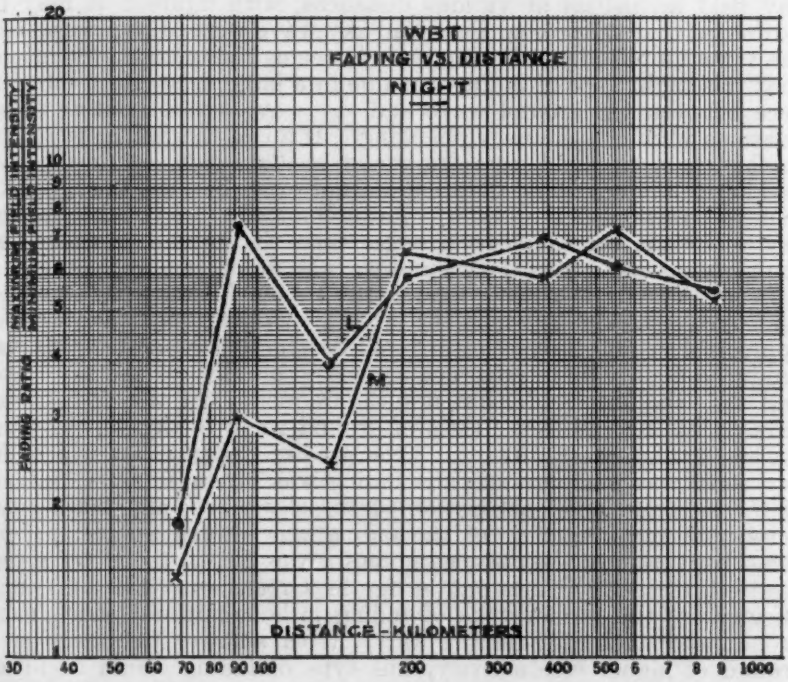

FIGURE 6.—*Amplitude ratios of night fading of emissions from* L *and mast antennas.*

The decrease of the amplitude of night fading over the three shortest paths by the use of the mast was a very great improvement. At Lexington the fading ratio for the mast as shown by an analysis of all the records obtained was only 0.4 that for the L, and at Greensboro, 0.6. Figure 4 does not show this clearly. These stations were in regions where night reception from the L was poor because of bad fading. It would be reasonable to conclude from these results that the night-service area was considerably increased by the use of the mast. At the more distant receiving stations the amplitudes of the fading ratios from the mast and the L were approximately equal. These latter fields were composed almost entirely of sky waves for

[4] See footnote 3.

both antennas. At the shorter distances the fields were composed of both sky waves and ground waves.

In addition to the amplitude of the fading ratios the rapidity of the fading is very important. It may be seen from figure 4 that fading at the closer receiving stations was much more rapid than at the more distant stations. This was especially noticeable at Lexington where the amplitude of the fading was great enough to be serious and the fading period was very short.

Fading may be produced in several ways, such as by phase interference between ground wave and sky wave or between two or more sky waves, by changing intensity of sky wave or rotation of the components of the field of sky waves. Ground waves are stable and sky waves unstable. By a comparison of figure 7, which shows the day field intensities at various distances, with figure 5 it may be estimated that the ground wave and sky wave were of approximately the same amplitude at Lexington. It seems reasonable to conclude that this rapid type of fading was due in a large measure to interference between the ground wave and sky wave whose relative phase relations were continuously changing. If all of the fading were due to this cause the field intensity would oscillate between fixed upper and lower limits. This condition did not exist, because the intensity and polarization of the sky wave also changed. At Greensboro the sky wave was considerably stronger than the ground wave and at the more distant points the ground wave is almost negligible at night.

From an analysis of all of the records obtained it may be concluded that over distances at which the ground wave and sky wave were of appreciably equal intensities, a rapid destructive type of fading was produced mainly by interference between ground wave and sky wave, and that the amplitude, but not the frequency, of this fading was reduced by increasing the ratio of ground wave to sky wave by the use of the high-mast antenna. Over greater distances, at which the sky wave was predominant, the fading was produced by variations of the intensity and polarization of the sky wave, and neither the amplitude nor frequency of the fading was altered appreciably by the substitution of the mast antenna for the L. In the WBT investigation, receiving points out as far as Greensboro (142 km) were affected by the former type of fading although it was much more pronounced at Lexington (91 km). With a lower frequency or a ground of higher conductivity, this type of fading would be found farther from the transmitting station. It seems that the frequency of the fading would be lower for a lower frequency.

Figure 7 shows the day field intensities from the mast and the L. The mast produced greater field intensities than the L at all recorder stations. The Boonton values are not shown on this graph.

As previously mentioned, the mast was used under several different conditions, i. e., with wires added to increase the top capacity and without the wires. The wires were used under two different conditions, i. e., half wires or wires from the top down to the waist of the tower and full wires or wires from the top nearly to the ground. In each case 4 wires were used and they were supported at the top by steel arms extending out horizontally. In studying the effect of the wires, records were available only for rather short periods for each condition, so that some of the variations are more likely to be accidental

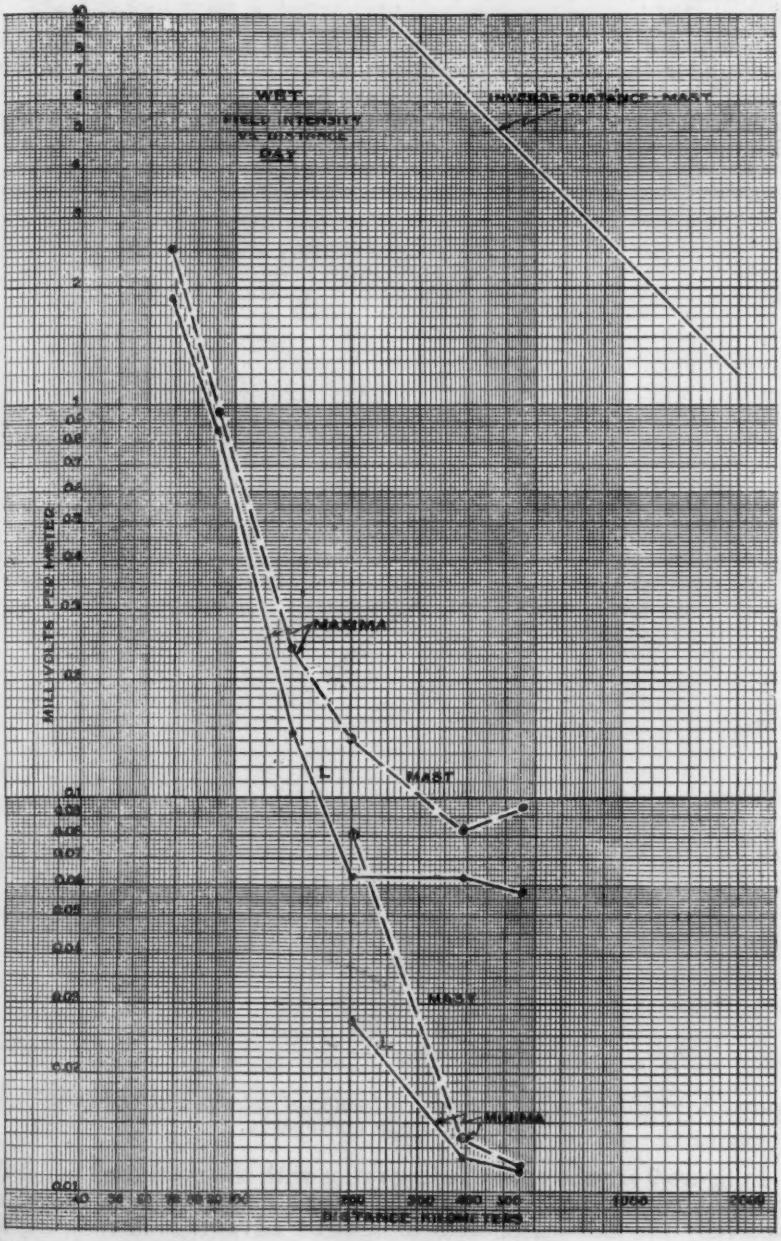

FIGURE 7.—*Average of 10-minute maximum and minimum day field intensities of emissions from* L *and mast antennas.*

than in the previous discussion. This is especially true for the Greensboro data because some of the late December records at this station were spoiled by receiving-set trouble.

In figure 8 are shown the field intensities with the mast antenna used under the different conditions described. The graph labeled "wires" includes the data for the days when both half wires and full wires were used. In general these results favor the use of the mast without the wires.

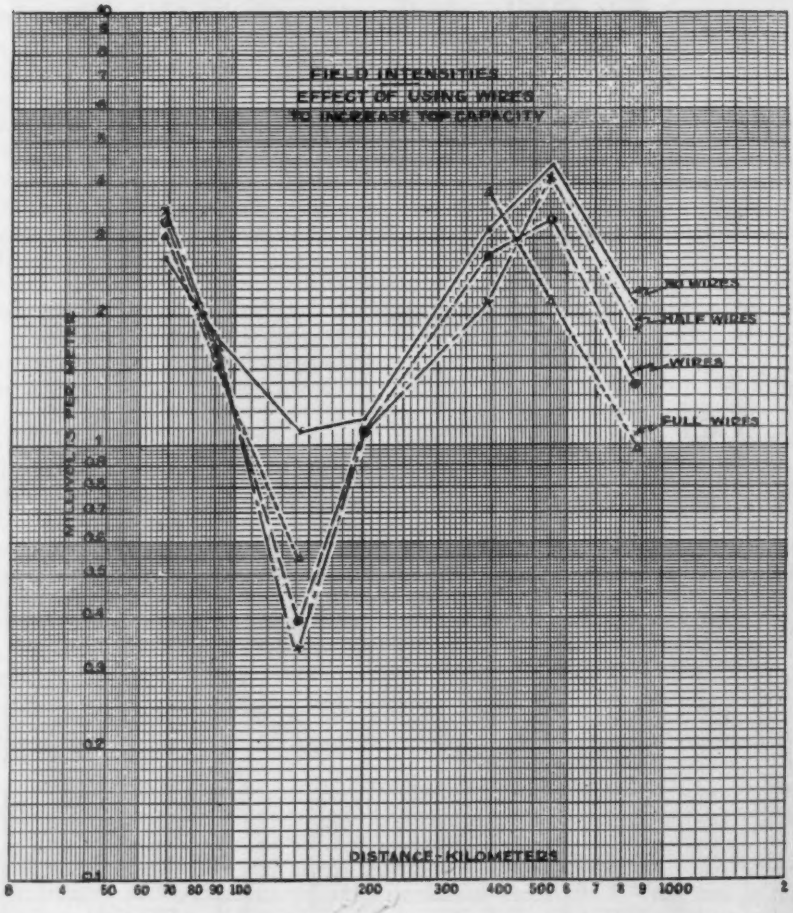

FIGURE 8.—*Field intensities of emissions from mast antenna with and without wires used to increase top capacity.*

In figure 9 are shown the fading ratios with the mast used under the different conditions. For the important nearby points the wires, especially the half wires, seem to have an advantage in reducing the fading. This problem should have further study. It should not be absolutely necessary to study the effect of antenna changes on the fading over a wide range of distances as was done in the WBT experiment, as much can be learned from a careful study at one well located station—Lexington, in the case at hand.

IV. CONCLUSIONS

The 429-foot mast antenna produced a ground-wave field intensity 1.75 times that produced by the old T, and twice that produced by the L.

The night field intensity at considerable distances was increased by a factor of about 1.5 by the substitution of the mast for the L.

The night-fading amplitude was decreased appreciably out to 150 km by the use of the mast. The fading amplitude was not appreciably decreased at distances over 200 km where sky wave was predominant from both antennas.

Fading was much more rapid and destructive within a distance of 150 km than for greater distances. The change of antennas did not appreciably affect the frequency of the fading but only the amplitude.

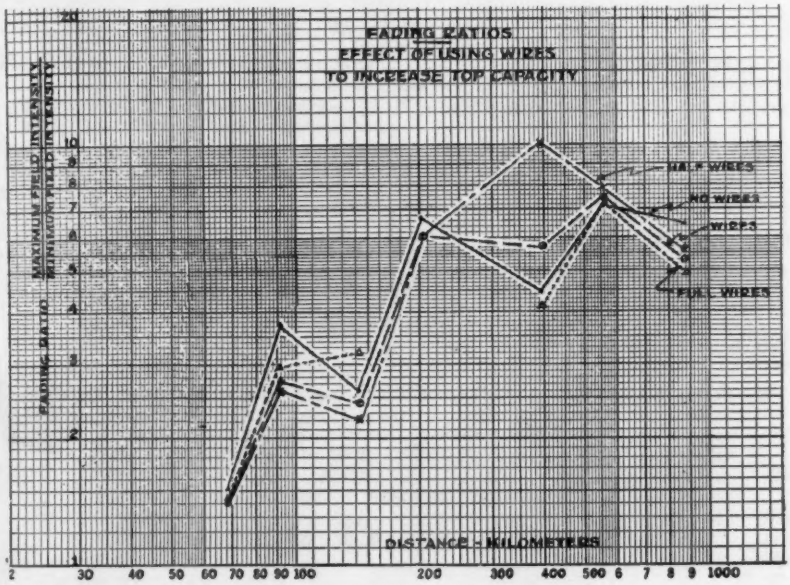

FIGURE 9.—*Amplitude ratios of night fading of emissions from mast antenna with and without wires to increase top capacity.*

The maximum sky-wave field intensity recorded was at Meadows, at a distance of 552 km from the transmitting station.

The use of wires to increase the top capacity and make the antenna current more nearly sinusoidal did not increase the field intensity, but there was some evidence that the fading was decreased over the first 150 km. The half wires were more effective than the full wires.

This investigation was made possible through the cooperation of the Columbia Broadcasting System, by arrangement with E. K. Cohan, Director of Engineering for that company. A. B. Chamberlin and W. B. Lodge, engineers for the Columbia Broadcasting System, assisted in the work.

S. E. Reymer of the National Bureau of Standards assisted in installing the recorders. Facilities for the installation of receiving equipment and recorders were furnished by T. M. Casey, Salisbury, N. C.; Fred Hunnicut and the firm Conrad, Linville, and Martin, Lexington, N. C.; Women's College, University of North Carolina, Greensboro, N. C.; Duke University, Durham, N. C.; University of Virginia, Charlottesville, Va.; and Ballantine Laboratories Inc., Boonton, N. J. S. Ballantine also operated the equipment installed in his laboratory.

WASHINGTON, January 29, 1936.

U. S. DEPARTMENT OF COMMERCE NATIONAL BUREAU OF STANDARDS

RESEARCH PAPER RP875

Part of Journal of Research of the National Bureau of Standards, Volume 16, April 1936

OXIDATION OF WOOL: EFFECT OF HYDROGEN PEROXIDE ON WOOL [1]

By Arthur L. Smith and Milton Harris [2]

ABSTRACT

The purpose of this investigation was to provide quantitative data showing the effect of oxidizing agents on wool as a basis for studying all processes in which wool is exposed to oxidation reactions. The work reported in this paper deals only with the effect of hydrogen peroxide.

Data are presented showing the effects on wool of varying the concentration, temperature, and pH of the hydrogen peroxide solutions, and the duration of treatment. The main point of attack during oxidation is the disulfide group of the cystine in the wool. The extent to which the wool is oxidized bears a functional relationship to the decrease in the cystine content and to the increase in the alkali-solubility of the wool.

CONTENTS

	Page
I. Introduction	301
II. Materials and methods	302
III. Results and discussion	303
1. Effect of varying the concentration of hydrogen peroxide	303
2. Effect of varying the temperature of the hydrogen peroxide solution	304
3. Effect of varying the duration of treatment with hydrogen peroxide	305
4. Effect of varying the pH of the hydrogen peroxide solution	306
IV. Conclusions	307
V. References	307

I. INTRODUCTION

In practical wool processing, such as bleaching, carbonizing, lustering, printing, chlorination and bromination for producing "unshrinkable" finishes, and in natural aging involving the action of light, air, and moisture, wool may become partially oxidized, the extent of oxidation depending on the severity of the conditions. The quantitative estimation of the oxidation is of great importance, since previous work [1][3] has shown that this oxidation increases the susceptibility of wool to deterioration by alkali treatments.

[1] This is the first paper of a series on studies relating to the oxidation of wool.

[2] Research associates at the National Bureau of Standards, representing the American Association of Textile Chemists and Colorists.

[3] The numbers in brackets here and elsewhere in the text refer to the numbered references at the end of this paper.

While there are several groups in proteins which may be attacked by oxidizing agents and alkalies, the evidence obtained from studies of the effects of these reagents on cystine [2, 3, 4, 5, 6, 7] indicates that the greatest effect is produced on the disulfide groups. However, Fruton and Clark [8] showed that the introduction of acyl groups into the amino groups of cystine greatly increases the oxidizability and its lability towards alkali. It is to be expected, therefore, that the reactivity of the disulfide group as it exists in the complex wool molecule will be very different from that of the disulfide group in pure cystine.

The present investigation was undertaken to obtain quantitative data showing the effects of various oxidizing agents on the disulfide groups in wool, and on the susceptibility of the oxidized wool to deterioration by subsequent alkali treatment. The work reported in this paper deals only with the effect of hydrogen peroxide.

II. MATERIALS AND METHODS

White worsted yarn prepared from raw wool which had been extracted with Stoddard solvent and washed with water, but which had received no chemical treatment, was used in this work. The yarn was further purified by extraction in a soxhlet apparatus with alcohol and ether for 6 hours each and then washed with water at 50° C. All the samples were conditioned and tested in a room maintained at a relative humidity of 65 percent and a temperature of 23° C, with the exception of those which became so gelatinous during alkali treatment that equilibrium was not readily obtained by conditioning. These samples were partially dried in an oven at about 50° C for 1 hour and then dried to constant weight at 105° C. The weights of the oven-dried samples were corrected to correspond with the moisture content of the original conditioned samples. The conditioned, untreated wool contained 13.2 percent of moisture, 14.3 percent of nitrogen, 3.23 percent of sulfur, and 11.6 percent of cystine.

The total nitrogen was determined by the micro-Kjeldahl method [9], total sulfur by the oxygen-bomb method [10], and cystine by the Sullivan method [11].

Resiliency tests were made with a compressometer [1]. Breaking-strength tests were made by the single-strand method on a pendulum-type machine, the yarn being tested while wet.

The stock hydrogen peroxide used was a 10-volume (3.03-percent) solution, about 0.005*N* with respect to sulphuric acid, and contained 0.3 percent of acetanilide as a preservative.

In the experimental procedure, 4-g samples of the wool yarn were treated with 400-ml portions of hydrogen peroxide solution. The supernatant liquor was poured off, the wool washed in running distilled water until 10 ml of the wash water would not decolorize 1 drop of a 0.075*N* solution of potassium permanganate, and then conditioned. The susceptibility of the wool to deterioration by alkalies (referred to as alkali-solubility in this paper) was determined by treating about 2-g portions of wool with 200 ml of 0.1*N* solution of sodium hydroxide at 65° C for 1 hour. The wool was filtered on a Büchner funnel, washed with about 2 liters of distilled water, and conditioned or dried as was necessary.

III. RESULTS AND DISCUSSION

1. EFFECT OF VARYING THE CONCENTRATION OF HYDROGEN PEROXIDE

Samples of wool yarn were treated for 3 hours at 50° C with hydrogen peroxide solutions varying in concentrations from 0.1 to 10.0 volume. Two-gram specimens of each oxidized sample were then given the alkali treatment previously described. The effects of the treatments on the physical and chemical properties of the wool are shown in tables 1 and 2. The results indicate that the oxidation treatment has caused no significant changes in wet breaking strength, resiliency, or total sulfur content. Both the cystine and nitrogen contents decrease with increasing concentrations of peroxide and exhibit a fairly sharp drop between concentrations of 4 and 6 volume.

TABLE 1.—*Effect on wool yarn of hydrogen peroxide solutions of various concentrations at 50° C for 3 hours*

Concentration of H_2O_2		Cystine content	Total sulfur	Nitrogen content	Wet breaking strength	Compressional resilience
Volume	*Percent*	*Percent*	*Percent*	*Percent*	kg	*Percent*
0.0	0.00	11.6	3.23	14.23	1.15	53
.1	.03	11.6	3.30	14.19	1.07	51
.5	.15	11.6	3.24	14.14	1.10	53
1.0	.30	10.8	3.24	14.17	1.09	52
2.0	.61	10.7	3.21	14.18	1.07	51
4.0	1.21	10.5	3.21	14.17	1.13	51
6.0	1.82	9.6	3.23	13.99	1.10	53
8.0	2.43	9.3	3.20	14.04	1.08	50
10.0	3.03	8.4	3.23	14.05	1.03	50

TABLE 2.—*Effect of 0.1N solutions of sodium hydroxide at 65° C for 1 hour on wool which has previously been treated with various concentrations of hydrogen peroxide at 50° C for 3 hours*

[See table 1 for the effect of the hydrogen peroxide alone]

Concentration of H_2O_2		Loss in weight	Cystine content	Total sulfur	Nitrogen content	Wet breaking strength	Compressional resilience
Volume	*Percent*	*Percent*	*Percent*	*Percent*	*Percent*	kg	*Percent*
0.0	0.00	12.8	2.2	1.61	14.03	0.30	42
.1	.03	18.3	2.2	1.73	14.07	----------	42
.5	.15	16.8	2.2	1.63	13.97	.19	40
1.0	.30	17.7	2.2	1.63	13.98	.17	37
2.0	.61	20.0	2.0	1.57	13.91	.13	36
4.0	1.21	20.9	2.2	1.76	14.01	.08	36
6.0	1.82	41.7	1.4	1.83	13.83	----------	----------
8.0	2.43	46.1	1.4	1.91	13.63	----------	----------
10.0	3.03	55.6	1.3	2.11	13.67	----------	----------

The alkali treatment greatly accentuates the differences produced by oxidation alone and shows an even more pronounced critical concentration of hydrogen peroxide between 4 and 6 volume. Whereas the oxidation alone showed no significant effect on the sulfur content, wet breaking strength, and resiliency of the wool, the subsequent alkali treatment produced a considerable decrease in all three. The samples treated with peroxide solution of concentrations greater than 4 volume became so gelatinous during alkali treatment that they dried to horny masses and the physical tests could not be made.

The sulfur content of each of the alkali-treated samples which had been oxidized with peroxide solutions below concentrations of 4 volume is about one-half of the sulfur content of the original wool. This is in accord with previous studies on the effect of alkalies on wool [1], in which it was shown that on continued treatment with alkali, the sulfur content decreased and approached a constant value at approximately half the sulfur content of the original wool. The increase in total sulfur content of the alkali-treated samples which had been treated with peroxide concentrations greater than 2 volume may be attributed to the oxidation of a portion of the sulfur to a form which tends to resist splitting from the molecule.

The increase in the alkali solubility of wool treated with increasing concentrations of peroxide is of special interest since it offers a simple

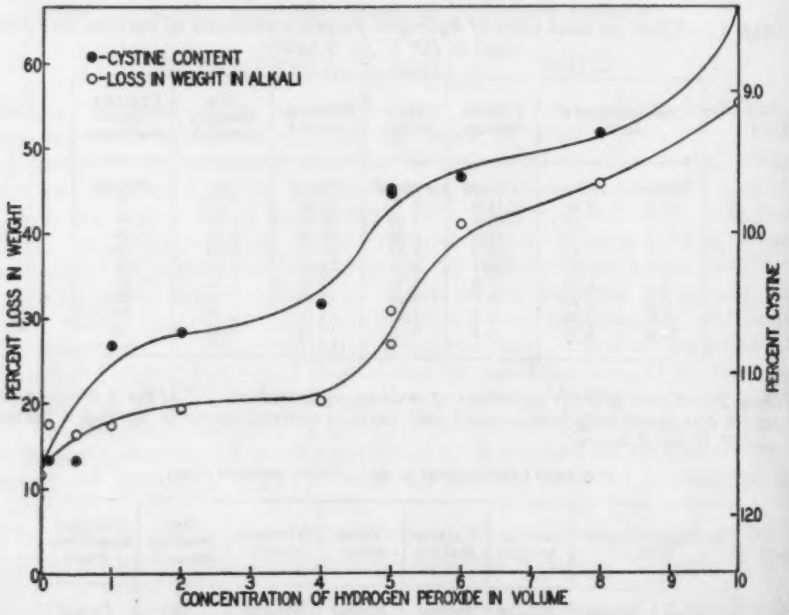

FIGURE 1.—*Effect on wool of various concentrations of hydrogen peroxide for 3 hours at 50° C.*

and reproducible method for measuring the extent of oxidation. It is also of interest to note that the decrease in the cystine contents of the peroxide-treated samples bears a functional relationship to the loss in weight of the corresponding samples after alkali treatment. The curves in figure 1 show graphically the relationship of decrease in cystine content of the oxidized wool to the loss in weight when the oxidized wool is subsequently treated with alkalies.

2. EFFECT OF VARYING THE TEMPERATURE OF THE HYDROGEN PEROXIDE SOLUTION

Samples of wool yarn were treated with 2-volume solutions of hydrogen peroxide for 3 hours at temperatures varying from 23 to 80° C. The cystine content and alkali solubility of the oxidized samples

were determined and are given in table 3. The cystine contents decreased and the losses in weight increased with increasing temperatures of the oxidizing bath, the rate of change increasing rapidly above 50° C. The loss in weight in alkali appears to be the more sensitive measure of the degree of oxidation.

TABLE 3.—*The effect on wool of 2-volume hydrogen peroxide solutions at temperatures varying from 23 to 80° C for 3 hours, and the alkali solubility of the treated wool*

Temperature of H_2O_2 solutions	Cystine content after treatment with H_2O_2	Alkali solubility
°C	*Percent*	*Percent*
23	11.2	9.7
35	11.3	13.6
50	10.8	19.4
65	9.8	31.6
80	7.4	100.0

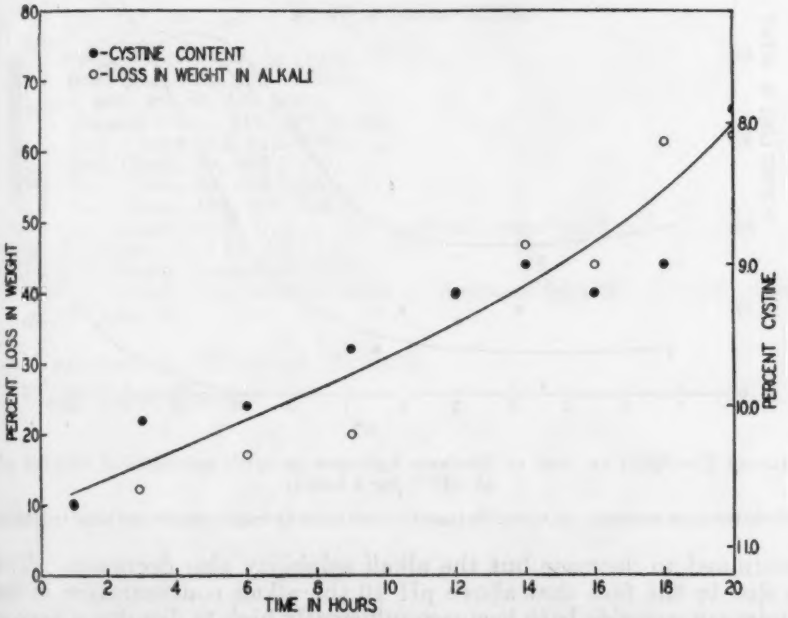

FIGURE 2.—*Effect on wool of 2-volume hydrogen peroxide solutions at 50° C for different lengths of time.*

3. EFFECT OF VARYING THE DURATION OF TREATMENT WITH HYDROGEN PEROXIDE

Samples of wool yarn were treated with 2-volume solutions of hydrogen peroxide at 50° C for periods of time varying from 1 to 20 hours. The effects on the cystine content and alkali-solubility of the wool are shown in figure 2. While the cystine content decreases, and the loss in weight in alkali increases with increasing time of treatment, there does not appear to be any critical time under the conditions of these experiments.

4. EFFECT OF VARYING THE pH OF THE HYDROGEN PEROXIDE SOLUTION

Samples of wool yarn were treated with 2-volume hydrogen peroxide solutions differing in pH[4] for 3 hours at 50° C and then analyzed for cystine content and alkali-solubility. The results, shown in figure 3, indicate that pH has no appreciable effect on the oxidation of wool by peroxide below about pH 7. Between pH 7 and pH 10 the alkali solubility increases and the cystine content decreases with increase in pH. Above pH 10 the cystine content

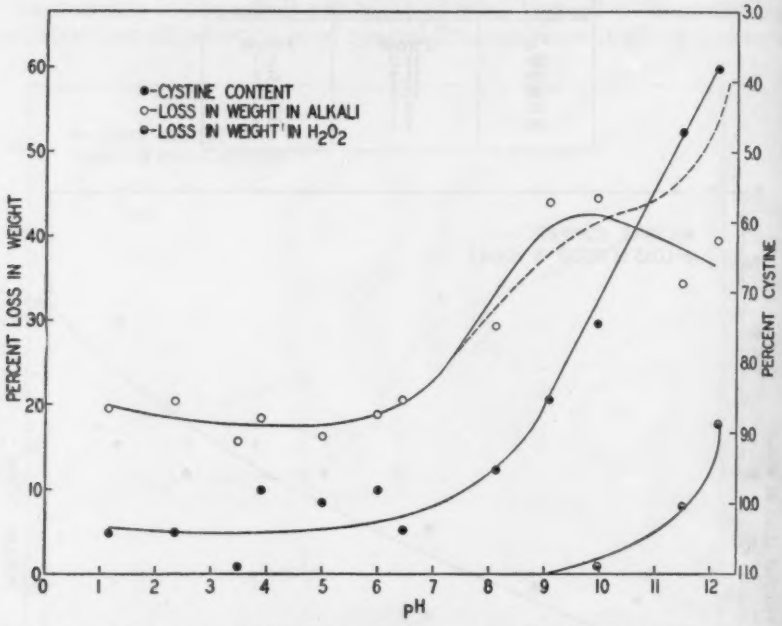

FIGURE 3.—*Effect on wool of 2-volume hydrogen peroxide solutions of varying* pH *at 50° C for 3 hours.*

The dotted curve represents the sum of the losses in weight in the hydrogen peroxide and alkali treatments.

continued to decrease but the alkali solubility also decreases. This is due to the fact that above pH 10 the alkali concentration in the hydrogen peroxide bath becomes sufficiently high to dissolve a portion of the wool that would ordinarily be removed in the subsequent alkali treatment. When the loss in weight in the peroxide treatment is added to the loss in weight in the alkali treatment, the total loss in weight (as shown by the dotted curve in fig. 3) is in better agreement with the decrease in cystine content.

[4] The buffers were prepared according to Clark [12] and were approximately *M*/50 with respect to salt.

IV. CONCLUSIONS

Wool which has been oxidized by hydrogen peroxide solutions has a lower cystine content and a higher alkali solubility than untreated wool. The extent to which the wool is oxidized bears a functional relationship to the decrease in cystine content and to the increase in alkali solubility. In general, the latter may be considered to be the better measure of the oxidation. This is due to the fact, that although the main point of attack during oxidation is the disulfide group, there is evidence [5] indicating that other groups may be attacked which may affect the alkali solubility but not the cystine content of the wool.

The extent to which wool is oxidized by hydrogen peroxide solutions depends on the concentration, temperature, and pH of the solutions and on the duration of treatment. The data obtained under the conditions of these experiments indicate critical values for the concentration, temperature, and pH of the hydrogen peroxide solutions, but not for the duration of treatment.

V. REFERENCES

[1] J. Research NBS **15,** 63 (1935), RP810.
[2] J. Biol. Chem. 80, 191 (1928).
[3] Rev. gén. sci. **45,** 593 (1934).
[4] Z. physiol. Chem. **216,** 193 (1933).
[5] J. Biol. Chem. **105,** 115 (1934).
[6] J. Biol. Chem. **78,** 463 (1928).
[7] J. Biol. Chem. **89,** 399 (1930).
[8] J. Biol. Chem. **106,** 667 (1934).
[9] Pregl, Quantitative Organic Microanalysis, second edition.
[10] J. Research NBS **13,** 617 (1934) RP731.
[11] Public Health Reports 86 (1930).
[12] W. M. Clark, The Determination of Hydrogen Ions, 106–7 (Williams and Wilkins Co.).

WASHINGTON, February 21, 1936.

[5] Investigation now in progress.

U. S. DEPARTMENT OF COMMERCE NATIONAL BUREAU OF STANDARDS

RESEARCH PAPER RP876

Part of Journal of Research of the National Bureau of Standards, Volume 16, April 1936

OXIDATION OF WOOL: THE LEAD ACETATE TEST FOR HYDROGEN PEROXIDE BLEACHED WOOL [1]

By Arthur L. Smith and Milton Harris [2]

ABSTRACT

The lead acetate test for distinguishing between untreated and hydrogen peroxide bleached wool has been investigated. The degree of darkening of the wool during lead acetate treatments is a function of pH, the maximum difference between untreated and bleached wool occurring at pH 5. The results indicate that hydrogen peroxide partially oxidizes the sulfur in wool and prevents the formation of lead sulfide. A mechanism by which lead sulfide is formed in untreated wool is described.

CONTENTS

		Page
I.	Introduction	309
II.	Materials and methods	310
III.	Results and discussion	310
IV.	References	313

I. INTRODUCTION

Previous work [1, 2] [3] has shown that in the action of hydrogen peroxide on wool, the disulfide group of the cystine is oxidized and the susceptibility of the wool to deterioration during alkali treatment is greatly increased. The extent to which the wool is oxidized bears a functional relationship to the decrease in the cystine content and to the increase in the alkali-solubility of the wool. While determinations of the cystine content or alkali-solubility of wool offer good quantitative methods for the control of hydrogen peroxide bleaching, there is a definite need for a qualitative test for distinguishing between unbleached and hydrogen peroxide bleached wool. Tests on the physical properties have been shown to be useless for this purpose [1]. Various dyeing tests [3, 4, 5] have been used, but with only partial success since they were designed to measure damage to wool in general and lack specificity.

It is well known that under suitable conditions wool will darken when treated with solutions of lead acetate or nitrate [6, 7, 8]. More recently, this treatment has been used by Beutel and Kutzelnigg [9] to distinguish between unbleached and bleached horn and wool. Presumably, the bleached materials remain unchanged, whereas the

[1] This is the second paper of a series of studies relating to the oxidation of wool.

[2] Research associates at the National Bureau of Standards representing the American Association of Textile Chemists and Colorists.

[3] The numbers in brackets here and elsewhere in the text refer to the numbered references at the end of this paper.

unbleached materials are darkened by the treatment. They also found that irradiated wool was readily darkened by the lead salts, but that the same wool after oxidation did not give the reaction. The method they have outlined is unsatisfactory since it fails in the presence of small amounts of acid or alkali. For example, unbleached wool containing a little acid is not darkened, while bleached wool in alkaline solution is darkened by lead acetate.

The present investigation was undertaken to study the effect of pH on the darkening of wool in lead acetate solutions, and to determine the optimum pH for distinguishing between unbleached and hydrogen peroxide bleached wool by the lead acetate test.

II. MATERIALS AND METHODS

The material used for these experiments was worsted cloth, plain weave, weighing about 5 ounces per square yard, mill-processed, and ready for dyeing. It was purified by extraction with alcohol for 8 hours in a soxhlet apparatus, after which it was soaked for 1 hour in water at 140° F. The cloth was then air-dried and cut into specimens 17.5 centimeters square.

The bleached wool was prepared from the purified worsted cloth described above by treating for 1 hour at 120° F with a 2-volume solution of hydrogen peroxide at pH 9.5, centrifuging to remove excess solution, and drying for 1 hour at 140° F. The cloth was then washed free of hydrogen peroxide and air-dried.

The alkali-treated wool was prepared from the purified worsted cloth by treating for 15 minutes at 130° F in a 0.5-percent solution of sodium carbonate. This cloth was immediately washed free of alkali and air-dried.

Approximately 5 g of the material to be tested was boiled for 40 minutes in 400 ml of a 0.05-percent solution of lead acetate of known pH, rinsed, and then dried at room temperature. The reflectance of the tested sample was measured with a Martens photometer [10].

III. RESULTS AND DISCUSSION

Preliminary spectrophotometric measurements at seven wave lengths in the range 405 to 703 millimicrons were made of the untreated and of the bleached cloths before and after the lead acetate treatments. The results indicated that measurements at wave lengths approximately 650 millimicrons would give a satisfactory measure of the darkening produced by the lead acetate test.

Samples of the untreated and of the bleached cloths were tested with lead acetate solutions varying in pH from 1 to 11, the pH of the solutions being obtained by suitable additions of hydrochloric acid or sodium hydroxide. The color of the untreated and bleached cloths tested at pH 1 was the same. The untreated cloth began to darken at about pH 2 and the bleached at about pH 3.5. Between these pH's and pH 11 the samples became darker with increasing pH. In this range the bleached samples were lighter in color than the untreated, the maximum differences occurring between pH 4 and 5.5. At pH 11 the color of the two materials became approximately the same.

Journal of Research of the National Bureau of Standards

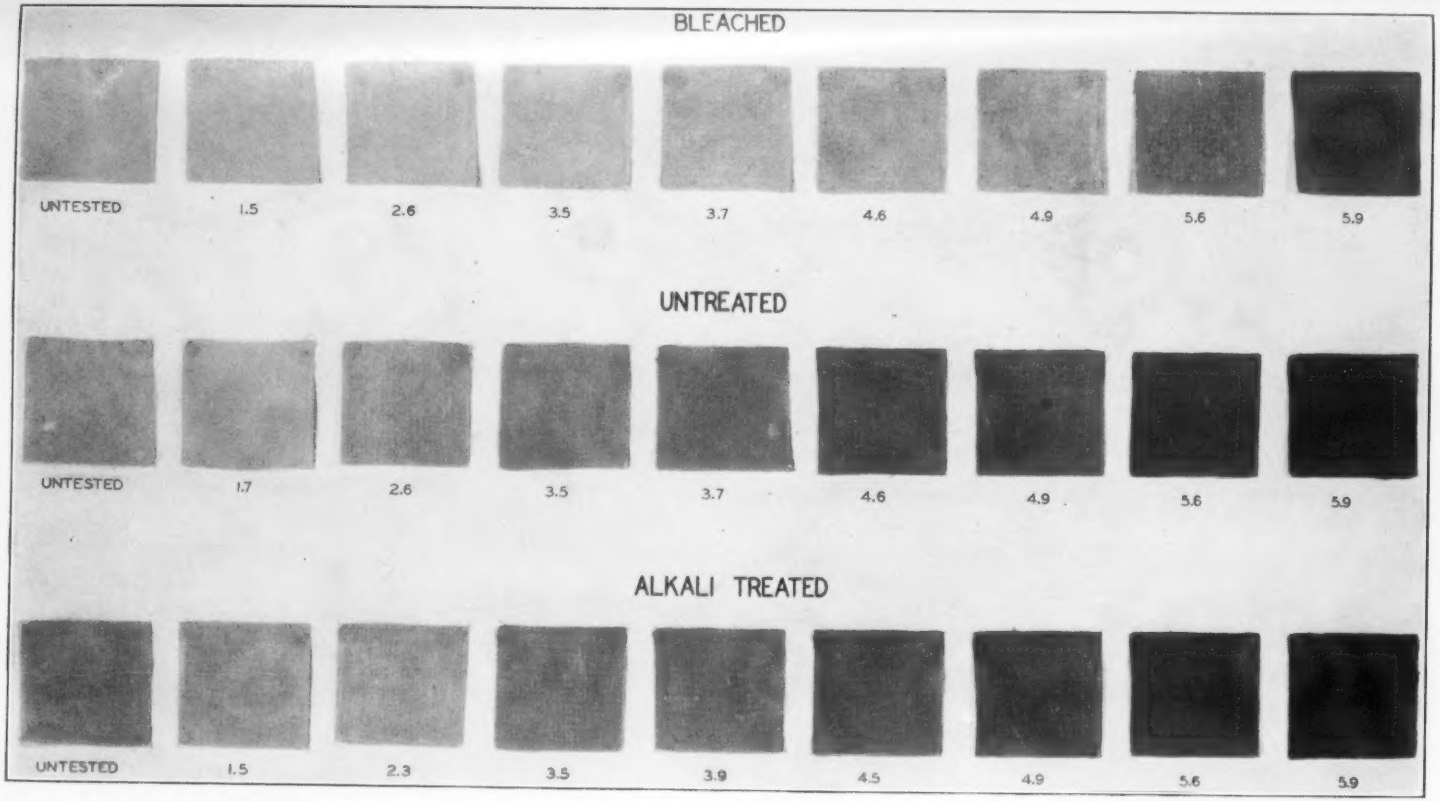

FIGURE 1.—*Appearance of the bleached, untreated, and alkali-treated wool after being boiled for 40 minutes in 0.05-percent lead acetate solutions of varying* pH.

UNIV. OF MICH.

In order to obtain a more definite maximum, and to eliminate the difficulties of regulating the pH with hydrochloric acid and sodium hydroxide solutions, lead acetate solutions, buffered with hydrochloric acid-sodium acetate mixtures were used [11]. A second series of untreated, bleached, and alkali-treated samples were treated with these solutions at intervals of about 0.5 pH between about pH 1.5 and pH 6. The effect of the treatments is shown in figures 1 and 2. A maximum difference in color and in reflectance at 650 millimicrons between the bleached samples and the untreated and alkali-treated samples was obtained at about pH 5.[4]

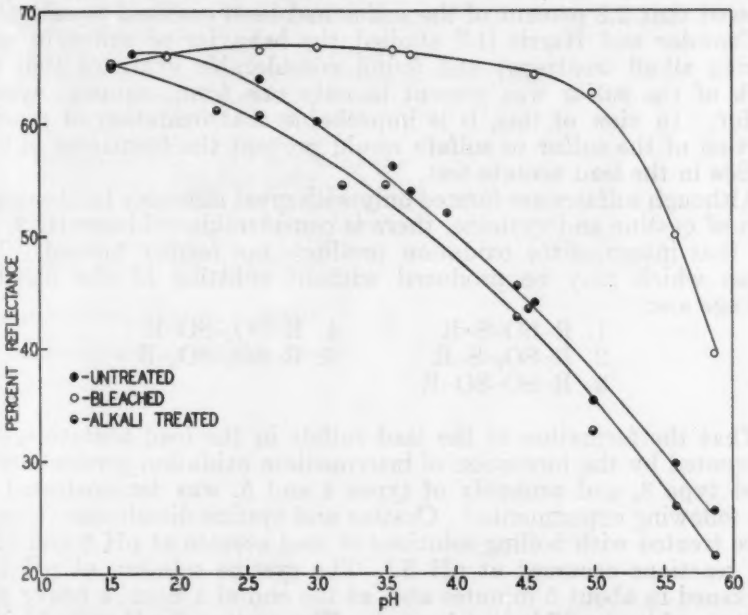

FIGURE 2.—*Relation between the* pH *of the lead acetate solution and the reflectance at wave length approximately 650* mμ *of the tested samples shown in figure 1.*

The alkali-treated samples [5] are, in general, slightly darker than the untreated samples. However, the differences in reflectances between the two series of samples are of the same order of magnitude as the variations obtained in a series of like samples at a given pH. The results, therefore, do not warrant the use of the lead acetate test as a method for the detection of alkali damage.

[4] Suitable buffer solutions for the lead acetate tests may be prepared according to either of the following formulas:

Formula 1			Formula 2		
Volume (ml)	Concentration	Component	Volume (ml)	Concentration	Component
200	1*N*	Sodium acetate.	200	1*N*	Sodium acetate.
20	2.5%	Lead acetate.	20	2.5%	Lead acetate.
50	1*N*	Hydrochloric acid.	68	1*N*	Acetic acid.
730		Water.	712		Water.

[5] The alkali treatment used in this work is more severe than alkali treatments to which wool is generally exposed in practical processing.

In their studies on keratins, Beutel and Kutzelnigg [9] postulated that during irradiation some of the sulfur in wool was converted to sulfide sulfur which readily reacted with lead salts. Since oxidation with hydrogen peroxide prevented the formation of black lead sulfide, they assumed that the sulfide sulfur had been oxidized to sulfate sulfur. It is known that in the photochemical oxidation of wool some sulfate is formed [12], but this accounts for only a small portion of the total sulfur. Furthermore, Blumenthal and Clarke [13] showed that by oxidation with bromine, only about 7 percent of the sulfur in wool was convertible to sulfate. Analyses for sulfates in the bleached samples used in this work, by the method of Mease [14], showed that 2.2 percent of the sulfur had been oxidized to sulfate.

Crowder and Harris [15] studied the behavior of sulfur in wool during alkali treatment and found considerable evidence that the bulk of the sulfur was present in only one form, namely, cystine sulfur. In view of this, it is improbable that oxidation of a small portion of the sulfur to sulfate would prevent the formation of lead sulfide in the lead acetate test.

Although sulfates are formed only with great difficulty by the oxidation of cystine and cysteine, there is considerable evidence [1, 2, 16, 17] that intermediate oxidation products are readily formed. The types which may be produced without splitting of the disulfide linkage are:

1. R–SO–S–R
2. R–SO_2–S–R
3. R–SO–SO–R
4. R–SO_2–SO–R
5. R–SO_2–SO_2–R

That the formation of the lead sulfide in the lead acetate test is prevented by the formation of intermediate oxidation products of at least type 3, and probably of types 4 and 5, was demonstrated by the following experiments.[6] Cystine and cystine disulfoxide (type 3) were treated with boiling solutions of lead acetate at pH 5 and 12.5. No reactions occurred at pH 5.[7] The cystine solution at pH 12.5 darkened in about 5 minutes and, at the end of 1 hour, a heavy precipitate of lead sulfide had formed. The cystine disulfoxide solution at pH 12.5 remained clear during this time, and only after prolonged boiling did a slight darkening occur.

The ease with which lead sulfide is formed on the untreated wool, especially with increasing pH, is in accord with the known lability of sulfur in wool and can be accounted for by the mechanism postulated by Crowder and Harris [15] according to the following scheme:

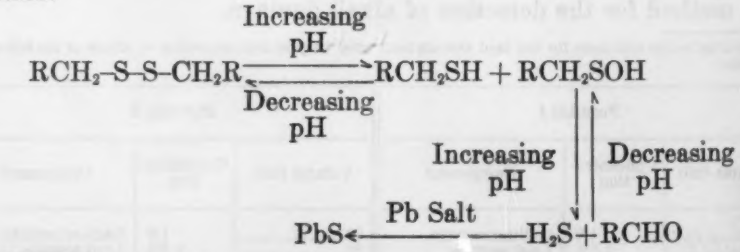

[6] This postulation may be made since it is known that the sulfoxides may be reduced to the sulfhydryl form, whereas the sulfones are not reduced under similar conditions.

[7] The sulfur in cystine itself is very much more stable than sulfur in cystine in the wool protein.

The darkening of the untreated wool samples in solutions below pH 5 indicates the extreme lability of the sulphur. While acid tends to drive the equilibrium in the above equation in the direction shown by the arrows, the results indicate that some hydrogen sulfide[8] is formed in acid solutions to about pH 2.

IV. REFERENCES

[1] J. Research NBS **16,**—(1936) RP—.
[2] J. Research NBS **15,** 63 (1935) RP810.
[3] Leipzig. Monatschr. Textil-Ind. **44,** 165, 211 (1929).
[4] Melliand Textilber. **9,** 326 (1928).
[5] Melliand Textilber. **12,** 768 (1931).
[6] Färber-Ztg. p. 45 (1912)
[7] Die Textilfasern, Berlin, p. 90 (1928).
[8] Die Rohstoffe des Tierreiches, Berlin, p. 1094 (1932).
[9] Monatsch. Textil-Ind. **64,** 183 (1934).
[10] Am. Dyestuff Reptr. **17,** 49 (1928).
[11] Britton, Hydrogen Ions, p. 180.
[12] J. Research NBS. (To be published.)
[13] J. Biol. Chem. **110,** 343 (1935).
[14] J. Research NBS **13,** 617 (1934) RP731.
[15] J. Research NBS. (To be published.)
[16] J. Am. Chem. Soc. **56,** 242 (1934).
[17] J. Biol. Chem. **105,** 107 (1934).

WASHINGTON, March 5, 1936.

[8] In alkaline solutions, Na_2S would be formed.

U. S. DEPARTMENT OF COMMERCE NATIONAL BUREAU OF STANDARDS

RESEARCH PAPER RP877

Part of Journal of Research of the National Bureau of Standards, Volume 16, April 1936

EVALUATION OF ULTRAVIOLET SOLAR RADIATION OF SHORT WAVE LENGTHS

By W. W. Coblentz and R. Stair

ABSTRACT

Technical details are given for evaluating ultraviolet solar radiation by two closely agreeing methods: (a) by means of a balanced thermopile and filter radiometer, calibrated against a standard of thermal radiation, and (b) by means of a photoelectric ultraviolet meter calibrated against a standard of ultraviolet radiation. A photoelectric cell and filter method for determining the solar ultraviolet spectral-energy distribution is described. Data are given on ultraviolet solar radiation intensities observed at Washington, D. C., San Juan, P. R., and Flagstaff, Ariz. The intensity of ultraviolet solar radiation of wave lengths shorter than and including 3132 A, in the clearest, midsummer, midday sunlight at Washington is about 75 $\mu w/cm^2$ decreasing to one-tenth this value (8 $\mu w/cm^2$) during the clearest, midwinter, midday sunshine. Extrapolation of the data observed at the three stations (Washington, San Juan, and Flagstaff) indicates an ultraviolet intensity of about 600 $\mu w/cm,^2$ outside the earth's atmosphere—a fivefold to eightfold increase as compared with a 20 to 30 percent increase in total intensity of all wave lengths.

CONTENTS

	Page
I. Introduction	316
II. Determination of the distribution of energy in the extreme ultraviolet of the solar spectrum	318
III. Evaluation of ultraviolet solar radiation with a balanced thermocouple and filter radiometer	324
1. Calibration of galvanometer-scale reading	325
2. Calculation of factor F	326
IV. Evaluation of ultraviolet solar radiation with a photoelectric cell and balanced-amplifier radiometer	330
1. Calibration of microammeter-scale reading	330
2. Calculation of factor G	332
3. Calculation of ultraviolet radiant flux	333
4. Summarizing comments	335
V. Ultraviolet solar-radiation data	336
1. Observations at Washington, D. C.	336
(a) Corrections to the Washington observations of September 1929 to June 1931	337
2. Observations at San Juan, P. R.	339
3. Observations at Flagstaff, Ariz.	342
(a) Corrections to the Flagstaff observations of August–September 1929	344
VI. References and notes	346

I. INTRODUCTION

The evaluation, in absolute units, of the energy in the short-wave-length ultraviolet region of the solar spectrum has been attempted by several methods. The most common procedure is to integrate the energy curve, observed throughout the whole solar spectrum, and calculate the fractional part that is contained in the band of wave lengths (for example, between 2900 to 3100 A) under investigation. Then, from a determination of the total radiant flux (the solar intensity Q, in gram-calories, as usually observed) the part in the short wave lengths is calculated. The objection to this method is the lack of accurate data on the spectral-energy distribution, particularly in the ultraviolet.

A proposed variation in this method is to calculate the spectral-energy distribution on the assumption that the radiation from the sun is comparable with that of a black body at 6,000° K. However, in view of the fact that the effective radiating surface of the sun emits selectively, this assumption is obviously untenable. In addition to this fact is the uncertainty of the atmospheric-transmission coefficients which are constantly changing. Hence, the method would be useful only in a very general way.

The most promising method of evaluation of the short-wave-length ultraviolet in solar radiation is by means of filters placed over either a selective (photoelectric) or a nonselective (thermopile) radiometer. This procedure requires a determination of the spectral-energy distribution and the radiant flux (the total intensity) within and adjacent to the band of wave lengths under investigation.

This Bureau's interest in the evaluation of the ultraviolet of short wave lengths in solar radiation began about 8 years ago, when, in connection with the widespread interest in light sources and window materials for therapeutic purposes [1],[1] it was urgent to obtain an estimate (having some degree of reliability) of the amount of ultraviolet in sunlight that has a therapeutic value, at least in healing rickets.

The earliest investigations [1, 2], using a thermocouple and filters of window glass, led to an estimate of the upper limit in intensities that might be expected in ultraviolet solar radiation, useful for therapeutic purposes.

From these crude beginnings, as the demand for more exact data increased, improvements were made in the filter methods of radiometry; and data were obtained on ultraviolet solar-radiation intensities at sea level and at high elevations [3]. For this purpose the best available ultraviolet spectral-energy measurements were used in calculating the amount of ultraviolet, of wave lengths 3132 A and shorter, in sunlight.

Since the ultraviolet intensities in the shortest wave lengths were extremely low, the investigation was undertaken anew, using a ("differential") balanced thermocouple and filter method, which greatly increased the accuracy of the measurements [3, 4].

However, there was an outstanding uncertainty in the ultraviolet solar-radiation measurements, which evidently was owing to the lack of knowledge of the spectral-energy distribution. This conclusion seemed to follow from the good agreement obtained on artificial

[1] Numbers in brackets refer to references and notes at the end of this paper.

sources, in which the radiation in a spectral band was integrated by spectroradiometric and filter methods [4], and it was further substantiated in a subsequent interlaboratory comparison of lamps [5], in which good agreement was obtained in the spectral-energy measurements.

Subsequent tests of the balanced thermocouple and filter radiometer as a standard ultraviolet dosage intensity meter [6] on artificial sources justify the belief that the device is reliable, provided the ultraviolet spectral-energy distribution of the source is known with sufficient accuracy. In the case of the sun it was evident that the spectral-energy distribution, in the extreme ultraviolet, is not known with sufficient accuracy, and that it should be determined at the time of the physiological or biological application of the radiation stimulus.

In view of the fact that the thermopile is not sufficiently sensitive to measure accurately, by means of filters, the spectral-energy distribution of solar radiation in the region of 2900 to 3200 A, the writers have devised a portable ultraviolet meter, consisting of a balanced amplifier, photoelectric cell, and microammeter [7], which is eminently adapted to determine the spectral quality of ultraviolet solar radiation, practically simultaneously with any biological tests that may be in progress.

Moreover, recent improvements in methods of calibrating the photoelectric ultraviolet meter against a standard of ultraviolet radiation [8] make it possible to use this instrument to determine (a) the spectral quality and (b) the total intensity (the latter in absolute value) thus greatly reducing the equipment, work, and expense in conducting field measurements of solar ultraviolet radiation.

There was recently published a preliminary outline [9, 10] of the procedure for determining the spectral-energy distribution in the extreme ultraviolet of the solar spectrum by means of a titanium photoelectric cell and filters [7]. It was shown [9] that: (a) because the ultraviolet solar spectral-energy curve is not known with sufficient accuracy (particularly in the region of the H and K lines; 3700 to 4000 A), and (b) because there are no suitable filters to place over a thermopile in order to confine its response to wave lengths shorter than about 3300 A (in which we are chiefly interested) a photoelectric cell which is insensitive to wave lengths longer than about 3300 A is especially adapted for determining the spectral-energy distribution in the band of wave lengths extending from 2900 to 3300 A, by the filter method.

The object of the present paper is to present technical details to serve as a guide in evaluating the ultraviolet of short wave lengths in solar radiation, by two closely agreeing methods: (a) by means of a balanced thermopile and filter radiometer which is calibrated against a standard of thermal radiation [11]; and (b) by means of a titanium photoelectric ultraviolet intensity meter [7], calibrated in absolute value against a standard of ultraviolet radiation [8].

At the outset, it is to be noted that, for small air masses, the previously published values of ultraviolet intensities remain practically unchanged; but, for large air masses, where the spectral-energy distribution was practically unknown prior to the adoption of the present method of spectral-energy evaluation, the ultraviolet intensities are appreciably lower than previously reported.

II. DETERMINATION OF THE DISTRIBUTION OF ENERGY IN THE EXTREME ULTRAVIOLET OF THE SOLAR SPECTRUM

A knowledge of the distribution of intensities in the spectrum, in relative units, is essential in order to evaluate the energy in a given band of wave lengths.

As shown in figure 2 of a previous paper [10], owing to the presence of the Fraunhofer absorption lines, caused by vapors of various elements in the solar atmosphere, and the absorption lines caused by ozone in the terrestrial atmosphere, the solar spectrum appears discontinuous when photographed under a sufficiently high dispersion. On the other hand, as ordinarily observed radiometrically, with a low dispersion, the ultraviolet spectral-energy curve is relatively smooth and free from indentations [12].

As indicated in the previous paper [10], by means of the titanium photoelectric cell and a group of four glass filters, the spectral band of ultraviolet, extending from 2900 A to about 3500 A, is separated into five parts. This procedure requires only a few minutes, thus securing the information desired without the necessity of making corrections for change in air mass.

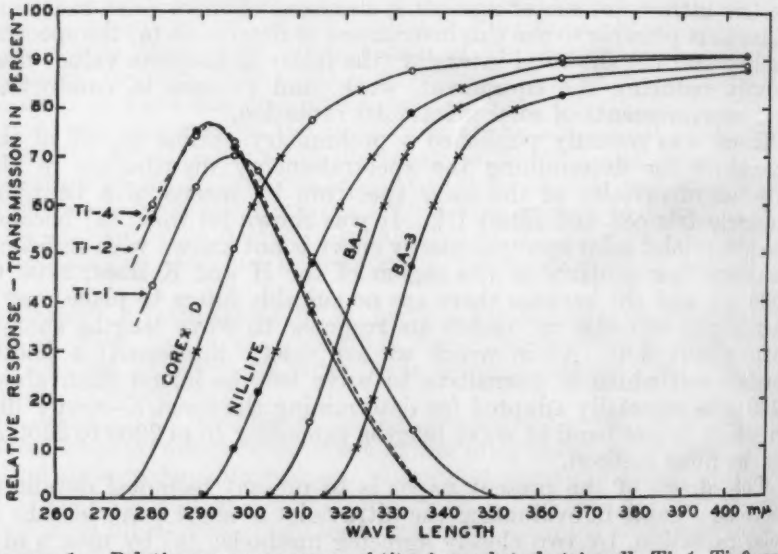

FIGURE 1.—*Relative response curves of titanium photoelectric cells* Ti–*1*, Ti–*2*, *and* Ti–*4 to an equal-energy spectrum; also spectral transmission of glass filters used* (*Corex* D, *Nillite; both trade names*); *and barium-flint glass* (Ba–*1 and* Ba–*3; thickness 1 mm and 3* mm, *respectively*).

Wave length 400 mμ=4000 A.

From a detailed study of the shape of the spectral-energy curve required to give calculated transmissions in agreement with the observed photoelectrically integrated filter transmissions, it appears that a relatively smooth curve with but slight indentations, as observed by Pettit [12], answers the purpose of evaluating the ultraviolet for use in medicine.

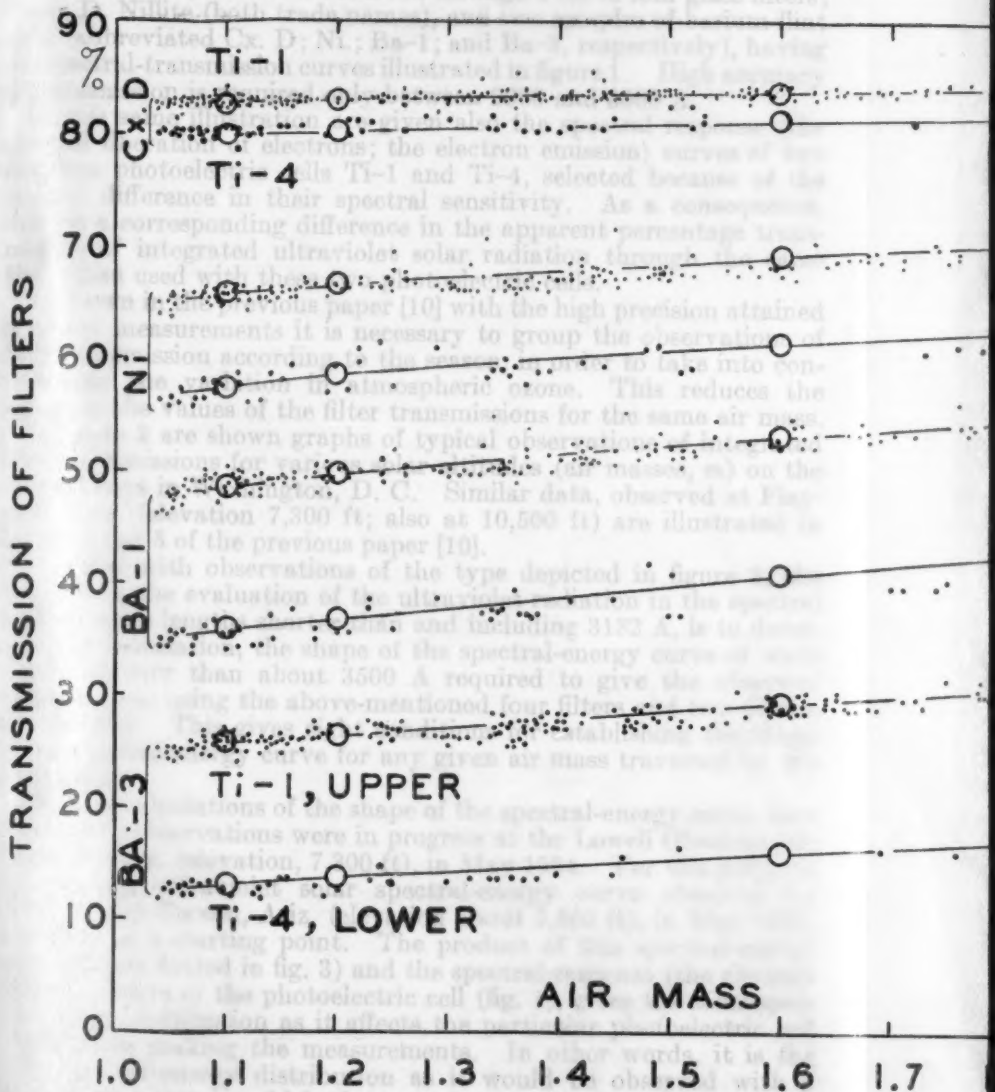

FIGURE 2.—*Diurnal variation in transmiss*

The large circles are the calculated transmissions for ultraviolet

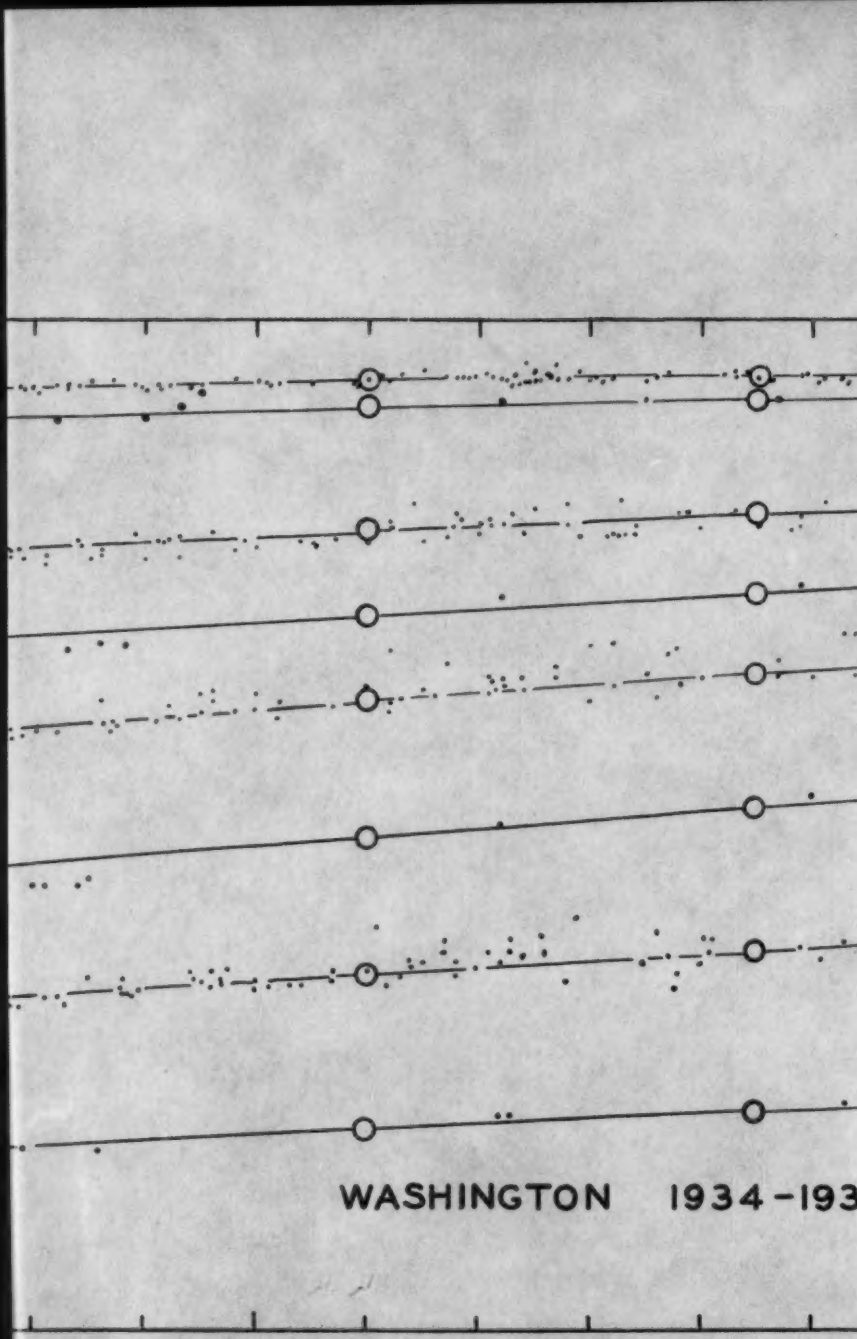

n transmission of ultraviolet solar radiation through standard filters (see figure 1) obs

for ultraviolet spectral-energy curves identified with the corresponding air masses, see figure 9. The blac

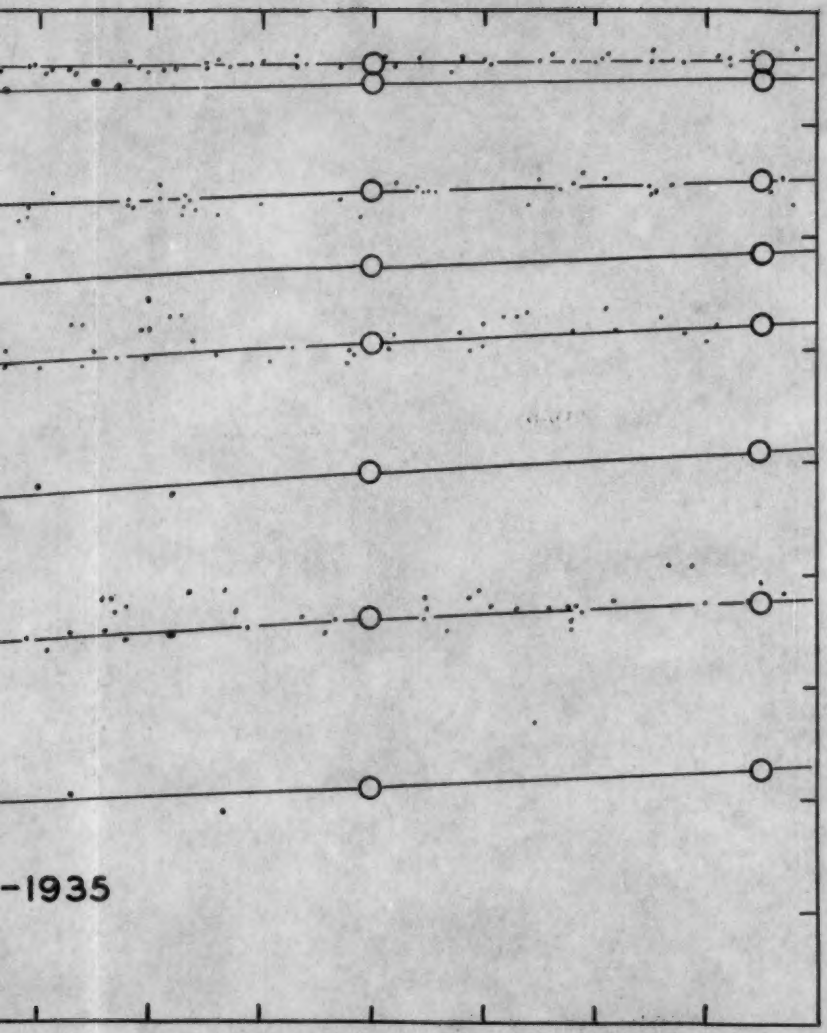

e 1) observed at Washington

The black dots represent observed values.

55384—36 (Face p. 318)

UNIV. OF MICH.

TRANSMISSION OF FILTERS
%
90
80
70
60
50
40
30
20
10
0
1.0
1.1
1.2
1.3
1.4
1.5
1.6
AIR MASS
Ti-4, LOWER
Ti-1, UPPER
Ti-1
Ti-4
Cx.D
Ni
BA-1
BA-3

The experimental procedure is to observe the percentage transmission of the ultraviolet solar radiation in the band extending from the extreme wave lengths that penetrate the atmosphere (about 2900 A) to the limit of response of the particular photoelectric cell used (3300 to 3500 A). This is observed through a set of four glass filters; Corex D, Nillite (both trade names), and two samples of barium-flint glass (abbreviated Cx. D; Ni.; Ba–1; and Ba–3, respectively), having the spectral-transmission curves illustrated in figure 1. High accuracy in transmission is required only between 2900 and 3500 A.

In this same illustration are given also the spectral response (the spectral liberation of electrons; the electron emission) curves of two titanium photoelectric cells Ti–1 and Ti–4, selected because of the marked difference in their spectral sensitivity. As a consequence, there is a corresponding difference in the apparent percentage transmission of integrated ultraviolet solar radiation through the same filter when used with these two photoelectric cells.

As shown in the previous paper [10] with the high precision attained in recent measurements it is necessary to group the observations of filter transmission according to the season, in order to take into consideration the variation in atmospheric ozone. This reduces the spread in the values of the filter transmissions for the same air mass.

In figure 2 are shown graphs of typical observations of integrated filter transmissions for various solar altitudes (air masses, m) on the clearest days in Washington, D. C. Similar data, observed at Flagstaff, Ariz. (elevation 7,300 ft; also at 10,500 ft) are illustrated in figures 4 and 5 of the previous paper [10].

Provided with observations of the type depicted in figure 2, the first step in the evaluation of the ultraviolet radiation in the spectral band of wave lengths shorter than and including 3132 A, is to determine, by calculation, the shape of the spectral-energy curve of wave lengths shorter than about 3500 A required to give the observed transmissions, using the above-mentioned four filters and two photoelectric cells. This gives eight conditions for establishing the shape of the spectral-energy curve for any given air mass traversed by the solar rays.

The first calculations of the shape of the spectral-energy curve were made while observations were in progress at the Lowell Observatory, Flagstaff, Ariz. (elevation, 7,300 ft), in May 1934. For this purpose, the average ultraviolet solar spectral-energy curve observed by Pettit [12] at Tucson, Ariz. (elevation about 2,500 ft), in May 1931, was used as a starting point. The product of this spectral-energy curve (shown dotted in fig. 3) and the spectral-response (the electron emission) curve of the photoelectric cell (fig. 1), gives the solar spectral-energy distribution as it affects the particular photoelectric cell employed in making the measurements. In other words, it is the solar spectral-energy distribution as it would be observed with a spectroradiometer in which the nonselective radiometer is replaced by a selective (photoelectric) radiometer. For the eye it is the "luminosity curve."

For example, curve Ti–1 is the spectral response of photoelectric cell Ti–1, when exposed directly to solar radiation whose spectral-energy distribution is shown by the dotted curve in figure 3. The product, at each wave length, of this photoelectric appraisal of the spectral energy by the corresponding percentage transmission of the filter (fig. 1) gives, in each case, the spectral-energy distribution as transmitted through the filters marked Cx. D.; Ni.; Ba–1; and Ba–3 in figure 3. The ratio of the area under each of these curves to the area under the curve Ti–1 gives, in each case, the fraction of the incident ultraviolet that is transmitted by the filter. Similar curves were obtained for the titanium photoelectric cell Ti–4.

As was to be expected, owing to the difference in altitude of the two observing stations (Tucson and Flagstaff), there were systematic deviations of the calculated from the observed photoelectrically integrated filter transmissions; these deviations being in agreement for both photoelectric cells. The spectral intensities taken from Pettit's

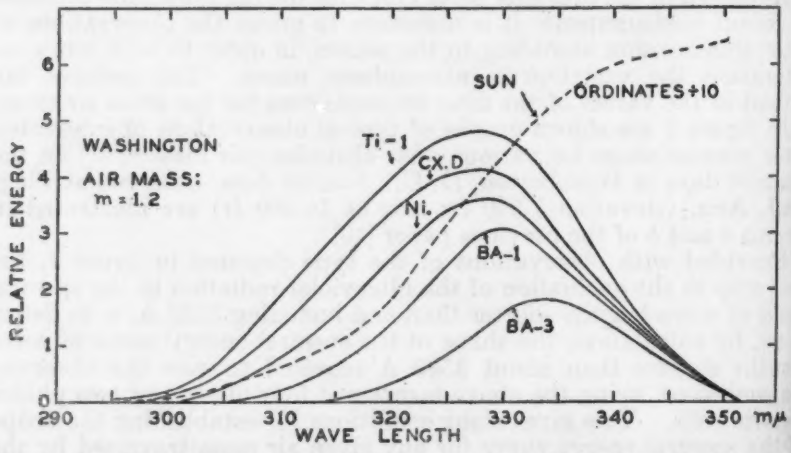

FIGURE 3.—*Spectral-energy curve of the sun as it would be observed with a non-selective radiometer and with a selective photoelectric radiometer,* Ti–*1, without a filter, and through the standard filters* Ba–*3, etc.*

Wave length 350 mμ=3500 A.

energy curve, in the region of 2950 to 3050 A were slightly too high, and the intensities at 3250 to 3550 A were appreciably too low (as was to be expected) to fit the observations at the higher elevation (7,300 ft) at Flagstaff, Ariz. By making slight changes in the assumed energy curve, in these two spectral regions, after one or two further trial adjustments and calculations, a set of calculated filter transmissions was obtained, for the two photoelectric cells and the four filters, which, within the experimental errors in the observations, was in good agreement with the transmissions observed in May and June at Flagstaff for an air mass, $m=1.35$, and with the transmissions observed at Washington, for $m=1.20$, in October and the first part of November 1934. This spectral-energy curve was, therefore, identified with the air mass $m=1.20$ at Washington and $m=1.35$ at Flagstaff.

Subsequently a prolonged investigation was made of the spectral transmissions of the filters and of thin samples (to determine the end points), by radiometric and photographic means; and a redetermination was made of the spectral photoelectric response curves of the photoelectric cells. In figure 1 the radiometric transmissions are indicated by dots and circles. The intervening parts of the curves (×××) were established by photographic means.

This investigation introduced slight changes in the spectral-transmission curves and in the spectral photoelectric response curves which, in turn, required a slight change in the assumed spectral-energy curve (fig. 3)—mainly increasing the indentation at 3250 A. As a result of this more exact determination of the spectral transmissions of the filters there was even better agreement than previously found between the observed and the calculated percentage transmissions of the integrated ultraviolet solar radiation through all the filters, except, perhaps, the filter of Nillite glass, which was a piece of special window glass that did not have a high optical polish and, hence, should not be given the same weight as the others.

The agreement attained between the calculated and the observed values is closer than required, because of the inevitable variations in the observed values caused by ever-changing atmospheric conditions.

In table 1 is given an example of the procedure in calculating the transmission of the photoelectrically integrated ultraviolet solar radiation through the various filters. In this table columns 2 and 3 give the spectral response (the spectral liberation of electrons), respectively, of the two photoelectric cells (Ti–1 and Ti–4), produced by an equal-energy spectrum.

Column 4 is the ultraviolet spectral-energy distribution (intensities are relative values) which is found to give the observed filter transmissions for an air mass $m=1.20$, at Washington. (See fig. 3.)

Columns 5 and 6 give the products of the ultraviolet solar intensities (column 4) and the spectral photoelectric responses (columns 2 and 3, respectively). The solar spectral-energy curve as it would be observed with titanium photoelectric cell Ti–1, attached to a spectroheliometer is illustrated in figure 3 (Ti–1). In other words, these two columns give the spectral distribution of the photoelectric response to the given solar radiation.

Columns 7, 8, 9, and 10 are the spectral transmissions, respectively, of filters Cx. D; Ni.; Ba–1; and Ba–3.

Columns 11, 12, 13, and 14 are the products of column 5 (solar energy times relative photoelectric response for Ti–1) and the spectral transmissions of the filters (columns 7, 8, 9, and 10, respectively). This gives the spectral distribution of the photoelectric response with titanium photoelectric cell Ti–1 observed through the various filters. (See fig. 3.)

Columns 15, 16, 17, and 18 give the spectral-energy distribution (photoelectric response) as observed with titanium photoelectric cell Ti–4, using the above-mentioned filters Cx. D; Ni.; Ba–1; and Ba–3.

The calculated transmissions of the photoelectrically integrated ultraviolet solar radiation, for air mass $m=1.20$, for the various filters, are obtained by taking the ratio of the areas under the curves (for example, the area under the curve Ba–3 to the area under the curve Ti–1, in fig. 3); or by taking the ratio of the summation of

TABLE 1.—*Example of the procedure followed in calculating the transmission coefficients of the filters, for a given distribution of energy (column 4), which were subsequently identified with the observed transmissions for air mass m=1.20, at Washington*

1	2	3	4	5	6	7	8	9	10	11	12	13	14	15	16	17	18
Wave lengths (angstroms)	Relative spectral response		Relative solar energy ($m=120$)	Relative solar energy × relative response		Transmission of filter				Transmission of filters × solar energy × relative response (Ti-1)				Transmission of filters × solar energy × relative response (Ti-4)			
	Ti-1	Ti-4		Ti-1	Ti-4	Cx. D	Ni.	Ba-1	Ba-3	Cx. D	Ni.	Ba-1	Ba-3	Cx. D	Ni	Ba-1	Ba-3
2950	0.70	0.75	0.005	0.004	0.004	0.46	0.067			0.002	0.001			0.002	0.001		
2975	.70	.71	.200	.140	.142	.54	.110			.076	.015			.077	.016		
3000	.69	.665	.465	.321	.309	.595	.155			.191	.050			.180	.048		
3025	.68	.62	.817	.555	.507	.645	.205			.358	.114			.327	.104		
3050	.64	.56	1.225	.784	.686	.687	.265			.539	.208			.471	.182		
3075	.59	.50	1.76	1.038	.880	.722	.33	0.034		.750	.343	0.035		.635	.290	0.030	
3100	.54	.45	2.30	1.242	1.035	.750	.39	.08		.931	.484	.099		.776	.404	.083	
3125	.50	.39	2.79	1.395	1.088	.772	.455	.14		1.077	.634	.195		.840	.639	.152	
3150	.455	.35	3.51	1.597	1.228	.792	.52	.215	0.013	1.264	.830	.343	0.021	.973	.639	.264	0.016
3175	.41	.30	4.41	1.808	1.323	.807	.58	.30	.043	1.459	1.048	.542	.078	1.068	.767	.397	.057
3200	.37	.25	5.75	2.128	1.438	.822	.635	.39	.08	1.749	1.351	.830	.170	1.182	.913	.561	.115
3225	.32	.20	8.01	2.563	1.602	.833	.68	.47	.125	2.135	1.743	1.205	.320	1.334	1.089	.753	.200
3250	.28	.16	10.4	2.912	1.664	.845	.728	.545	.195	2.461	2.120	1.587	.568	1.406	1.211	.907	.324
3275	.24	.12	12.1	2.904	1.452	.853	.745	.61	.27	2.477	2.163	1.771	.784	1.239	1.082	.886	.392
3300	.20	.085	14.0	2.800	1.190	.861	.768	.665	.35	2.411	2.150	1.862	.980	1.025	.914	.791	.417
3325	.155	.055	15.6	2.418	.858	.868	.790	.704	.435	2.099	1.910	1.702	1.052	.745	.678	.604	.373
3350	.12	.025	17.5	2.100	.437	.872	.807	.734	.52	1.831	1.695	1.541	1.092	.381	.353	.321	.227
3375	.095	.01	18.9	1.795	.189	.878	.823	.76	.59	1.577	1.477	1.364	1.059	.166	.156	.144	.112
3400	.07	.00	20.0	1.400		.882	.833	.78	.645	1.235	1.166	1.092	.903				
3425	.05		20.5	1.025		.885	.843	.795	.685	.907	.864	.815	.702				
3450	.03		21.0	.630		.888	.853	.81	.72	.559	.537	.510	.454				
3475	.015		21.3	.320		.890	.859	.821	.745	.285	.275	.262	.238				
Total				31.879	16.032					26.373	21.178	15.755	8.421	12.827	9.342	5.893	2.233
Total transmissions, in percent (for comparison with the observed transmissions)										82.7	66.5	49.4	26.4	80.1	58.2	36.8	13.9

columns 14 and 5 (or 18 and 6 for Ti–4) in table 1, to obtain the transmission through the filter Ba–3; and a similar procedure is followed for the other filters.

The last line in table 1 gives, for the assumed spectral energy distribution, the calculated percentage transmissions of the four filters, Cx. D; Ni.; Ba–1; and Ba–3, as used with photoelectric cells Ti–1 and Ti–4.

Using the spectral-energy curve for air mass $m=1.20$, and factors based upon Pettit's [12] atmospheric transmission coefficients, other spectral-energy curves were calculated. Proceeding as indicated above (see fig. 1), on multiplying, point by point, these spectral-energy curves by the spectral-response curves of the two photoelectric cells and by the spectral transmissions of the respective filters, calculated photoelectrically-integrated ultraviolet transmissions were obtained for the four filters, using the two photoelectric cells (eight determinations), which (after several minor adjustments of these spectral-energy curves) were in close agreement with the observed filter transmissions for air masses $m=1.10$, 1.20, 1.60, etc. (see table 2), at Washington, and correspondingly equivalent air masses (lower solar altitudes) at Flagstaff.

TABLE 2.—*Ultraviolet solar spectral-energy distribution (relative intensities; unrelated for different air masses) corresponding with the observed filter transmissions (four filters with two* Ti *photoelectric cells) at the various air masses, at Washington*

Wave lengths (angstroms)	Air mass; m										
	1.10	1.20	1.60	2.00	2.35	2.70	3.05	3.40	3.70	4.00	4.35
2950	0.05	0.005	0.001								
2975	.28	.20	.019	0.005	0.002	0.001					
3000	.60	.465	.164	.056	.018	.007	0.002				
3025	1.00	.817	.326	.122	.049	.018	.004	0.002	0.001		
3050	1.50	1.225	.546	.230	.100	.041	.018	.006	.003	0.001	
3075	2.05	1.76	.830	.404	.180	.083	.040	.016	.008	.004	0.0015
3100	2.7	2.30	1.16	.585	.304	.148	.071	.033	.017	.009	.004
3125	3.3	2.79	1.57	.838	.463	.240	.119	.066	.034	.018	.009
3150	4.0	3.51	2.01	1.20	.700	.370	.195	.113	.060	.036	.017
3175	4.8	4.41	2.74	1.62	.989	.564	.317	.186	.109	.064	.033
3200	6.4	5.75	3.73	2.30	1.46	.866	.507	.306	.191	.160	.063
3225	8.9	8.01	5.41	3.48	2.30	1.40	.854	.547	.352	.224	.126
3250	11.5	10.4	7.11	4.67	3.15	1.99	1.23	.799	.522	.340	.195
3275	13.3	12.1	8.58	5.78	4.02	2.60	1.66	1.105	.743	.497	.293
3300	15.1	14.0	10.18	7.07	5.02	3.35	2.20	1.50	1.04	.715	.438
3325	16.9	15.6	11.63	8.17	5.91	3.98	2.66	1.84	1.29	8.96	.552
3350	18.8	17.5	13.05	9.30	6.82	4.65	3.15	2.21	1.57	1.112	.695
3375	20.3	18.9	14.30	10.35	7.67	5.31	3.64	2.59	1.87	1.336	.847
3400	21.3	20.0	15.30	11.20	8.40	5.90	4.10	2.95	2.15	1.560	1.000

In table 2 are given the spectral-energy distributions (relative intensities) found to correspond with the observed filter transmissions for the air masses indicated at the top of the table.

In figure 2 the large circles show the agreement between the calculated and the observed transmissions at different solar heights (air masses), using titanium photoelectric cells Ti–1 and Ti–4, and the four filters Cx. D, Ni.; Ba–1; and Ba–3.

Having proved the trustworthiness of the method, and having established the shape of the spectral-energy curve, it should suffice in actual practice to determine the shape of the spectral-energy curve with one or two filters at the time of making the observations; and

from this information, the reduction factor for evaluating the ultraviolet can be taken from previously tabulated data that apply to the particular photoelectric cell used. In fact, during the clearest days, it probably will be unnecessary to determine the spectral quality by making filter measurements.

It is to be noted that these spectral-intensity curves give the average energy distribution in the solar spectrum; whereas, using a large dispersion, spectroradiometric measurements of the radiation between the absorption lines (see fig. 2 of the previous paper [10]) would give an energy curve filled with indentations. However, the slope of the envelope drawn through the intensities measured between the absorption lines would decrease with the wave length as observed spectroradiometrically [12] and as indicated by the filters.

As pointed out in previous papers, owing to the highly selective spectral response of the photoelectric cells, the effect of the low-intensity radiation at 2900 to 2950 A is greatly magnified in the transmission measurements. However, after correcting for this selective magnification, the spectral-energy curves, as determined by the photoelectric cell and filter method, appear to be in good agreement with the few spectroradiometric data that are avaliable for comparison. Another check on the accuracy of this method will be obtained by calculation of the atmospheric-transmission coefficients.

In concluding this discussion it is to be emphasized that heretofore, owing to the almost complete lack of solar spectral-energy data, of wave lengths shorter than about 3100 A, at low elevations (Washington), the data used in evaluating the ultraviolet in sunlight at low altitudes were little more than extrapolations of measurements made at high altitudes.

Since the calculated spectral-energy curve that gives the observed filter transmissions fits the observed spectral-energy curve at high altitudes (due allowance being made for the difference in altitude of the two stations, Tucson and Flagstaff, Ariz.); and since there is no good reason for doubting (see, however, section V–2) that at low elevations, for the equivalent air mass (higher atmospheric pressure but shorter column traversed by the solar rays), the same relative spectral-energy distribution obtains as observed at high altitudes, there is ample justification in using the ultraviolet spectral-energy curves, derived by the above-described filter method, in evaluating the ultraviolet in sunlight at stations of low elevation.

III. EVALUATION OF ULTRAVIOLET SOLAR RADIATION WITH A BALANCED THERMOCOUPLE AND FILTER RADIOMETER

In view of the uncertainty of the solar spectral-energy curve in the region of 3800 to 4100 A, it is necessary to limit the spectral range to the narrowest band of wave lengths readily obtainable, in order to attain the high accuracy desired in the most recent evaluation of the ultraviolet (in absolute units). For this purpose the balanced thermocouple is covered with an especially selected sample of optically polished red-purple Corex A glass (no. 986), which was found to have the same homogeneity (the same percentage transmission) through the two widely separated areas that cover the openings leading to the two receivers of the balanced thermocouple. The sample of red-

purple glass used in previous measurements [4] was not so perfect optically.

In figure 4 is shown the spectral transmission of the red-purple Corex A glass (no. 986, thickness 3.1 mm), which is practically opaque to wave lengths longer than 425 mμ (4250 A). Used in connection with the cell of water, 1 cm in thickness, the transparency of this glass in the infrared is practically eliminated, and the thermopile response is confined principally to the violet and ultraviolet, as obtains in a titanium photoelectric cell. The small amount of infrared transmitted by the combined filters is determined by inserting, temporarily, a filter of Noviol A glass, which shuts out the ultraviolet (fig. 4). The transmission curves of the Ba-flint exclusion filter and the Corex A compensating filter are also given in figure 4.

1. CALIBRATION OF THE GALVANOMETER-SCALE READING

The first step in the evaluation of ultraviolet radiation by means of a balanced thermoelectric radiometer is to calibrate the thermopile-

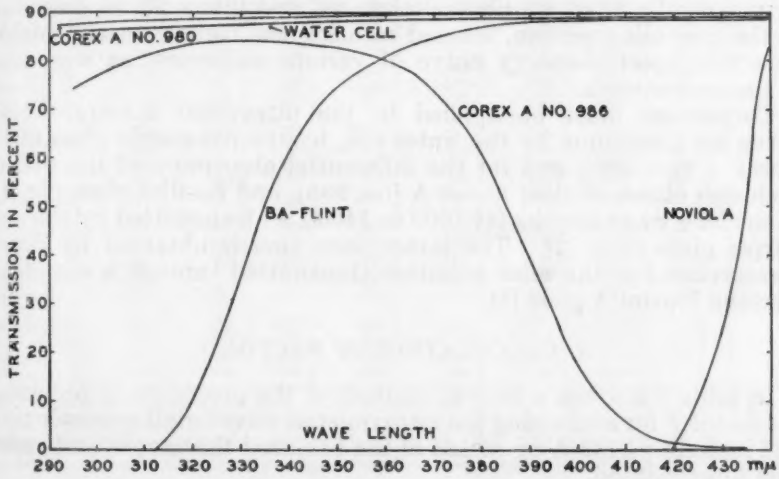

FIGURE 4.—*Transmission of filters used in the balanced-thermopile and exclusion-filter method of evaluation of ultraviolet.*

Wave length 420 mμ=4200 A.

galvanometer deflection, in absolute value, against a standard of radiation [11]. For this purpose the water cell and the red-purple Corex A filters are removed, and the receivers (first the one, then the other) are exposed to the standard lamp as described on page 731 of a previous paper [4]. If these filters were kept in place the calibration would have to be made by the method used with photoelectric cells (see section IV–1).

Since the galvanometer sensitivity is subject to variations, a standard sensitivity (with a means of testing it, as described in previous papers) is adopted; and all the ultraviolet solar-radiation measurements (for example, column 3 of table 4) are reduced to this sensitivity.

The radiation sensitivity of the thermopile (no. 254),[2] determined at various times during the past three years, has remained constant within the errors of observation; the average value of the scale reading being 1 cm=44.55 μw/cm^2, see column 7 of table 4.

The next procedure is to make a series of measurements of ultraviolet solar radiation by means of the barium-flint glass exclusion filter and the compensating filter of clear Corex A glass (no. 980), as described on page 731 of the previous paper [4]; and at closely the same time measurements are made of the spectral quality of the sunlight, as described in section II.

For, as already stated, a knowledge of the ultraviolet spectral-energy curve, in relative units, is necessary in order to determine the factor F, required to evaluate the fractional part of wave lengths shorter than and including 3132 A, relative to the total ultraviolet excluded by the filter.

The present experimental procedure differs from that previously employed [3, 4] in that the spectral-energy curve, in the region of 2900 to 3550 A, is determined directly at the time of the energy evaluation, by means of a titanium photoelectric cell and filters [7], as described in the preceding section, instead of using the composite and highly uncertain spectral-energy curve of various observers, as was done in the earlier work.

Corrections must be applied to the ultraviolet spectral-energy curve for absorption by the water cell, by the red-purple glass filter, Corex A (no. 986), and for the differential absorption of the pair of exclusion filters, of clear Corex A (no. 980), and Ba-flint glass (fig. 4), in the long wave lengths (at 7000 to 14000 A) transmitted by the red-purple glass filter [3]. The latter correction is obtained by direct measurement of the solar radiation transmitted through a sample of Corning Noviol A glass [4].

2. CALCULATION OF FACTOR F

In table 3 is given a typical example of the procedure in obtaining the factor F for evaluating the ultraviolet of wave lengths shorter than and including 3132 A by means of the balanced thermopile and exclusion filter method.

[2] Balanced thermopile no. 254 consists of two complete linear thermopiles of Bi–Ag, joined in opposition. Each thermopile consists of 4 couples, with individual receivers, 1.2 by 2.2 mm, mounted on a small fiber support, 25 mm in diameter, depicted in figure 1, of BS Sci. Pap. 17, 188 (1921) S413. By removing the circular part, along the common edge of the two mountings, the combination fits in a box 4.5 cm in diameter. The linear receivers facilitate adjustment of the two thermopiles to the same radiation sensitivity.

TABLE 3.—*Typical example of the calculation of the factor F for evaluating ultraviolet solar radiation of wave lengths shorter than and including 3132 A, by means of the balanced thermopile and exclusion-filter radiometer*

[The solar spectral energy is for air mass $m=1.20$ at Washington]

1	2	3	4	5	6	7	8	9	10
Wave lengths (angstroms)	Transmission; Corex A, no. 980 (2.08 mm)	Transmission; Ba-flint (3.12 mm)	Col. 2–3	Correction; fluorite window (2.40 mm)	Transmission H_2O cell (1 cm)	Transmission; Corex, no. 986 (3.10 mm)	Products of col. 4×5×6×7	Relative solar energy ($m=1.20$)	Col. 8×9. Calculated spectral energy excluded
2950	0.875	0.000	0.875	0.961	0.864	0.740	0.537	0.005	0.003
3000	.877	.000	.877	.963	.866	.768	.562	.465	.26
3050	.880	.000	.880	.966	.868	.792	.585	1.225	.72
3100	.883	.000	.883	.968	.869	.810	.602	2.30	1.38
3150	.884	.025	.859	.970	.870	.823	.597	3.51	2.10
3200	.885	.10	.785	.972	.871	.830	.551	5.75	3.17
3250	.887	.22	.667	.973	.871	.834	.471	10.4	4.90
3300	.888	.35	.538	.974	.872	.835	.381	14.0	5.34
3350	.888	.51	.378	.975	.872	.835	.268	17.5	4.69
3400	.889	.61	.279	.977	.873	.834	.1985	20.0	3.97
3450	.891	.69	.201	.978	.874	.832	.143	21.0	3.00
3500	.893	.745	.148	.979	.875	.828	.105	21.7	2.28
3550	.895	.78	.115	.980	.876	.817	.0807	24.5	1.98
3600	.896	.81	.086	.980	.877	.802	.0593	28.3	1.68
3650	.898	.83	.068	.981	.877	.783	.0458	30.7	1.41
3700	.899	.846	.053	.981	.878	.745	.0340	33.3	1.13
3750	.899	.86	.039	.982	.879	.685	.0231	34.6	.80
3800	.900	.87	.030	.982	.880	.605	.0157	36.2	.57
3850	.900	.875	.025	.983	.880	.500	.0108	40.3	.44
3900	.900	.88	.020	.983	.881	.380	.0066	48.3	.32
3950	.901	.882	.019	.983	.882	.270	.00445	57.5	.26
4000	.901	.883	.018	.983	.883	.170	.0027	68.7	.19
4050	.901	.884	.017	.983	.884	.102	.0015	71.0	.11
4100	.901	.884	.017	.984	.885	.055	.0008	73.5	.06
4150	.901	.884	.017	.984	.886	.030	.0004	76.0	.03
4200	.901	.884	.017	.984	.887	.011	.00016	79.0	.01
4250	.901	.884	.017	.984	.888	.006	.00009	82.0	.01
4300	.901	.884	.017	.984	.889	.004	.00006	85.0	.00
4350	.901	.884	.017	.985	.890	.002	.00003	87.0	.00
Total energy measured									40.82
Total energy of wave lengths less than 3132 A								4.36	

The factor $F=4.36\div40.82=0.107$, for $m=1.20$

In table 3, columns 2 and 3 give the spectral transmissions, respectively, of the balancing filter of Corex A glass (no. 980) and the exclusion filter of barium-flint glass. The difference in transmission of these two filters is given in column 4.

Column 5 gives the correction for the fluorite window, which is a fixed part of the balanced thermopile and consequently present when the thermopile is calibrated by means of a standard of radiation. The fluorite window decreases uniformly in transmission from 0.916 in the near infrared to 0.903 at 4350 A and 0.880 at 2950 A.

Column 8 is the product of columns 4, 5, 6, and 7 and is a constant of the instrument. The product of column 8 and the solar spectral energy for an air mass, $m=1.20$ (column 9), gives the solar spectral energy (column 10) excluded by the Ba-flint glass filter.

The ratio of the area (4.36) under the spectral-energy curve, of wave lengths shorter than and including 3132 A, to the total area (40,823) is $F=0.107$, for $m=1.20$, Washington.

Using the data given in column 8 of table 3 and the spectral-energy data for different air masses (table 2), additional factors are calculated. This forms the graph of reduction factors F in figure 5, for determining the amount of ultraviolet radiation of wave lengths shorter than and including 3132 A, relative to the total measured.

These factors are somewhat smaller than the values previously used [4]. This is owing to changes in the assumed spectral-energy curve, especially for large air masses, where the previous curves resulted from uncertain extrapolations in the short wave lengths.

An example of the reduction of the observed data, which procedure is relatively simple, is given in table 4. Column 3 gives the observed average galvanometer deflection on insertion of the Ba-flint glass exclusion filter and the balancing filter of clear Corex A (no. 980) glass.

TABLE 4.—*Reduction of data observed on May 18, 1935, using a balanced thermopile with filters of* Ba-*flint and Corex* A *(no. 980), in conjunction with a red-purple filter, Corex* A *(no. 986), and a water cell*

1	2	3	4	5	6	7	8
Time	Air mass	Observed galvanometer deflection	Correction for infrared effect	Differences of col. 3—4	Factor F	Thermopile-galvanometer sensitivity (1 cm)	Total ultraviolet of wave lengths shorter than and including 3132 A; col. 5×6×7
a. m.		cm	cm	cm		$\mu w/cm^2$	$\mu w/cm^2$
9:16	1.33	10.29	0.35	9.94	0.094	44.55	41.6
9:55	1.21	11.32	.23	11.10	.105	44.55	51.9
10:36	1.13	12.22	.44	11.78	.114	44.55	59.8
11:30	1.06	12.89	.62	12.27	.122	44.55	66.7
11:50	1.06	13.04	.40	12.64	.122	44.55	68.7
p. m.							
12:31	1.06	12.93	.38	12.55	.122	44.55	68.2
12:50	1.08	12.85	.55	12.30	.120	44.55	65.8
1:36	1.13	11.85	.35	11.50	.114	44.55	58.4
1:55	1.16	11.65	.57	11.08	.111	44.55	54.8
2:39	1.27	10.03	.38	9.65	.099	44.55	42.5
3:00	1.35	9.71	.40	9.31	.092	44.55	38.1

Column 4 gives the galvanometer deflection on insertion of the Ba-flint and Corex A filters (noted in the preceding paragraph) when the thermopile is covered with a filter of Noviol A glass which shuts out the ultraviolet. The transmission of this filter (82 percent) is determined as explained in the previous paper [4]. The values in column 4 are the observed galvanometer deflections divided by the transmission of this filter. This (infrared) correction is relatively small. Column 5 gives the total ultraviolet, of wave lengths shorter than about 4000 A, shut out by the Ba-flint glass filter.

Column 6 gives the factor F (read from fig. 5 for the air mass at the time of making the measurements) which serves to deduce, from the total ultraviolet measured (column 5), the amount that is of wave lengths shorter than and including 3132 A.

Column 7 is the radiation sensitivity of the thermopile, in microwatts per square centimeter ($\mu w/cm^2$), for 1-cm deflection of the galvanometer, observed by exposure to the standard of radiation [11].

Column 8, which is the product of columns 5, 6, and 7, is the total flux of ultraviolet solar radiation, in microwatts per square centi-

meter, of wave lengths shorter than and including 3132 A, incident at Washington, on May 18, 1935, which was a very clear day, with a

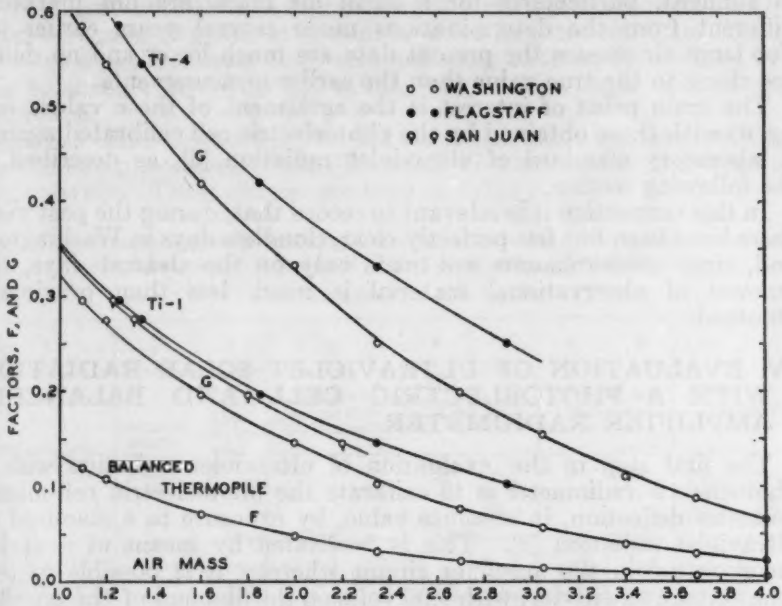

FIGURE 5.—*Reduction factors used in determining the amount of ultraviolet solar radiation of wave lengths shorter than and including 3132 A, relative to the total radiation measured when using a balanced thermopile and exclusion-filter radiometer, F, and when using a photoelectric cell, G.*

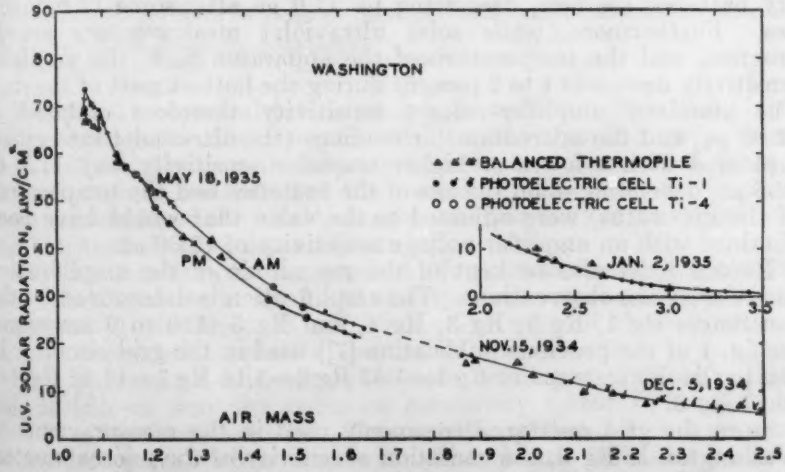

FIGURE 6.—*Measurements of ultraviolet solar-radiation intensities at Washington, showing the agreement in the results obtained by two methods of evaluation: (1) by means of a balanced thermopile and filter radiometer, calibrated against a standard of thermal radiation, and (2) by means of a photoelectric ultraviolet meter, calibrated against a standard of ultraviolet radiation.*

cloudless sky, small corona, and light west wind; but with somewhat lower intensities in the afternoon. (See fig. 6.)

Considering the changes made in the ultraviolet solar spectral-energy curve in the meantime, the present values of the ultraviolet in sunlight, particularly for a small air mass, are not markedly different from the determinations made several years earlier [4]. For large air masses the present data are much lower and no doubt are closer to the true value than the earlier measurements.

The main point of interest is the agreement of these values (see fig. 6) with those obtained by the photoelectric cell calibrated against a laboratory standard of ultraviolet radiation [8], as described in the following section.

In this connection it is relevant to record that, during the past year, there have been but few perfectly clear, cloudless days in Washington; and, since measurements are made only on the clearest days, the amount of observational material is much less than previously obtained.

IV. EVALUATION OF ULTRAVIOLET SOLAR RADIATION WITH A PHOTOELECTRIC CELL AND BALANCED-AMPLIFIER RADIOMETER

The first step in the evaluation of ultraviolet radiation with a photoelectric radiometer is to calibrate the photoelectric cell-microammeter deflection, in absolute value, by exposure to a standard of ultraviolet radiation [8]. This is facilitated by means of a device incorporated in the amplifier circuit whereby it is possible to test (the voltage sensitivity, with 1.90 volts on the filament of the type 32, screen-grid tube) the constancy of the amplification in terms of the microammeter-scale reading [7].

In the present apparatus the amplifier voltage sensitivity (the microammeter scale reading) is 12.5 microamperes (μa) when the dry batteries are new, decreasing to 11.0 μa after some 12 months' use. Furthermore, while solar ultraviolet measurements are in progress, and the temperature of the apparatus rises, the amplifier sensitivity decreases 1 to 2 percent during the hottest part of the day. The standard amplifier-voltage sensitivity therefore adopted is 12.00 μa; and the microammeter readings (the ultraviolet intensities, measured with a lower or higher amplifier sensitivity, say 11.3 to 12.5 μa, depending upon the age of the batteries and the temperature of the apparatus) were adjusted to the value that would have been obtained with an amplifier voltage sensitivity of 12.00 μa.

Record must also be kept of the magnitude of the amplification used during the observations. The amplification is determined by the resistances Rg 1, Rg 2, Rg 3, Rg 4, and Rg 5 (120 to 0 megohms; see fig. 1 of the previous publication [7]) used in the grid circuit. In this particular instrument Rg 1=1.57 Rg 2=3.16 Rg 3=11.86 Rg 4=39.87 Rg 5.

Since the grid resistance commonly used in the measurements in Washington is Rg 3, the radiation sensitivity of the microammeter-scale reading, for the two photoelectric cells Ti–1 and Ti–4, exposed to the standard of ultraviolet radiation [8], was determined for the grid resistance Rg 3 and an amplifier sensitivity of 12.00 μa.

1. CALIBRATION OF MICROAMMETER-SCALE READING

The following is an example of the determination of the radiation sensitivity of the microammeter for the grid resistance Rg 3 and an

amplifier sensitivity of 12.00 μa, when used with titanium cells Ti–1 and Ti–4, respectively.

The ultraviolet radiant flux from the Uviarc lamp (covered with a filter of Corex D glass, to eliminate wave lengths less than 2804 A) of wave lengths shorter than and including 3132 A, determined with the balanced thermopile and filters, was 81.0 μw/cm². This is used in table 5.

At the same distance from the lamp the microammeter readings for the two photoelectric cells Ti–1 and Ti–4 were 5.250 and 4.840 μa, respectively. These values are used in table 5.

TABLE 5.—*Example of the procedure followed in calibrating the balanced photoelectric amplifier, using a standard Uviarc lamp with a Corex* D *filter*

[Data obtained on December 11, 1935]

1	2	3	4	5	6	7	8	9	10	11
Wave length (angstroms)	Relative energy through Corex D	Absolute energy through Corex D	Relative response of titanium cells		Energy×relative response		μa value for each wave length		Factor P	
			Ti–1	Ti–4	Col. 3×4 Ti–1	Col. 3×5 Ti–4	Ti–1	Ti–4	Col. 6 / Col. 8 (Ti–1)	Col. 7 / Col. 9 (Ti–4)
		μw/cm²					μa	μa		
3342	13.2	6.6	0.134	0.035	0.884	0.231	0.101	0.029		
3132	106.6	53.2	.49	.39	26.068	20.748	2.989	2.569	8.72	8.08
3024	37.0	18.5	.68	.62	12.580	11.470	1.443	1.420	8.72	8.08
2967	14.0	7.0	.70	.72	4.900	5.040	.562	.624	8.72	8.08
2890	3.6	1.8	.64	.73	1.152	1.314	.132	.163	8.72	8.07
2804	1.0	.5	.43	.57	.215	.285	.025	.035		
Total	[1] 162.2	[1] 81.0			45.799	39.088	[2] 5.250	[2] 4.840	[3] 8.72	[3] 8.08

[1] Totals for 3132 A and shorter wave lengths. The value observed with balanced thermocouple and filter radiometer is 81.0 μw/cm².
[2] Observed photoelectric-microammeter readings.
[3] Mean values of the factor P: for Ti–1=8.72; Ti–4=8.08, for Rg. 3.

The relative spectral intensities of the radiation from the Uviarc lamp, through the above-mentioned filter of Corex D glass, as measured with a spectroradiometer, are given in column 2 of table 5. Column 3 gives, for each line, the intensity in absolute value derived from column 2 and the total intensity (81.0 μw/cm²) as measured with the balanced thermopile and filters [8].

Column 6, which is the product of columns 3 and 4, gives the spectral intensities in terms of the spectral response (the electron emission) of photoelectric cell Ti–1. The sum of these photoelectrically (weighted) appraised spectral values is 45.799.[3]

This produced a microammeter-scale reading of 5.25 μa. From this it follows that the radiation sensitivity factor P, when using Ti–1 is (45.799÷5.25=8.72. This sensitivity factor P is a constant of the instrument when used with photoelectric cell Ti–1, and together with the factor G (see sec. III–2), it is used to evaluate the incident radiation in absolute units (microwatts per square centimeter).

[3] This is the spectral photoelectrically weighted value in microwatts per square centimeter. If the photoelectrical response (the electrons liberated per unit incident radiation) were the same at each wave length, then the integrated value would be 81.0 μw/cm²—the same as would be used in calibrating a nonselective radiometer. The factor G restores the photoelectrically appraised solar radiation to the true value.

Similarly, column 7, which is the product of columns 3 and 5, gives the evaluation of the lamp with the photoelectric cell Ti–4, the sum of the photoelectrically (weighted) appraised spectral values being 31.310. This produced a microammeter reading of 4.84 μa. Hence, the sensitivity factor P, when using Ti–4, is (39.088÷4.840=)8.08. This factor P is a constant of the instrument when used with Ti–4, and, together with the factor G (pertaining to Ti–4), it is used to evaluate the incident radiation (the microammeter-scale reading) in absolute units.

In view of the attempt made to calibrate the microammeter-scale reading, in absolute value, by means of homogeneous radiation of wave length 2967 A [8], columns 8, 9, 10, and 11, of table 5 are included to show how the values of factor P, for the photoelectric cells Ti–1 and Ti–4, may be derived from the use of single wave lengths, even when not isolated spectroscopically. For example, columns 8 and 9 show how the observed microammeter readings, 5.25 and 4.84 μa, respectively, may be apportioned according to the relative intensities of the various spectral lines given in columns 6 and 7, respectively. The factor P, as calculated for each spectral line, is in agreement with the value derived from the integrated heterogeneous radiation, and it is believed that the same value would have been obtained with spectroscopically isolated radiation, for example, of wave length 3024 A.

The foregoing values of the radiation-sensitivity factor P=8.72 and 8.08 [weighted μw/cm^2], respectively, for the photoelectric cells Ti–1 and Ti–4 (noted in a previous paper [8]) are determinations made on a single date. The average values of four calibrations, made between January 22 and December 16, 1935, are P=9.06 and 8.20 [weighted μw/cm^2,] respectively. These values (given in column 7 of table 7) are used in evaluating the measurements (the microammeter readings) with these two photoelectric cells, given under a subsequent section.

2. CALCULATION OF FACTOR G

The ultraviolet solar-radiation intensities, I_0, for evaluation in absolute units, are obtained in connection with the measurements of the filter transmissions $I_f \div I_0$, used in determining the spectral-energy curve (sec. II). This spectral-energy distribution is necessary in order to deduce the factor G, required to calculate the fractional part (of wave lengths shorter than and including 3132 A) of the total measured by the particular photoelectric cell used.

In table 6 is given a typical example of the procedure in obtaining the factor G, for evaluating the ultraviolet of wave lengths shorter than and including 3132 A from the total measured. In this table column 2 gives the solar spectral-energy for air mass m=1.20. (See tables 2 and 3.)

Column 3 gives the spectral response of photoelectric cell Ti–1 for an equal-energy spectrum. Column 4 (the products of the data in columns 2 and 3) gives the solar spectral-energy distribution as it would be measured with the photoelectric cell Ti–1. (See curve Ti–1 in fig. 3.)

The ratio of the area under the solar spectral-energy curve, column 2, of wave lengths shorter than and including 3132 A,[4] relative to the

[4] By taking this area from column 2, instead of column 4, the correction is applied for reducing the measurements to what would be observed with a nonselective radiometer.

total area under the spectral-energy curve as observed with the photoelectric cell, column 4, gives the factor G (8.72÷31.879=0.274) for evaluating the ultraviolet radiation of short wave lengths, when measured with the titanium photoelectric cell Ti–1.

A similar calculation (column 6) gives the factor G (8.72÷16.032=0.544) for evaluating the ultraviolet solar radiation of wave lengths shorter than and including 3132 A, when measured with titanium photoelectric cell Ti–4.

TABLE 6.—*Typical example of the calculation of the factor G, for evaluating ultraviolet solar radiation of wave lengths shorter than and including 3132* A, *by means of a photoelectric radiometer, consisting of titanium photoelectric cells Ti–1 and Ti–4, and a balanced amplifier*

[The solar spectral energy is for air mass m=1.20 at Washington]

1	2	3	4	5	6
Wave lengths (angstroms)	Relative solar energy (m=1.20)	Relative spectral response (Ti–1)	Product of column 2×3	Relative spectral response (Ti–4)	Product of column 2×5
2950	0.005	0.70	0.004	0.75	0.004
2975	.20	.70	.140	.71	.142
3000	.465	.69	.321	.665	.309
3025	.817	.68	.555	.62	.507
3050	1.225	.64	.784	.56	.686
3075	1.76	.59	1.038	.50	.880
3100	2.30	.54	1.242	.45	1.035
3125	2.79	.50	1.395	.39	1.088
3150	3.51	.455	1.597	.35	1.228
3175	4.41	.41	1.808	.30	1.323
3200	5.75	.37	2.128	.25	1.438
3225	8.01	.32	2.563	.20	1.602
3250	10.4	.28	2.912	.16	1.664
3275	12.1	.24	2.904	.12	1.452
3300	14.0	.20	2.800	.085	1.190
3325	15.6	.155	2.418	.055	.858
3350	17.5	.12	2.100	.025	.437
3375	18.9	.095	1.795	.01	.189
3400	20.0	.07	1.400	----------	----------
3425	20.5	.05	1.025	----------	----------
3450	21.0	.03	.630	----------	----------
3475	21.3	.015	.320	----------	----------
Total	----------	----------	31.879	----------	16.032

Total less than 3132 A=8.72 (column 2).

The factor G=8.72÷31.879=0.274 for Ti–1; and 8.72÷16.032=0.544 for Ti–4.

Using the spectral response data of the two photoelectric cells Ti–1 and Ti–4, given in columns 3 and 5, respectively, of table 6, and the ultraviolet solar spectral energy data for different air masses (table 2), additional factors are calculated. In this manner are obtained the graphs of reduction factors G, for determining the amount of ultraviolet solar radiation of wave lengths shorter than and including 3132 A, illustrated in figure 5.

3. CALCULATION OF ULTRAVIOLET RADIANT FLUX

Supplied with the foregoing data, the evaluation of the ultraviolet solar intensities, as measured with the photoelectric cells, is relatively

simple. An example of the calculations involved is given in table 7, which is similar to table 4.

TABLE 7.—*Reduction of data observed on May 18, 1935, using titanium photo electric cells* Ti–1 *and* Ti–4 *and the balanced amplifier*

1	2	3	4	5	6	7	8
Time	Air mass	Photo-electric cell used	Observed deflection	Correction for reducing observed value to sensitivity 12.0 μa	Factor G	Radiation sensitivity of photo-electric cell amplifier radiometer (factor P)	Total ultra-violet of wave lengths shorter than 3132 A (Col. 4×5×6×7)
a. m.			μa				μw/cm²
8:16	1.65	Ti–1	13.54	0.999	0.189	9.06	23.2
8:39	1.52	Ti–4	7.62	1.003	.441	8.20	27.6
9:30	1.27	Ti–1	12.68	1.005	.253	14.55	46.9
10:12	1.17	Ti–4	12.00	1.015	.553	8.20	55.2
10:49	1.10	Ti–1	7.65	1.011	.299	28.72	66.4
11:01	1.09	Ti–4	13.36	1.012	.584	8.20	64.7
p. m.							
12:02	1.06	Ti–4	13.73	1.017	.596	8.20	68.2
12:13	1.06	Ti–1	15.89	1.012	.313	14.55	73.2
12:59	1.08	Ti–1	15.48	1.014	.306	14.55	69.9
2:07	1.18	Ti–1	13.48	1.017	.275	14.55	54.8
2:22	1.21	Ti–4	10.77	1.017	.540	8.20	48.5
3:23	1.45	Ti–4	15.17	1.023	.460	4.08	29.1
3:43	1.57	Ti–1	13.12	1.023	.200	9.06	24.3
3:51	1.63	Ti–1	12.30	1.023	.191	9.06	21.8

In column 4, table 7, are given the observed microammeter readings, after the usual corrections for errors in the scale calibration, and for the shunt used in the amplifier circuit. This shunt (about 1,100 ohms) is connected in parallel with the microammeter to introduce critical damping.

Column 5 gives the corrections of the voltage sensitivity of the amplifier, which was practically 12.00 μa at the start but decreased to 11.73 μa in the afternoon. The factor G is given in column 6 (see fig. 5 from which the data were obtained).

In column 7 is given the radiation sensitivity factor P (in microwatts per square centimeter) of the microammeter for the particular photoelectric cell used; Ti–1=9.06 for Rg 3, and Ti–4=8.20 for Rg 3, when used as calibrated.

In some cases the microammeter deflection was reduced by means of a resistance in series (see fig. 1 of the previous paper [7]). This increased the factor to 14.55 (column 7). Late in the afternoon the amplifying resistance Rg 2 was used. Since in this instrument, Rg 3÷Rg 2=2.01, the sensitivity factor P, with Ti–4, is reduced from 8.20 to 4.08.

Column 8, table 7, gives the total flux of ultraviolet solar radiation of wave lengths shorter than and including 3132 A, in microwatts per square centimeter, as observed with the two photoelectric cells Ti–1 and Ti–4 on May 18, 1935. These data are in agreement with the observations with the balanced thermocouple and filter radiometer (table 4).

The ultraviolet solar-radiation intensities as measured by these two photoelectric cells (standardized as just described), and as measured with a balanced thermopile (described in section IV–2)

are depicted in figure 6. The agreement in the observations appears to be closest for large air masses. This is perhaps to be expected, in view of the fact that the photoelectric cells magnify the intensities in the shortest wave lengths, and this would be most apparent for small air masses. In view of the impracticability of making simultaneous measurements by means of these three radiometers (two photoelectric cells and one thermopile) the agreement in the results is satisfactory. Similar variations in the observations were recorded in previous intercomparisons of methods of evaluating ultraviolet solar radiation [4].

4. SUMMARIZING COMMENTS

Probably the most outstanding result of these studies of various methods of evaluating the short-wave-length ultraviolet in sunlight is the repeated observation of a radiant flux (intensity) almost twice as large as the value calculated on the basis of early observations of the ultraviolet spectral-energy curve.

Unable to find serious errors in their work, and unable to make their results agree with the older ideas of much lower values of ultraviolet solar intensities than they were obtaining, the writers have tried various methods of attack, including the determination of the ultraviolet solar spectral energy.

All methods seem to be in agreement in indicating that the ultraviolet radiant flux, of wave lengths shorter than and including 3132 A, in the clearest midsummer midday sunlight, in Washington, is about 75 $\mu w/cm^2$. In arriving at this conclusion the following three distinctly different methods of evaluation were used:

(1) The radiometer was a single thermocouple receiver [3], covered permanently with a cell of water to absorb the infrared rays, and with a filter of Corning red-purple glass, Corex A, no. 986, to isolate the ultraviolet rays of wave lengths shorter than about 4000 A. This combination reduces the intensity to about 8 percent of the total incident upon the receiver. The apparatus was used also without this filter, thus admitting about 75 percent of the full intensity (the part transmitted by the water cell) upon the thermocouple receiver.

Two exclusion filters of Ba-flint glass were used (singly and in combination) to eliminate some of the uncertainty of the assumed ultraviolet spectral-energy distribution (of wave lengths shorter than 3132 A), which was based upon the few, highly discordant measurements available. The radiant flux of ultraviolet of wave lengths shorter than and including 3132 A was determined in absolute value, in terms of the total incident solar-radiation intensity Q, measured with a pyrheliometer [3].

(2) A balanced thermocouple and filter radiometer were used [4], either with or without the red-purple filter of Corex A glass (no. 986). A single-exclusion filter of Ba-flint glass (and a balancing filter of clear Corex A glass no. 980) were used to isolate the ultraviolet of short wave lengths.

This method requires a knowledge of the spectral-energy curve in only the ultraviolet of short wave lengths, instead of the whole spectrum as used in the preceding method. Nevertheless, a direct comparison of these two widely different methods of evaluating ultraviolet solar radiation gave concordant results [4]; the uncertainty of the

magnitude of the absolute values being ascribable to the uncertainty of the spectral-energy curve employed in reducing the observations.

(3) The third method (described in this paper) consists in evaluating the ultraviolet of short wave lengths by means of a titanium photoelectric cell calibrated, in absolute value, against a standard of ultraviolet radiation [8].

This method differs also from the two preceding methods in that the solar spectral-energy distribution, in the extreme ultraviolet, is determined directly by means of a titanium photoelectric cell and filters, at the time of the ultraviolet radiation measurements, instead of using the highly uncertain extrapolations, previously employed.

Comparative measurements of ultraviolet solar intensities were made also with the balanced thermocouple and exclusion filter of Ba-flint glass, as described in method (2), but employing the directly observed ultraviolet spectral-energy curve in reducing the data. The balanced thermocouple and filter method, therefore served as a means of comparing the three methods of evaluating the ultraviolet in sunlight.

The ultraviolet solar intensities, measured by the herein described photoelectric and thermoelectric radiometers, using the ultraviolet spectral-energy distributions as observed with the herein described photoelectric-cell and filter method, are in good agreement.

The fact that the absolute values, particularly for large air masses, are somewhat lower than previously observed [4], is ascribable to changes in the ultraviolet spectral-energy curves, which are somewhat lower in the extreme ultraviolet than previously used. There is also a possibility that the recently observed values of ultraviolet intensities may be lower, owing to a lower solar emission of ultraviolet of short wave lengths.

From a comparison of the data obtained by these three widely different methods of evaluation it appears that the average intensity of the solar ultraviolet, of wave lengths shorter than and including 3132 A, during the clearest midsummer weather, at midday, in Washington, is about 75 $\mu w/cm^2$, decreasing to about 8 $\mu w/cm^2$ at noon in midwinter.

V. ULTRAVIOLET SOLAR-RADIATION DATA

In a preceding paper various factors affecting ultraviolet solar radiation were discussed [10], but no numerical data of radiation intensities were given. In the present caption measurements are given of ultraviolet intensities at Washington, D. C., San Juan, P. R., and Flagstaff, Ariz.

1. OBSERVATIONS AT WASHINGTON, D. C

The average values of the filter transmissions of ultraviolet solar radiation, observed with the titanium photoelectric radiometer [7] in 1935, seem to be somewhat lower than similar measurements made in 1934. Furthermore, the total ultraviolet intensities appear to be somewhat higher in 1935 than observed in 1934 (see fig. 7). Both methods of appraisal seem to indicate that the stratosphere was somewhat clearer of ozone in 1935. As a consequence the ultraviolet spectral-energy curves that give calculated transmissions in agreement with the observed transmissions for 1935, should probably

be identified with air masses that are a trifle larger than mentioned in the preliminary announcements, namely, $m=1.23$, instead of $m=1.20$ [9, 10]. In the present calculations the spectral-energy curve identified with the average transmissions for air mass $m=1.20$ is used.

The ultraviolet solar intensities (of wave lengths shorter than and including 3132 A) observed at Washington in 1934 and 1935, are depicted in figure 7. It is to be noted that the recent measurements were made only on the clearest, cloudless days and, hence, there is not such a wide range of intensities, for the same air mass, as was recorded in previous papers [3, 4]. However, as already mentioned, even on the clearest days (for example, May 18, 1935, fig. 6) the ultraviolet solar radiation is subject to relatively large changes in intensity.

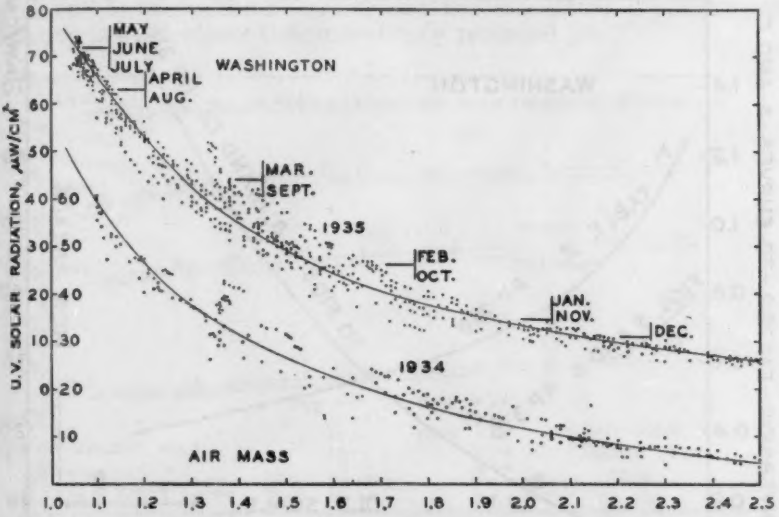

FIGURE 7.—*Measurements of ultraviolet solar-radiation intensities, of wave lengths shorter than and including 3132 A, during some of the clearest days at Washington.* (See fig. 6.)

From the data depicted in figures 6 and 7 it appears that the intensity of ultraviolet solar radiation, of wave lengths shorter than and including 3132 A, during the clearest weather, at a midlatitude sea-level station (Washington) at the noon-hour ranges from about 75 $\mu w/cm^2$ in midsummer, to 0.1 this value (about 8 $\mu w/cm^2$) in midwinter. In figure 7 the noon-hour intensities, at the middle of each month (Feb., Oct.), are indicated at the intersection of short horizontal and vertical lines.

(a) CORRECTIONS TO THE WASHINGTON OBSERVATIONS OF SEPTEMBER 1929 TO JUNE 1931

In a supplemental note to the paper describing the ultraviolet solar measurements, made with a single thermocouple receiver and a pair of barium-flint exclusion filters (p. 976 of reference [3]), attention was called to the fact that the ultraviolet intensities required a correction (an increase in value) of 10 to 20 percent.

The intensities observed in Washington from September 1929 to January 1931, can be corrected by means of factors taken from graphs A or B in figure 8, which were worked out from the average data given in figure 7 of the previous publication [3] and from figures 6 and 7 of the present paper.

From graph A it can be seen that for air mass $m=1.05$ the ultraviolet intensities must be increased to $(1.25\times56=)$ 70 $\mu w/cm^2$, and for $m=3$ they must be decreased to $(0.4\times3.8=)$ 1.5 $\mu w/cm^2$. For $m=1.25$ the values remain unchanged. Graph B, figure 8, converts the old microwatt scale to the new. For example, 56 $\mu w/cm^2=$ 70 $\mu w/cm^2$, new scale.

The foregoing survey shows that, for low air masses, the previously estimated increase (of 10 to 20 percent) in the values of the solar

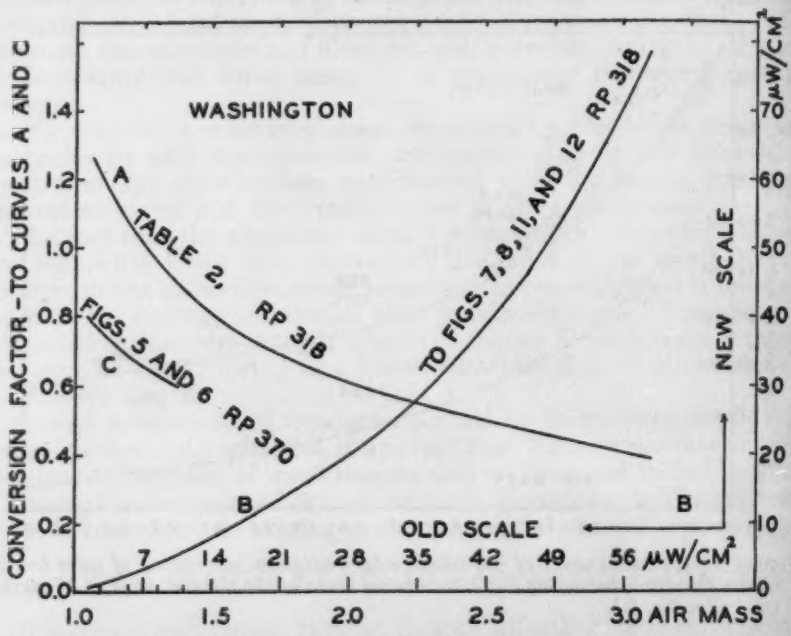
WASHINGTON
A
TABLE 2, RP 318
TO FIGS. 7, 8, 11, AND 12 RP 318
FIGS. 5 AND 6 RP 370
C
B
B
OLD SCALE
7 14 21 28 35 42 49 56 μW/CM²
NEW SCALE
μW/CM²
CONVERSION FACTOR - TO CURVES A AND C
0.0 0.2 0.4 0.6 0.8 1.0 1.2 1.4
0 10 20 30 40 50 60 70
1.0 1.5 2.0 2.5 3.0 AIR MASS

FIGURE 8.—*Factors for correcting the ultraviolet solar-radiation intensities observed at Washington in 1929 and 1931.*

Graph B relates the old microwatt scale to the new scale of intensities.

intensities was close to the herein recorded factors. But for large air masses the values must be decreased. These high intensities, for large air masses, resulted from the use of erroneous spectral-energy curves, which, in the entire absence of observational data, were uncertain extrapolations.

It is of course possible that in 1929–30 the ultraviolet intensities were lower than average, as appears to be the case for the observations made in 1934 (fig. 7); but owing to the errors of observations, and to the diverse atmospheric conditions under which these earlier measurements were made, it is impracticable to attempt a closer evaluation. They served their purpose at the time they were obtained, and with the development of more refined methods of measurement, these data are chiefly of climatological interest, showing the wide difference in intensities observed on clear and on hazy days.

The observations made in June 1931 with the balanced thermocouple and exclusion-filter radiometer, depicted in figures 5 and 6 of an earlier paper [4], may be corrected by means of graph C in figure 8. The data are comparative, obtained under similar conditions, for several types of radiometers. The same solar spectral-energy curves were used, and the good agreement in the observations, made with the various instruments, is not affected by applying the corrections taken from graph C in figure 8.

The practical significance of this correction is that in the physiological (erythemal) tests the total ultraviolet solar energy required to produce a minimum perceptible erythema is probably 10 to 15 percent lower than previously published [4, 6]. However, since, for the same person, skin sensibility is subject to a variation of 2 to 3 fold, this correction is of minor importance. If such a correction is made the agreement between the observed and the calculated erythemogenic efficiency is even closer than previously recorded [6].

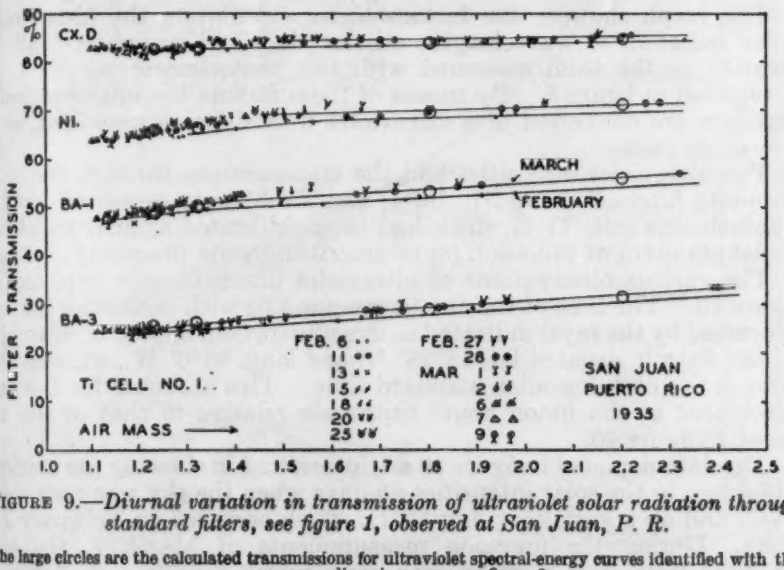

FIGURE 9.—*Diurnal variation in transmission of ultraviolet solar radiation through standard filters, see figure 1, observed at San Juan, P. R.*

The large circles are the calculated transmissions for ultraviolet spectral-energy curves identified with the corresponding air masses, see figure 2.

2. OBSERVATIONS AT SAN JUAN, P. R.

The measurements of ultraviolet solar intensities at San Juan, Puerto Rico, were made during February and the first half of March 1935.

A brief description of climatic conditions was given in a previous paper [10]. It will, therefore, suffice to state that during the forenoon the measurements were often interrupted by alternate cloudiness (rapidly moving fracto-cumulus clouds) and sunshine. By noon, and often continuing throughout the entire afternoon, the whole sky was cloudless, except over the inland mountains to the south and southwest, where the morning clouds (now cumulus and strato-cumulus) had been blown by the prevailing north and northeast winds. Judged by the filter transmissions the air seemed to be the quietest and clearest (transmissions lowest) a short time after the sun had passed the meridian (see fig. 9).

The ultraviolet transmissions through the filters for various solar altitudes are depicted in figure 9. As mentioned in the earlier paper [10] owing to an apparent increase in ozone there was a marked increase in the transmissions after February 6. The general trend of the transmission curves for San Juan, figure 9, seems somewhat different from that of similar observations in Washington, figure 2. Moreover, for the same solar altitude, the percentage transmission is somewhat lower in the tropics, as previously noted [10]. As a result the assumed spectral-energy curves that give calculated transmissions in agreement with the observations at Washington, for air masses $m=1.10$, 1.20, 1.6, 2.0, etc. (see heavy circles, fig. 2), are in good agreement with the San Juan observations for larger air masses, respectively, $m=1.23$ 1.32, 1.80, 2.20, etc. (see large-size circles, fig. 9). It is to be noted that there is no regularity in the differences in the corresponding air masses, giving the same filter transmissions, at these two stations. However, owing to the paucity of the observations, this is probably to be expected.

The graph showing the factors G, for calculating the ultraviolet solar radiation of wave lengths shorter than and including 3132 A, relative to the total measured with the photoelectric cell Ti–1, is illustrated in figure 5. By means of these factors the microammeter readings are converted into ultraviolet intensities as described on a preceding page.

The ultraviolet intensities and the transmissions through the four standard filters (Cx. D, Ni., Ba–1, and Ba–3) were measured with a photoelectric cell, Ti–1, which had been calibrated against an ultraviolet standard of radiation [8] as described in the preceding caption.

The various observations of ultraviolet intensities are depicted in figure 10. The time of the day (corresponding with certain air masses traversed by the rays) indicated in this illustration, applies to March 1.

San Juan is situated lat. 18°28′ N. and long. 66°6′ W., whereas the time is the 60th meridian standard time. This accounts for the displacement of the (noon hour) time-scale relative to that of the air mass, in figure 10.

The data depicted in figure 10 are interesting in showing the marked difference in the solar intensities on days when the sky was very clear (VC) and on a very hazy day (VH), which occurred on February 25, 1935. During the forenoon measurements of March 7, the sky changed from very clear to very hazy, which condition is shown in the short graph (between 10 and 11 a. m.) in figure 10.

The smallest air mass through which measurements were made was $m=1.10$, the ultraviolet intensity being about 85 $\mu w/cm^2$ (March 7, 1935). This may be compared with similar measurements on a very clear day in Washington, May 18, 1935 (fig. 6) when the ultraviolet intensity was 67 $\mu w/cm^2$ for $m=1.10$. This difference in intensity, amounting to 21 percent is, no doubt, to be attributed to differences in the ozone content of the stratosphere, as noted in a previous paper [10].

From the data in figure 10, it appears that for an air mass $m=1.00$ to 1.01, which occurs during the noon hour for about 4 months in San Juan [10], the ultraviolet intensity, of wave lengths shorter than and including 3132 A, is 95 to 98 $\mu w/cm^2$, or about 20 percent higher than is ever attained in Washington (u.v. $Q=75$ $\mu w/cm^2$ for $m=1.05$). In this connection reference is made to a discussion of this subject in an earlier paper [10].

In concluding the discussion of the foregoing measurements, it is to be noted that the calculated and the observed filter transmissions for the four filters (fig. 9) do not coincide so nicely as obtains in the

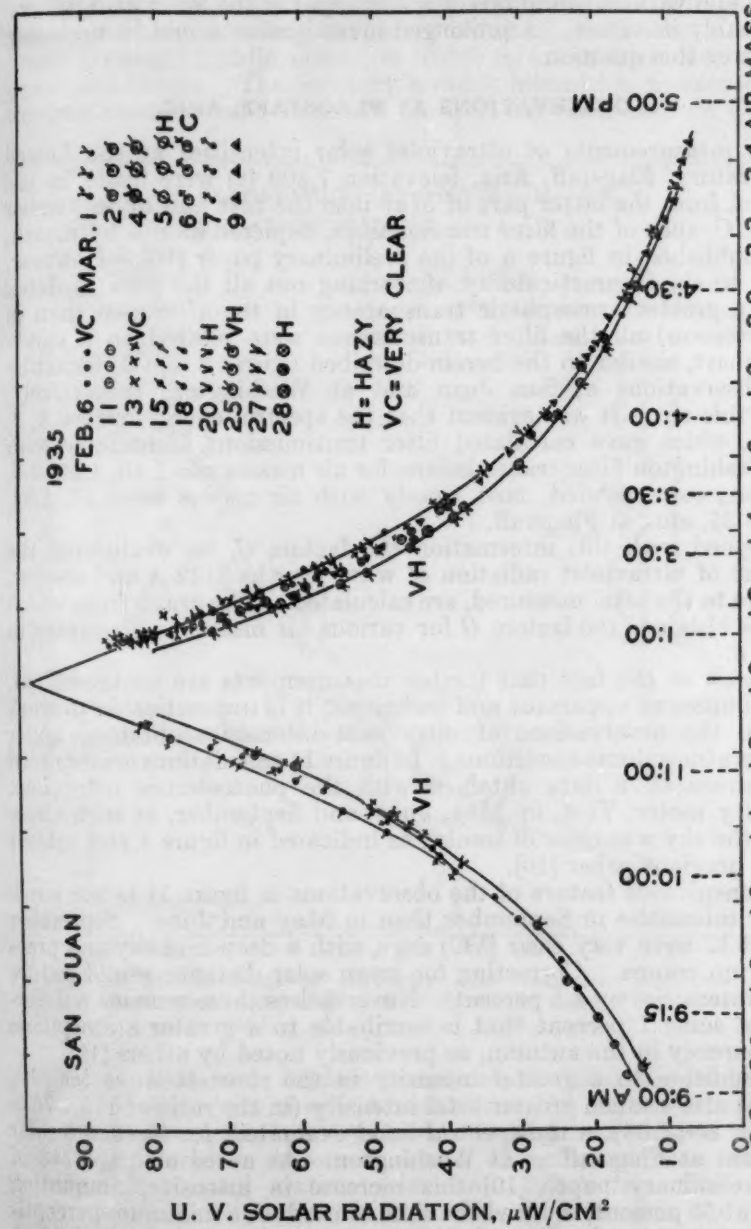

FIGURE 10.—*Measurements of ultraviolet solar-radiation intensities of wave lengths shorter than and including 3132 A at San Juan, P. R. in 1936.*

Washington observations (fig. 2). With rapidly changing local atmospheric conditions (cloudy a. m., clear p. m.) and with a lower ozone content in the stratosphere, it is probable that the ultraviolet

spectral-energy curves, for different air masses traversed by the rays, are slightly different from the ones used in the calculations. That is to say, the assumption of reciprocity of density and length of air path traversed, for a heterogeneous combination of ozone in the stratosphere and various conditions of water vapor in the lower atmosphere, is probably incorrect. A prolonged investigation would be necessary to answer this question.

3. OBSERVATIONS AT FLAGSTAFF, ARIZ.

The measurements of ultraviolet solar intensities at the Lowell Observatory, Flagstaff, Ariz. (elevation 7,300 ft) were made in the interval from the latter part of May into the first half of September 1934. Graphs of the filter transmissions, depicted month by month, were published in figure 5 of the preliminary paper [10]. However, owing to the impracticability of working out all the data in detail (with a greater atmospheric transparency in the afternoon than in the forenoon) all the filter transmissions were plotted on a small-scale chart, similar to the herein-described figures 9 and 2, depicting the observations at San Juan and at Washington, respectively. From this chart it was evident that the spectral-energy curves 1, 2, 3, etc., which gave calculated filter transmissions identifiable with the Washington filter transmissions for air masses $m=1.10$, 1.20, 1.6, 2.9, etc., corresponded most closely with air masses $m=1.25$, 1.35, 1.85, 2.35, etc., at Flagstaff.

Supplied with this information the factors G, for evaluating the amount of ultraviolet radiation of wave lengths 3132 A and shorter, relative to the total measured, are calculated. The graph from which may be obtained the factors G for various air masses is illustrated in figure 5.

In view of the fact that further measurements are contemplated, using improved apparatus and technique, it is impracticable to work out all the observations of ultraviolet intensities obtained under various atmospheric conditions. In figure 11 calculations are depicted of representative data obtained with the photoelectric ultraviolet intensity meter, Ti–4, in May, June, and September, at such times when the sky was clear of smoke, as indicated in figure 4 and table 1 of the previous paper [10].

A conspicuous feature of the observations in figure 11 is the much higher intensities in September than in May and June. September 11 and 12 were very clear (VC) days, with a deep-blue sky and practically no corona. Correcting for mean solar distance would reduce these intensities by 4.5 percent. Nevertheless there remains a difference of some 7 percent that is ascribable to a greater atmospheric transparency in the autumn, as previously noted by others [10].

In addition to a greater intensity in the shortest wave lengths, there is also a much greater total intensity (in the ratio of $115 \div 75 = 1.53$ for $m=1.05$) in the spectral band evaluated, for the same solar elevation at Flagstaff as at Washington. As noted on page 143 of the preliminary paper [10] this increase in intensity, amounting to about 50 percent, reduced the time to produce a minimum perceptible erythema to about one-half (9 to 10 minutes) that required at Washington. This lack of correlation of energy and time to produce a minimum perceptible erythema, at these two stations, is owing to

a change in spectral quality of the ultraviolet at the higher elevation, where there is a rapid increase in spectral intensity in the region of 2900 to 2950 A, which is in the region of the maximum of the spectral erythemic reaction at about 2967 A.

On page 146 of the preliminary paper [10] attention was called to two sets of measurements that were obtained on the San Francisco Peaks (Fremont Saddle, elevation 10,500 ft) under fairly clear atmospheric conditions. The total ultraviolet intensities, measured with the two titanium cells Ti–1 and Ti–4, at the noon hour on June 12

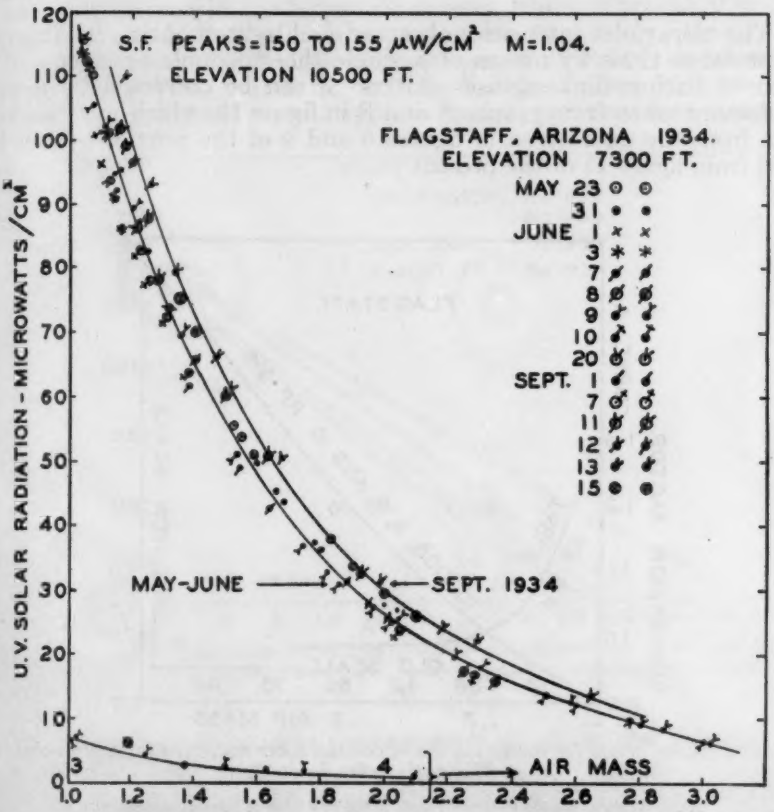

FIGURE 11.—*Measurements of ultraviolet solar radiation intensities of wave lengths shorter than and including 3132* A, *during some of the clearest days at Flagstaff, Ariz., in 1934.*

and July 5, 1934, were in close agreement, the intensity values being about 155 $\mu w/cm^2$ for $m=1.04$ and about 150 $\mu w/cm^2$ for $m=1.08$. These values are about $(155 \div 115 = 1.35)$ 35 percent higher than the maximum intensities observed during the clearest noon hours at Lowell Observatory station (elevation 7,300 ft). The smaller difference (12 to 15 percent) in intensities, mentioned in the preliminary report [10], is owing to the fact that no allowance was made for a difference in the factors G, for these two stations.

No controlled erythema tests were obtained. Such a test, undertaken on June 12, was interrupted by smoke from a forest fire on Crater Hill, some 6 miles to the west of the observatory. However, from the sunburn resulting from exposure of the face and hands, at this high altitude, it may be expected that a minimum perceptible erythema will be produced on the untanned skin in a proportionately shorter time (6 to 7 minutes) than that observed (9 to 10 minutes) at the Flagstaff station.

(a) CORRECTIONS TO THE FLAGSTAFF OBSERVATIONS OF AUGUST-SEPTEMBER 1929

The ultraviolet intensities observed at Flagstaff, Ariz., in August-September 1929, by means of a single thermocouple receiver and a pair of barium-flint exclusion filters [3] can be corrected by means of factors taken from graphs A and B in figure 12, which were worked out from the data given in figures 6 and 9 of the previous paper [3] and from figure 11 of the present paper.

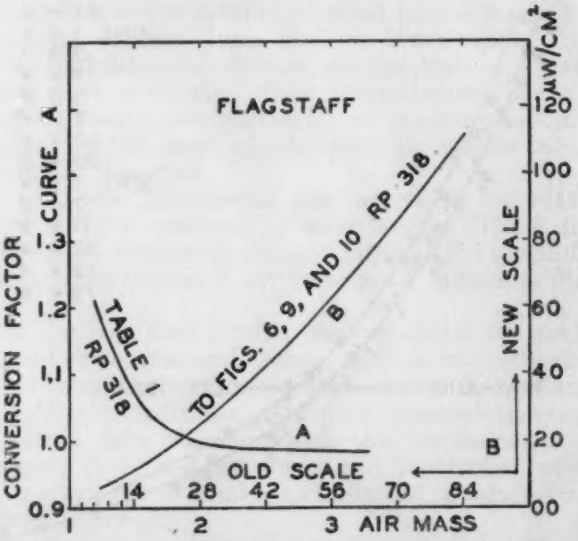

FIGURE 12.—*Factors for correcting the ultraviolet solar radiation intensities observed at Flagstaff, Ariz., in 1929.*

Graph B relates the old microwatt scale to the new scale of intensities, see figure 8.

From figure 12 it can be seen that for air masses $m=2$ to $m=3$, the earlier data remain practically unchanged; but for smaller air masses there is a gradual increase in the numerical values 42 μw/cm^2 (old)=42 μw/cm^2 (new scale); 56 μw/cm^2 (old)=63 μw/cm^2 (new scale); 70 μw/cm^2 (old)=86 μw/cm^2 (new scale).

In concluding the presentation of the data on ultraviolet solar-radiation intensities (of wave lengths shorter than and including 3132 A) at these three stations (Washington, San Juan, and Flagstaff), it is of interest to obtain an approximate estimate of the intensity outside of the terrestrial atmosphere.

Following the procedure commonly employed in meteorology, this estimate is obtained by plotting the observed intensities on a loga-

rithmic scale (ordinates in fig. 13) against the corresponding air masses, as abscissas, and extrapolating the graphs to zero air mass.

Figure 13 is a small-scale reproduction of the graphical determination of the extraterrestrial ultraviolet solar intensity by this method. Graph A represents the average curve drawn through the observations, at Washington, taken from figure 7 for the year 1934. Similarly graph B depicts the data observed in 1935. These curves, when extrapolated to zero air mass, intersect at the same point (at 560 $\mu w/cm^2$), as they should if the atmospheric (ozone) absorption which was higher in 1934 is eliminated. It is to be noted that all these graphs are slightly curved in the larger air masses, which is probably to be expected, since the radiation is not homogeneous.

Graph C represents the intensities observed at San Juan when it was very clear (VC). It is taken from the upper curve in figure 10, and on the logarithmic scale it appears to be approximately a straight

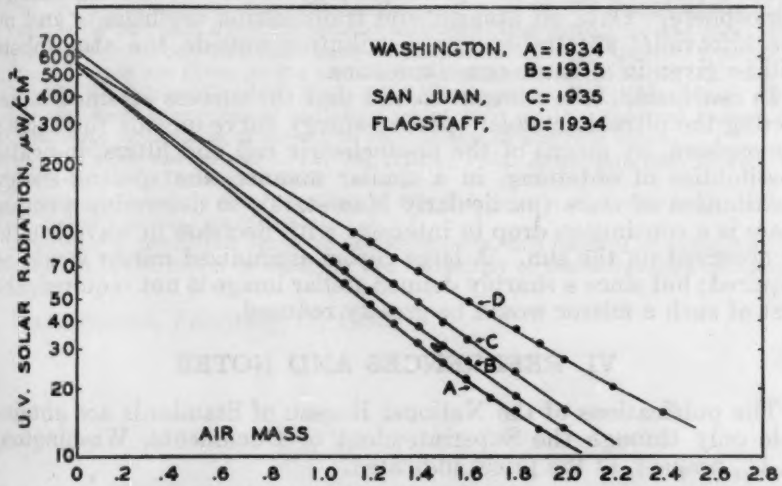

FIGURE 13.—*Ultraviolet solar intensities plotted on a logarithmic scale and extrapolated to zero air mass in order to obtain an estimate of the intensity outside the earth's atmosphere.*

line. When extrapolated to zero air mass an ultraviolet intensity of 650 $\mu w/cm^2$ is indicated.

Graph D represents the intensities observed at Flagstaff in 1934. It is the average curve taken from figure 11, and on the logarithmic scale it appears to be slightly curved for large air masses. When extrapolated to zero air mass an ultraviolet intensity of 590 $\mu w/cm^2$ is indicated.

The average value of the ultraviolet solar intensity for zero air mass, determined by extrapolation of these four graphs, is 590 $\mu w/cm^2$. The close agreement in the extrapolated values is probably to be considered fortuitous [13].

It is to be noted that this estimated value of about 600 $\mu w/cm^2$ represents the intensity of the radiation comprised in the spectral band of wave lengths shorter than 3132 A, and does not include appreciable radiant flux, of wave lengths shorter than 2900 A, that may be present outside the terrestrial atmosphere. This is a five- to eight fold

increase as compared with a 20 to 30 percent increase in the total intensity of all wave lengths.

Whether there is appreciable radiation of wave lengths shorter than about 2900 A outside the earth's atmosphere is an interesting question. In a recent communication Pettit [12] calls attention to his observations which show that, even after presumably completely eliminating the absorption by ozone, there is an abrupt and continuous drop in the solar spectral-energy curve, of wave lengths shorter than 3000 A, outside the earth's atmosphere—a well-known phenomenon for all known terrestrial sources, and probably to be expected of the complex radiation emanating from different depths of the solar surface.

The spectral intensities of the above-described energy curves for different air masses, when extrapolated to zero air mass, show a continuous drop with decrease in wave length, in good agreement with Pettit's [12] average solar spectral-energy curve outside the earth's atmosphere. Data on atmospheric transmission coefficients and on the ultraviolet spectral-energy distribution outside the atmosphere will be given in a future communication.

In conclusion, it is relevant to add that the success attained in depicting the ultraviolet solar spectral-energy curve outside the earth's atmosphere, by means of the photoelectric cell and filters, indicates possibilities of obtaining, in a similar manner, the spectral-energy distribution of stars (particularly blue stars), to determine whether there is a continuous drop in intensity with decrease in wave length, as observed on the sun. A large chrom-aluminized mirror would be required; but since a sharply defined stellar image is not required, the cost of such a mirror would be greatly reduced.

VI. REFERENCES AND NOTES

The publications of the National Bureau of Standards are obtainable only through the Superintendent of Documents, Washington, D. C., prepaid, at the prices indicated.

[1] W. W. Coblentz, Trans. Illum. Eng. Soc. **23,** 287 (1928).

[2] W. W. Coblentz and R. Stair, BS J. Research **3,** 629 (1929) RP113 (15¢). Data on spectral characteristics of light sources and window material. From four methods of attack the conclusion arrived at (page 642) was that, at the most, less than 0.3 percent of the total incident solar radiation (and more likely only 0.1 of this value) at sea-level stations has a therapeutic effect in healing rickets.

[3] W. W. Coblentz and R. Stair, BS J. Research **6,** 951 (1931) RP318 (10¢). A description is given of quantitative measurements (at Washington, D. C. and Flagstaff, Ariz.) of extreme ultraviolet solar radiation, of wave lengths less than 3130 A, using a nonselective thermocouple receiver and two filters of barium-flint glass. A preliminary statement is given of the performance of a balanced ("differential") thermocouple and filter method.

[4] W. W. Coblentz, R. Stair, and J. M. Hogue, BS J. Research **7,** 723 (1931) RP370 (10¢). A complete description is given of the construction, calibration, and operation of a balanced ("differential") thermocouple and exclusion-filter radiometer. A comparison of solar ultraviolet intensities, measured with the balanced thermocouple and filter method and with the previously used single thermocouple and exclusion filter; also physiological (erythemal) tests using measured intensities of ultraviolet of the sun and of artificial sources; and tests of the integration of ultraviolet radiation by spectroradiometric and by filter methods.

[5] Report of the Illum. Eng. Soc. Subcommittee on Measurement and Evaluation of Ultraviolet Radiation, Trans. Illum. Eng. Soc. **28,** 684 (1933).

[6] W. W. Coblentz, R. Stair, and J. M. Hogue, BS J. Research **8,** 759 (1932) RP450 (10¢).

Description of the evaluation of ultraviolet in different commercial sources by means of a balanced thermocouple and filter radiometer used as a dosage intensity meter. On page 769 are enumerated the advantages in using homogeneous radiation of wave length 2967 A as a standard source for correlating the physiologic (erythemal) reaction with the radiation stimulus.

[7] W. W. Coblentz and R. Stair, BS J. Research, **12,** 231 (1934) RP647 (5¢).
Description of the construction and performance of a portable ultraviolet intensity meter consisting of a photoelectric cell of titanium, a balanced amplifier circuit, and a microammeter

[8] W. W. Coblentz and R. Stair, J. Research NBS **16,** 83 (1936) RP858 (5¢).
The advantages and disadvantages of sources emitting either a continuous or a discontinuous spectrum are considered in connection with the use of such lamps as a standard of ultraviolet radiation. A description is given of a commercial vertical quartz-mercury arc for use as a standard source of ultraviolet for calibrating photoelectric ultraviolet intensity meters, in absolute units.

[9] W. W. Coblentz, Puerto Rico J. Public Health and Tropical Medicine **11,** 1 (1935).
The problem of evaluating ultraviolet radiation for use in medicine is discussed. An outline is given of the procedure in determining the solar ultraviolet spectral-energy distribution by means of a photoelectric cell and filters [7].

[10] W. W. Coblentz and R. Stair, J. Research NBS **15,** 123 (1935) RP816 (5¢).
Various factors that affect ultraviolet solar-radiation intensities are discussed. The photoelectric cell and filter method of determining the spectral quality is outlined. Data are given on the variation of ozone with altitude and latitude.

[11] W. W. Coblentz and R. Stair, BS J. Research **11,** 79 (1933) RP578 (5¢).
Verification of standards of radiation maintained by the National Bureau of Standards for calibrating nonselective radiometers in absolute value.

[12] E. Pettit, Astrophys. J. **75,** 185 (1932); Publ. Astronom. Soc. of the Pacific, 47, No. 280, December 1935.
A spectroradiometric determination of the distribution of energy in the ultraviolet end of the solar spectrum.

[13] Using a prolonged series of measurements, this method of reducing the data should prove useful in studying the variability of the ultraviolet radiation of the sun.

WASHINGTON, February 12, 1936.

U. S. DEPARTMENT OF COMMERCE NATIONAL BUREAU OF STANDARD

RESEARCH PAPER RP878

Part of Journal of Research of the National Bureau of Standards, Volume 16, April 1936

SIMPLIFIED APPARATUS FOR TECHNICAL SUGAR COLORIMETRY [1]

By Joseph F. Brewster

ABSTRACT

The apparatus consists of a Dubosecq colorimeter and an incandescent light source with suitable spectral filters and glass photometric standards for the measurement of absorbancy in sugar solutions. The absorbancy of all except very pale solutions, may be determined at 560 mμ by using a special yellow-green filter. Solutions of high-grade sugar products having little color are treated as a special case, and using a blue filter, measurements are made at 460 mμ. The results obtainable are satisfactory for technical purposes.

CONTENTS

		Page
I.	Introduction	349
II.	Spectrophotometric terminology	350
III.	Colorimeters	351
IV.	Spectral filters	352
	1. For 560 millimicrons	352
	2. For 460 millimicrons	352
V.	Glass photometric standards	353
VI.	Method of observation and calculation of results	355
VII.	Comparative results	356
VIII.	Calibration of working standards	358

I. INTRODUCTION

The value of methods of sugar colorimetry based upon spectrophotometry or the measurement of light absorbed by sugar solutions at definite wave lengths is well recognized. The general adoption of such methods for routine factory purposes has been delayed chiefly because adequate instruments, of which there are several, are considered too complicated, too delicate, or too expensive. It is possible, however, to obtain satisfactory results by means of abridged methods and with inexpensive apparatus.

What is perhaps the first attempt at simplification resulted in the apparatus devised by Bates and associates,[2] which consists of a Stammer colorimeter with a rotating sectored disk of known transmission fitted under the open tube to serve as a photometer. With mercury-arc illumination, and with appropriate spectral filters at the eyepiece, the transmittancy of sugar solutions is measured at wave

[1] Parts of this article were read before the Division of Sugar Chemistry at various meetings of the American Chemcial Society, as follows:
Glass Standards and the Dubosecq Instrument in Sugar Colorimetry, Buffalo, N. Y., August 1931.
A Color Filter for Visual Sugar Colorimetry, Washington, D. C., March 1933.

[2] (Abstract), Int. Sugar J. 22, 654 (1920).

lengths 435.8, 546.1, and 578 mμ. The same kind of photometric device and illumination is adaptable to other types of the Duboscq colorimeter. By interpolation between data obtained at 546.1 and 578 mμ, Peters and Phelps [3] later showed that the specific absorptive index at 560 mμ may be calculated with sufficient accuracy for technical purposes, $-\log \mathbf{t}$ at 560 mμ having been shown to be a nearly correct estimate of color in sugar products.[4]

A further step in simplification, as described in the present paper, results from the use of a filter that isolates a narrow spectral band at 560 mμ, permitting the direct determination of $-\log \mathbf{t}$ at this wave length with ordinary incandescent tungsten illumination. Another filter with optical centroid at 460 mμ is recommended for nearly colorless solutions. These filters may be employed with any suitable photometric device such as the Hess-Ives, the Pulfrich, the Martens photometer, or the modified Stammer referred to above.

With the idea of employing readily available and well known equipment in the present case, a standard type of Duboscq colorimeter was used as the comparator. Glass plates calibrated for transmission at one or both wave lengths served as photometric standards.

II. SPECTROPHOTOMETRIC TERMINOLOGY

Spectrophotometric terminology as relating to sugar solutions was published by Peters and Phelps [5] in complete form under the title Color Nomenclature in the Sugar Industry, in which the recommendations of the Committee on Spectrophotometry of the Optical Society of America [6] were strictly followed insofar as they adequately covered the ground. Since these publications are no longer readily available it is considered necessary to repeat here such definitions as apply directly to the methods to be described.

In the case of light, homogeneous with respect to wave length, incident upon a transparent, nondiffusing solid with plane parallel faces such as a polished glass plate

T = transmission, the fraction of light that gets through and is not reflected at the surfaces nor absorbed by the solid. T may also refer to the transmission of a cell with parallel glass end plates.

In the case of solutions contained in cells with parallel glass end-plates

$T_{sol.}$ = the transmission of a given cell containing solution.

$T_{sov.}$ = the transmission of the same or another similar cell containing the solvent.

$\mathbf{T} = \frac{T_{sol.}}{T_{sov.}}$ = transmittancy, the transmission after correction for reflection at the surfaces and the absorption, if any, by the solvent.

$-\log \mathbf{T}$ = absorbancy (of solutions).

$\mathbf{t}$ = specific transmissivity = transmittancy reduced to unit conditions regarding thickness and concentration.

b = thickness (in centimeters) of absorbing medium.

c = concentration (gram sugar dry substance per 1 ml solution).

[3] BS J. Research **2**, 335 (1929) RP38.
[4] Tech. Pap. BS **21**, 267 (1927) T338.
[5] Tech. Pap. BS **21**, 261 (1927) T338.
[6] J. Opt. Soc. Am. and Rev. Sci. Instr. **10**, 160-241 (1925).

$\mathbf{t}=\sqrt[bc]{\mathbf{T}}$, or $-\log \mathbf{t}=\frac{1}{bc}(-\log \mathbf{T})$=Lambert-Beer law to which sugar solutions and caramel conform.

$-\log \mathbf{t}$, the specific absorptive index, is the absorptive index of a solution reduced to unit conditions regarding thickness and concentration. It is a measure of the coloring or light-absorbing power of the unknown amount of coloring matter associated with 1 g of sugar dry substance.

λ=wave length.

$m\mu$=millimicron=meter$\times 10^{-9}$, a measure of λ.

III. COLORIMETERS

A Bausch and Lomb Duboscq colorimeter with 10 cm-scales, as illustrated in figure 1, permits the determination of transmittancies ranging from less than 10 to above 90 percent. In some colorimeters, depending upon their construction, the half-fields do not match, as they should, when scale readings are too widely separated. In the present instrument, with distilled water in the cups, it was found that the half-fields match at a difference in scale reading as great as 8.5 cm, affording a sufficient range. The illuminating mirror is glass, with the under surface silvered and the outer surface ground. The inclined eyepiece, as already offered by some manufacturers, is a feature to be recommended. In this case the inclination was accomplished by introducing a 60° prism in a suitable housing in the telescope tube. To support the glass photometric standard, a brass shelf, with heavy bracket, is rigidly fastened with two screws to the vertical column, leaving a clearance of 1 cm between the shelf and the lowest position of the cup stages. The two orifices of the shelf centered below the cups are 25 mm in diameter. A plate carrier with a 25-mm orifice, over which the standard is placed, slides between guides on the shelf. A stop at the center of the shelf engages in a slot in the carrier and serves to center the orifices under either stage when the carrier is moved from side to side.

Some Duboscq instruments have an open space between the top of the plungers and the rhombs in which the standard may be inserted and the shelf is then unnecessary. Whatever the construction of the instrument, provision is to be made for easy change of standards from one side to the other.

A Klett colorimeter with short cells allowing a useful range of about 5 cm has given good results. Satisfactory results were not obtained when the long cells were used. A pair of extra stages mounted below the cells supported the standards.

IV. SPECTRAL FILTERS

1. FOR 560 MILLIMICRONS

Two filters have been devised that are suitable for the measurement of absorbancy in sugar solutions at 560 mμ, with incandescent tungsten illumination, one by the writer [7] and a later one by Gibson.[8] The composition [9] of these filters is as follows:

Brewster		Gibson	
Material	Thickness	Designation of glass	Thickness
			mm
Wratten filter 21	1 layer	Corning 351	4.55
Wratten filter 61	1 layer	Corning didymium	5.82
Corning didymium glass	6.5 mm	Jena VG–3	1.99
Colorless glass	1 to 2 mm	Jena BG–18	1.94

The components are sealed together with canada balsam and the edges may be bound with black tape. The colorless glass in the Brewster filter serves to protect the gelatin film. Transmission curves of these filters are shown in figure 2. For the writer's filter the spectral centroid of the transmitted light for incandescent tungsten illumination at 2,848° K is 558.8 mμ. There is slight leakage of light between 600 and 630 mμ and between 680 and 700 mμ, but this has little or no effect upon the results. The dyed gelatin components are stable for at least one year and are easily renewed.

For Gibson's filter the spectral centroid of the transmitted light for tungsten at 2,848° K is given as 560.0 mμ. Advantages of this filter over the older one are: (1) optical permanence, (2) the location of the spectral centroid exactly at 560.0 mμ, (3) the higher transmission at 560 mμ, and (4) the higher ratio of height to width of its transmission curve. Before publication of his description, Dr. Gibson kindly placed his filter at the writer's disposal for trial in sugar colorimetry, some results of which are included in a later section. Either filter is capable of yielding satisfactory results in sugar colorimetry, and for convenience may be of such size as to fit in the eyepiece tube of the colorimeter and rest upon a diaphragm or the lower lens mounting.

2. FOR 460 MILLIMICRONS

Highly desirable as it may be that all measurements be made at 560 mμ, this is a matter of considerable difficulty in the case of very pale solutions, such as those of highest-grade refinery products, where special arrangement must be made for liquid columns long enough to provide measurable absorption, regardless of what type of instrument is being used. At the shorter wave lengths in the blue and violet where absorption caused by yellowish coloring matter is greater,

[7] J. F. Brewster, (Abstract), Facts About Sugar, **28**, 228 (1933).
[8] K. S. Gibson, J. Research NBS **14**, 545 (1935) RP785; J. Opt Soc. Am. **25**, 131 (1935).
[9] The materials composing these filters are described in advertising booklets as follows:
Wratten filters, Eastman Kodak Co., Rochester, N. Y.
Glass color filters, Corning Glass Works, Corning, N. Y.
Jena Colored Optical Filter Glasses For Scientific and Technical Purposes, obtainable from Fish-Schurman, Inc., 230 East Forty-fifth Street, New York, N. Y.

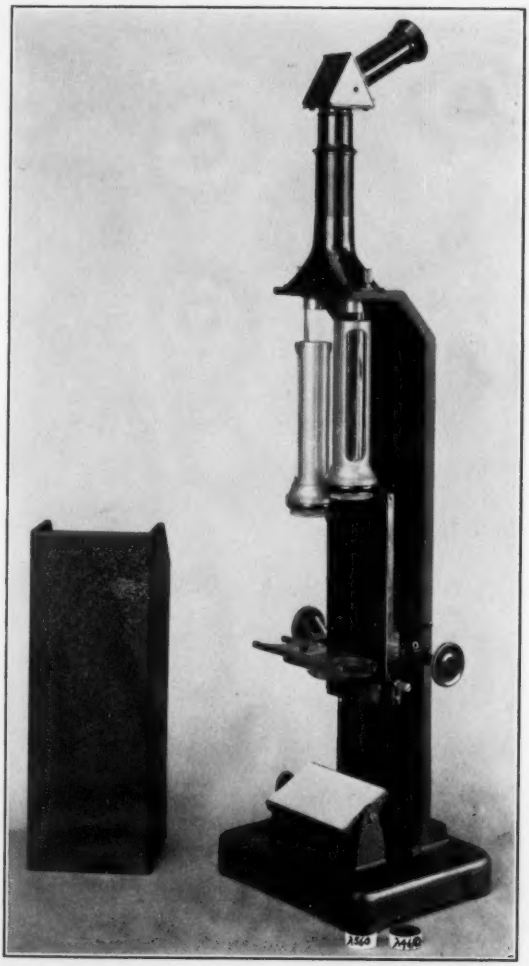

FIGURE 1.—*Duboscq colorimeter for measurement of sugar color, showing inclined eyepiece, mounting of the glass standard, and spectral filters.*

UNIV. OF MICH.

shorter columns may be used (see uppermost curve, fig. 3). In consideration of the relative visibility of light and ease of matching field intensities (see curve V, fig. 2) it is preferable to use the longest wave length in this region compatible with sufficient absorption by the sample. The filter chosen for this purpose consists of a single blue glass designated as Jena BG–12.[10] The thickness is 3.42 mm. The spectral centroid of the band transmitted by this filter for incandescent tungsten at 2,848° K is 459.9 mμ, and the transmission at 460 mμ is 0.294. No advantages accrued by reducing the width of the transmitted band by various means. The transmission curve of this filter is shown in figure 2. The small dotted curve at the bottom of the chart gives a comparison of the visibility of the energy transmitted by this filter as against that by the two 560 mμ filters.

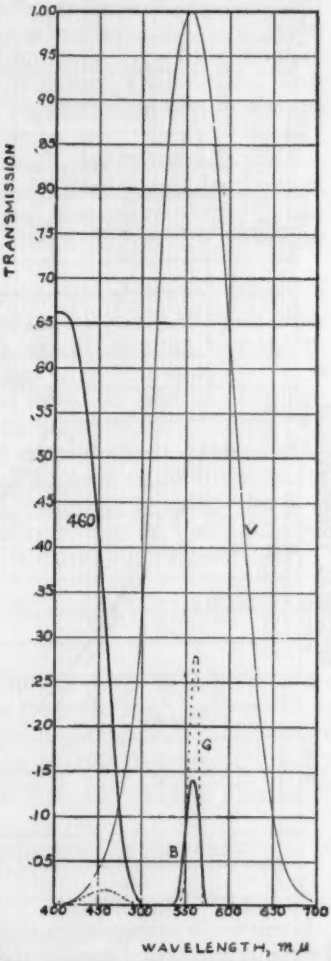

FIGURE 2.—*Transmission of spectral filters.*

460=Jena BG-12, 3.42 mm thick; G=Gibson filter for 560 mμ; B=Brewster filter for 560 mμ; V=relative visibility of radiant energy.

Although colored glasses may not be precisely reproducible in spectral transmission from one melt to another, it is believed that any differences will be too small to cause a serious shift of the spectral centroid, particularly in the case of the Jena BG–12 glass, if the deviation from the specified thickness is not greater than 0.02 or 0.03 mm.

V. GLASS PHOTOMETRIC STANDARDS

For the colorimetry of darker sugar products, polished plates of carbon amber glass, calibrated in terms of transmission at 560 mμ, are used as comparison standards. This glass is produced in various shades ranging from dark amber to pale yellow.[11] By reference to figure 3, spectral-transmission curves (percent T at λ) of some of these glasses may be compared with similar curves for caramel preparations, the caramel in either case being so diluted that in a 1-cm layer at 560 mμ, $\mathbf{T}$ is approximately equal to T of the respective glass. The similarity in the slope of each pair of curves in the spectral region 440 mμ to about 600 mμ, which includes the bands inclosed by the filters, is to be noted. Due to this similarity, it is possible to obtain a good chromaticity match in this region between glass and a sugar solution with filters that include rather wide spectral bands. From 600 to 700

[10] See footnote 9.

[11] The writer desires to express his thanks to Dr. E. D. Tillyer, American Optical Co., Southbridge, Mass., for supplying specimens of amber glass and for information concerning them.

mμ the curves diverge, the caramel having an increasingly higher transmission than the glass for the orange and red, so that when compared under ordinary conditions of incandescent illumination, the sugar color appears more red than the glass and an accurate match of

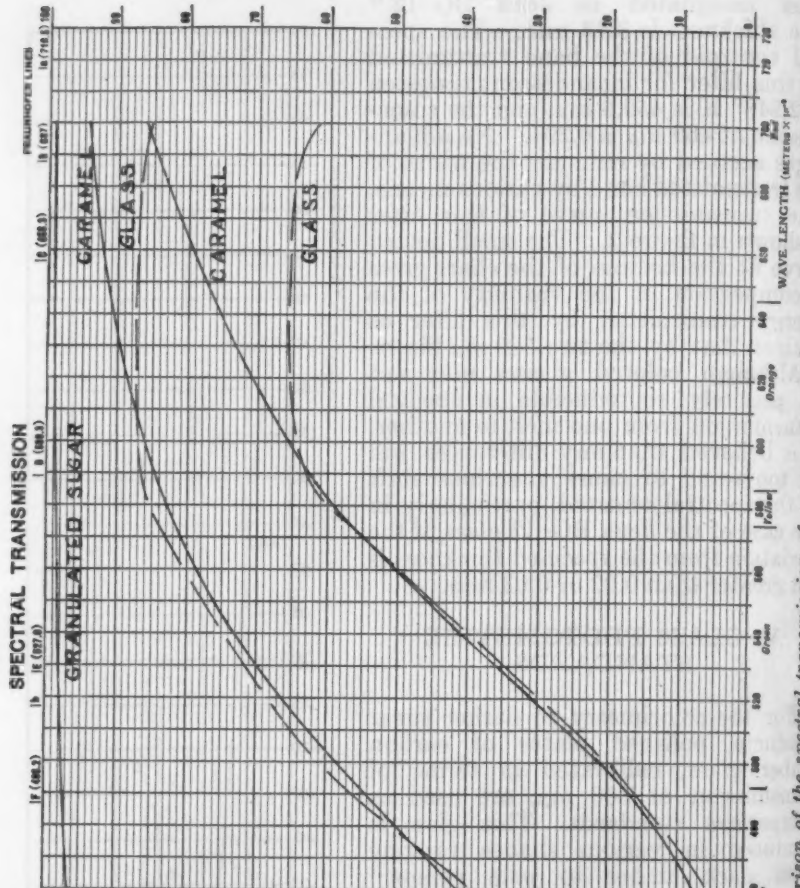

FIGURE 3.—*Comparison of the spectral transmission of aqueous caramel preparations and amber glasses.*

intensities is difficult. This is the familiar defect of the Stammer method. However, since the spectral centroid of light transmitted by a combination of sugar solutions and a filter of broad spectral range shifts with change in concentration of sugar coloring matter, the use of filters transmitting only a narrow spectral band is imperative for accurate results.

Standard plates in three shades of amber glass are a sufficient number for the colorimetry of products ranging from the darkest that may be read, up to and including off-color granulated sugar. It is recommended that the transmission of these plates, controlled by shade and thickness of glass, be close to 0.50, 0.70, and 0.80, respectively. Since the plates are to be calibrated independently, it is unnecessary in purchasing to specify a transmission tolerance closer to these values than ± 0.02, a condition easily attained in their manufacture. The glass is customarily supplied in 2-inch polished squares, free from imperfections and with satisfactory parallelism of faces. Other sizes and shapes may be specified to conform to the construction of the instrument.

Stammer plates, unless previously calibrated, are worthless for the present scheme, or any other scheme of sugar colorimetry, because of possible variation in transmission among them, not only at 560 mμ, but over the entire visible spectrum, as has been shown by Spengler and Landt.[12]

For the colorimetry of very pale solutions, a calibrated plate of colorless optical glass may be used. The optical density of such glass is due principally to reflection at the surfaces rather than to absorption, and, in good specimens, the transmission at 560 and 460 mμ is the same within the limits of observational error, so that the calibration value as determined for 560 mμ may be adopted for 460 mμ.

For high accuracy, glass plates to be employed as photometric standards should be sent to the National Bureau of Standards for calibration. With one such standard so calibrated, however, it is possible, as described later, to calibrate others that are suitable for working standards in cases where extreme accuracy is unnecessary.

VI. METHOD OF OBSERVATION AND CALCULATION OF RESULTS

Since Beer's law does not hold for turbid sugar solutions these are to be rendered transparent by filtration through asbestos, as described elsewhere.[13] The Brix of the solution, which should be 60.0 or higher, is determined preferably by a refractometer, and the dry substance, c, in grams per milliliter is found by calculation, thus,

$$c=\frac{\text{Brix}\times\text{true density (Plato)}}{100},$$ or more conveniently by reference to

the density table of Brewster and Phelps.[14] A portion of the solution is added to each colorimeter cup and with the appropriate filter in place at the eyepiece the zero setting is checked. Since a perfect zero setting is not easily attained, compensation is made for this error, and for any others due to asymmetry of the instrument by a transposition method as follows:

A standard plate is centered under one of the cups, the corresponding scale set to a definite "blank" reading, say 0.5 or 1.0 cm, and five readings taken in the usual manner. The plate is now centered under the opposite cup, the same blank scale reading set above it, and another series of five readings taken.

[12] Z. Ver. deut. Zucker Ind. **83**, 223 (1933).
[13] BS J. Research **10**, 365 (1933) RP536. See also Tech. Pap. BS **21**, 261 (1927) T338.
[14] See page 370 of BS J. Research **10**, (1933) RP536.

The mean of the ten readings, minus the blank setting, expressed in centimeters gives the depth b of liquid for which $\mathbf{T}$[15] of the solution = T of the standard plate as given by calibration. The value of $-\log \mathbf{T}$ is found by reference to log tables or to the convenient colog table given by Peters and Phelps.[16] The data are substituted in the Beer's law equation, $-\log \mathbf{t}=\frac{1}{cb}(-\log \mathbf{T})$. The results may be expressed as $-\log \mathbf{t}_{560}$, or $-\log \mathbf{t}_{460}$, depending upon the filter used.

The following example of the determination of $-\log \mathbf{t}$ at 560 mμ in the case of a solution of washed raw sugar is an illustration:

Refractometric Brix, 60.9, corresponding to true density, 20°, 1.29176.

$$c=\frac{60.9\times 1.29176}{100}=0.7867$$

Standard plate, $T=0.579$ or $-\log T=0.2373$.

Photometric measurements:

	cm.
Right scale, mean of 5 settings	3.332
Left scale, mean of 5 settings	3.028
Mean of 10 settings	3.180
Subtracting blank setting	1.000
b	2.180

Substituting in the Beer's law equation

$$-\log \mathbf{t}=\frac{0.2373}{2.18\times 0.7867}=0.1384.$$

The calculation of results is simplified by using a slide rule with reciprocal scales.

VII. COMPARATIVE RESULTS

To gain an idea of the reliability of the present method, some results obtained with the Duboscq colorimeter and a Bausch and Lomb spectrophotometer may be compared by reference to tables 1, 2, and 3. The spectrophotometer is controlled by means of known wave-length and transmission standards and is capable, particularly in the case of amber glass or solutions at 560 mμ, of yielding results in error by considerably less than 1 percent of the transmission. Differences or errors in the final results are cumulative and attributable to both instruments.

In table 1 are given results of measurements of $-\log \mathbf{t}$ at 560 and at 460 mμ in the case of solutions of sugars. Sugar 1, column 1, was a washed Cuban raw; 2, 3, and 4 were solutions made by diluting sample 1 with colorless sirup; 5, 6, and 7 were granulated sugars; and nos. 8 and 9 were tablets and confectioners crystals, respectively. Measurements were made on portions of each solution with the colorimeter and with the spectrophotometer. Column headings 1 to 8 will be understood from the description of the method as given in the preceding section. In columns 9 and 10 the differences, D, in $-\log \mathbf{t}$ and $\mathbf{t}$ as found with the two instruments are expressed as the percentage of the spectrophotometric values.

[15] Strictly the quantity measured is the transmittance. However, since the absorption by the solvent, water, is negligible in the thicknesses used, the transmittance and the transmittancy are numerically equal, and the symbol $\mathbf{T}$ is used in the present discussion, since it is the quantity ordinarily determined with the spectrophotometer for which the proposed apparatus is a substitute.

[16] Tech. Pap. BS 21, 261 (1927) T338.

TABLE 1.—*Determination of* $-\log \mathbf{t}$ *in sugar solutions*

DUBOSCQ COLORIMETER					SPECTROPHOTOMETER				
1	2	3	4	5	6	7	8	9	10
Sugar	c, g/ml	b, cm	$-\log T$	$-\log \mathbf{t}$	b, cm	$-\log \mathbf{T}$	$-\log \mathbf{t}$	D, %, $-\log \mathbf{t}$	D, % t
560 mμ—BREWSTER FILTER									
1	0.79330	1.182	0.2373	0.25307	2	0.39794	0.25081	+0.90	−0.52
2	.78668	2.180	.2373	.13837	2	.21896	.13916	−.06	+.13
3	.79496	4.461	.2373	.06691	2	.10513	.06612	+1.20	−.69
4	.79165	7.274	.2373	.04121	5	.16494	.04167	−1.10	+.52
5	.79662	6.909	.03245	.00589	12	.05502	.00576	+2.25	−.21
6	.79496	6.224	.03245	.00656	12	.06298	.00660	−0.61	.09
460 mμ FILTER									
7	.8083	1.705	.03953	.0288	12	.29158	.03050	−5.58	+0.43
8	.7966	6.999	.03953	.00709	12	.07058	.00733	−3.27	+.47
9	.8033	7.707	.03953	.00639	20	.09864	.00608	+4.93	−.11

In table 2 are given results of measurement of $-\log \mathbf{T}$ at 560 and 460 mμ in the case of some caramel preparations. For the measurements at 560 mμ the darkest preparation designated as 100 in column 1 was analyzed with the Duboscq colorimeter and the spectrophotometer, the results given in the first two lines being practically identical. The preparation was then diluted volumetrically with water to contain the volumes, in percent, of the original that follow in column 1. The remaining four solutions of this series were not analyzed with the spectrophotometer, but the calculated values for $-\log \mathbf{T}_{1\,cm}$ are percentages of original $-\log \mathbf{T}_{1\,cm}$ corresponding to the dilution. In the 460 mμ series all of the caramel preparations were analyzed with both instruments. In columns 2, 3, and 4 are given, respectively, depth b, as found with the colorimeter; $-\log T$ of the glass standard; and $-\log \mathbf{T}_{1\,cm}$ (values in column 3 divided by corresponding values of column 2). In column 5 the values of $-\log \mathbf{T}_{1\,cm}$ are calculated as percentages of the original corresponding to the concentrations in column 1. The experimental and calculated values of $\mathbf{T}_{1\,cm}$ appear in columns 6 and 7, respectively, and the differences as the percentage of the calculated values of $-\log \mathbf{T}_{1\,cm}$ and $\mathbf{T}_{1\,cm}$ in columns 8 and 9.

TABLE 2.—*Absorbancy and transmittancy of caramel preparations*

1	2	3	4	5	6	7	8	9
Conc. orig. prep. ml/100	b, cm	$-\log \mathbf{T}$	$-\log \mathbf{T}_{1\,cm}$ Found	$-\log \mathbf{T}_{1\,cm}$ Calculated	$\mathbf{T}_{1\,cm}$ Found	$\mathbf{T}_{1\,cm}$ Calculated	D, %, $-\log \mathbf{T}$	D, %, $\mathbf{T}$
SPECTROPHOTOMETER								
100	1.100	----------	0.61617	----------	0.242	----------	----------	----------
DUBOSCQ—BREWSTER 560 mμ FILTER								
100	0.366	0.22548	0.6160	0.6162	0.242	0.242	0.00	0.00
50	.734	.22548	.3072	.3081	.493	.492	−0.30	+0.20
25	1.501	.22548	.1502	.1540	.708	.702	−2.42	+.85
20	.996	.11919	.1196	.1232	.759	.753	−2.92	+.80
10	1.971	.11919	.0605	.0616	.870	.868	−1.79	+.23
DUBOSCQ—460 mμ FILTER								
----------	0.620	0.2660	0.4290	0.4220	0.372	0.378	+1.66	−1.25
----------	1.309	.2660	.2003	.2022	.630	.628	−0.94	+0.32
----------	4.048	.2660	.0657	.0648	.860	.861	+1.39	−0.12

VIII. CALIBRATION OF WORKING STANDARDS

The results obtained in the calibration at 560 mμ of some amber and colorless plates, as described below, are given in table 3.

The amber reference standard $T=0.703$ at 560 mμ, was calibrated by the colorimetry section of this Bureau. An aqueous preparation of caramel was made by diluting a small amount of a commercial product, available in the form of a thick tarry paste, so that a layer of solution 1 cm thick approximately matched the reference standard. Such dilute preparations fade slowly and are subject to infection with organisms. It was, therefore, used the same day it was prepared. With solution in both cups, and using a 560-mμ filter, a series of matchings (10 on each side) was made and the mean of the 20 readings taken to represent thickness b, of the layer wherein $\mathbf{T}=T$. Dividing $-\log \mathbf{T}$ by b gave $-\log \mathbf{T}$ for 1 cm thickness of caramel, which then was employed as a secondary standard. The data relating to this calibration appear as the first line of figures in table 3. The unknown plates were substituted, one by one, for the reference standard and matched against the caramel, giving the mean values for b in column 2. The value of $-\log \mathbf{T}_{1\text{ cm}}$ in column 3 multiplied by b gave $-\log T$, column 4, for each plate. The antilog T is given in column 5, which may be compared with the direct spectrophotometric value in column 6. The values of D in column 7 represent the percentage deviation from the spectrophotometric values. The last three calibrations with a Gibson filter, as indicated in table 3, were performed at a later time than the others. The average deviation, as expected, is smaller than with the older filter.

TABLE 3.—*Calibration of glass plates at λ 560*

1	2	3	4	5	6	7
Plate	b, cm	$-\log \mathbf{T}_{1\text{ cm}}$	$-\log T$	T Duboscq	T Spectrophotometer	D, % T
BREWSTER FILTER						
Caramel	1.1885	0.12877	0.15304	----------	0.703	----------
3.54	1.7775	.12877	.2290	0.590	.589	+0.17
2.96	.9630	.12877	.1240	.752	.754	−.26
2.78	.9195	.12877	.1184	.761	.760	+.13
1.39	.5670	.12877	.0730	.845	.847	−.24
Colorless	.2380	.12877	.0306	.932	.928	+.43
GIBSON FILTER						
3.54	1.940	0.1207	0.2341	0.583	0.585	−0.34
2.78	.9825	.1207	.1184	.761	.761	.00
Colorless	.2720	.1207	.03282	.927	.928	−.13

To reduce the probability of error in calibration the custom may be followed of taking the mean of a larger number of observations (at different times if necessary) and by more than one observer.

WASHINGTON, March 3, 1936.

U. S. DEPARTMENT OF COMMERCE NATIONAL BUREAU OF STANDARDS

RESEARCH PAPER RP879

Part of Journal of Research of the National Bureau of Standards, Volume 16, April 1936

GLOSS INVESTIGATIONS USING REFLECTED IMAGES OF A TARGET PATTERN

By Richard S. Hunter

ABSTRACT

A target pattern of concentric rings varying from fine lines to broad bands has been placed in the open face of a desk lamp. This luminous target is useful in the study of the gloss characteristics of the more glossy surfaces. The lines and bands of various sizes in the pattern provide means for studying surfaces of a wide range of "distinctness-of-reflected-image" gloss. Records may be made of which lines and bands are visible by reflection from different surfaces. Such records serve as permanent gloss values for the different surfaces studied. The dark areas of the target immediately adjacent to the luminous areas provide ideal conditions for the identification of surface "bloom." The best gloss differentiations are made when the lamp is used in a darkened room, so that the luminous pattern is the only source of light illuminating the surfaces inspected. Photographic records of gloss and unusual gloss effects are discussed.

CONTENTS

	Page
I. Introduction	359
II. Apparatus and method	360
III. Representative results	362
IV. Identification of differences in bloom, objective gloss, and texture	363
V. Value of gloss photographs	365
VI. General technique	366

I. INTRODUCTION

In a recent circular [1] of the scientific section of the National Paint, Varnish, and Lacquer Association, the author described an instrument to measure "distinctness-of-reflected-image" gloss and to study other gloss effects. In this gloss comparator two identical, illuminated targets consisting of concentric rings varying from fine lines to wide bands were used. The narrowest lines which could be seen after reflection from any given surface were used as the criterion of the distinctness-of-image gloss of that surface. A measuring device which gave variable amounts of diffusion to one of the targets was used to arrange these distinctness-of-image comparisons on a continuous scale.

Shortly after this gloss comparator was introduced, it was realized that perhaps the luminous target itself, without the accompanying instrument, might be useful in gloss-control work and studies of gloss differences. Accordingly, an enlargement of the gloss-comparator target was printed on a photographic plate and mounted in the face

[1] Scientific Section Circular 493 of the NPVLA, Washington, D. C. (October 1935). In this circular are described the gloss comparator and also the different appearance effects identified with glossiness. A bibliography on gloss-measuring methods is included.

of a desk lamp, as illustrated in figure 1. This lamp has proved so useful in studies of gloss that it is thought worth-while to describe its use in detail.

II. APPARATUS AND METHOD

In figure 2, a 90-degree quadrant of the target is reproduced to full scale. Each of the lines and bands in the target is designated with a letter by which it may be identified. The advantages which the device offers when used for studies of gloss and gloss differences are: (1) it affords reproducible conditions for the study of glossy materials; (2) the lines and bands of varying size in the target provide means for studying surfaces over a wide range of distinctness-of-image gloss; (3) permanent records of this type of gloss may be obtained by identification of the rings and bands which are visible after reflection from any given surface; and (4) the dark areas in the target may be used for determining the differences in bloom between glossy surfaces.

The design of the circular target was reached through a trial-and-error development during the building of the earlier instrument.[1] Rectangular and straight-line targets were tried first, but it was discovered that the images reflected by many surfaces varied as the surfaces were rotated in their own plane. The circular target, of course, gives the imaging powers from source lines in all directions. The widths of the lines and bands have been graded to give fairly even steps in distinctness-of-image reflection. To illustrate the differentiations thus made possible, three pairs of typical target images have been photographed with the combination of camera and lamp shown in figure 1. These photographs are reproduced in figure 3.

The lamp makes possible the finest distinctions in gloss when it is used in an otherwise darkened room. However, since the ordinary glossy appearance of any surface varies with the surrounding field of view and with other illuminations, it is, in many cases, advisable to make gloss comparisons with outside light present in order to realize more closely the actual conditions of gloss observation. It is best to obtain flat panels of the materials to be studied as curved surfaces reflect distorted images, which are more difficult to evaluate. A mild example of this distortion is seen in figure 3, where the panel a-l possesses a slight curvature.

For detecting gloss differences, the two panels to be compared are placed side by side and viewed so that part of the image of the face of the lamp is seen reflected from each surface. The distance of the surfaces from the lamp and the angle of view are always important and should be noted where permanent records are to be kept. If the test panels are moved toward the lamp, finer lines in the target may be distinguished. Also, a shift of the surfaces toward the lamp will make their lightness and color characteristics more pronounced. When the surfaces are moved away from the lamp, the finer lines in the pattern disappear, and color and lightness become more difficult to recognize. As the angle of view approaches grazing incidence, images reflected in the surfaces become more distinct. Thus many of the very flat, mat surfaces will reflect distinguishable images at near-grazing incidence.

When the lamp is used as a source for obtaining distinctness-of-image gloss ratings of individual surfaces, instead of simply for com-

[1] See footnote 1.

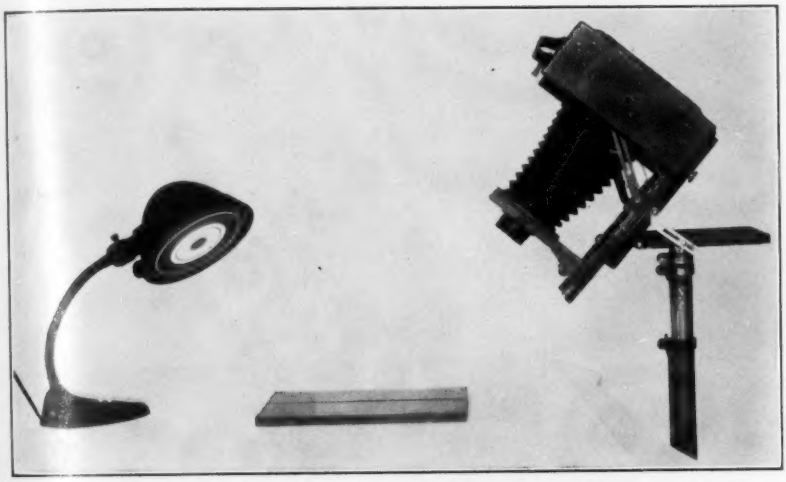

FIGURE 1.—*Target pattern mounted in desk lamp, two panels in position for comparison, and camera to photograph images of target pattern reflected in panel surfaces.*

UNIV. OF MICH.

paring two surfaces, these surfaces must, in turn, all be placed in the same position relative to the lamp and should be viewed from the same position. The exterior-lighting conditions must also be constant and the following factors specified in presenting the results:

1. Distance from lamp to test surface.
2. Distance from observer to test surface.
3. Direction of view (unless otherwise specified, approximately 45°).
4. Amount of light present from sources outside the lamp. When these factors are recorded, reproducible conditions for the identification of the lines of the target are established, and observations made

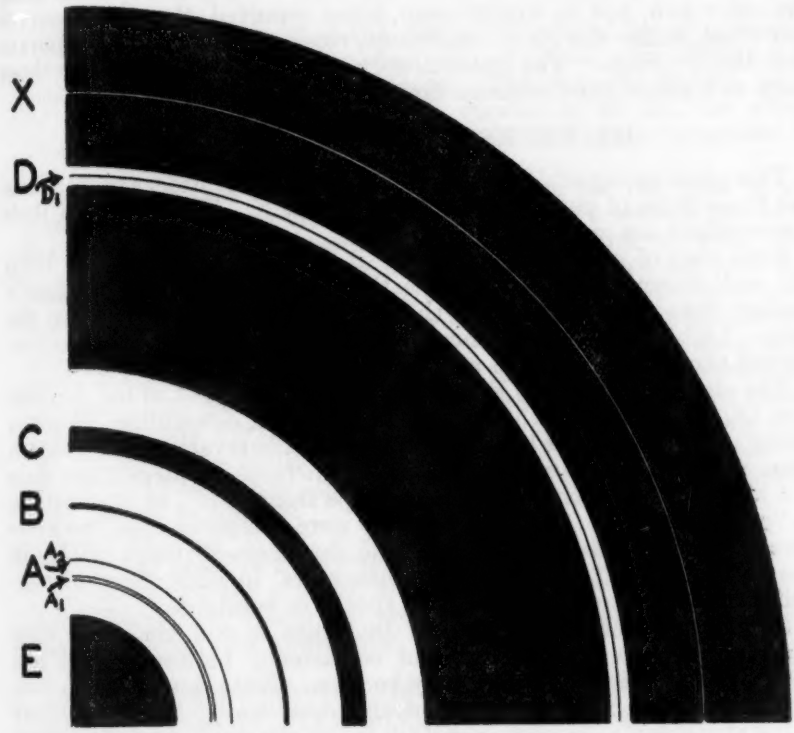

FIGURE 2.—*One-quarter circle of the target pattern reproduced full scale, with letters to identify the different rings and lines.*

at separate times may be used as records of the gloss of the surfaces tested.

The observer who wishes to describe the appearance of the target image reflected in some particular glossy surface, names and describes the appearance of the least-distinct ring. That is, he records the letter which identifies this ring and perhaps a modifying letter to indicate whether this ring is sharp, fairly plain, or indistinct; also whether it appears as a continuous ring, or shows only irregularly from certain parts of the surface. In order of descending distinctness-of-image, the letters identifying the rings in the target are A_1, A_2, A, B, C, D, and E. In addition, there are two auxiliary rings (D_1 and X), which are occasionally used in describing the appearance of surfaces.

The following modifying letters are suggested for the above designations: g, good definition; f, fair definition; and p, poor definition. This system gives a distinctness-of-image gloss scale of 7 letter ratings and 21 steps, 3 steps for each rating. Three letters, which serve to indicate the appearance of a surface aside from its distinctness-of-image gloss, are suggested: n, nonuniform; w, wavy; and s, specks and scratches. Other characteristics of surfaces, such as bloom, particular types of texture, and unusual appearance may also be designated.

In the innermost band of rings, the letter A_1 represents resolution by the eye of the two rings close together just outside the center of the target. A_2 represents resolution of the third ring as separate from the other two, but A_2 would mean, when reported, that the observer could not, under the given conditions, resolve the A_1 pair as separate and distinct rings. The letter A indicates identification of the three rings as a single band without their separate resolution.

III. REPRESENTATIVE RESULTS

This gloss-rating scale was used by a number of observers to grade the three pairs of panels illustrated in figure 3. The results of their observations are given in table 1.

Each pair of panels was observed at two distances from the lamp (30 and 90 cm); in each instance the observer's eyes were slightly farther from the test surfaces than the test surfaces were from the lamp. Light was incident upon the specimens at 45°, and the observer viewed the images reflected at 45°; the room was dark.

The observer's rating, *g*, *f*, or *p*, is placed to the right of the designation (A_1, A_2, ...) of the ring which was least discernible. A mean rating is assigned at the bottom of each set of observations. To obtain these means, it is assumed that the distinctness-of-image gloss scale is a uniform, continuous scale of 21 steps from "*p*E", at the bottom, to "*g*A_1", at the top. Tenths of a step were computed from the averages of the six observers. Below the sharpness-of-image ratings in the table are "x's" to indicate the observers' identifications of nonuniformities, surface waviness, and specks or scratches.

From the photographic record in figure 3 and the gloss data recorded in table 1, the degree of consistency between visual and photographic records of gloss may be seen. Note, for instance, that panels a–l and b–r, figure 3, were designated "wavy" by all observers in the visual test; also these panels in the photograph show the typical distortion due to waviness. The distinctness of the images reproduced in the figure do not exactly correspond to the 30-cm ratings given in table 1, because of slight changes in reproduction introduced in the various printing processes.

When it is considered that the gloss-inspection lamp and the method of rating gloss were both new to these observers, the agreement among them seems quite satisfactory. The lamp is shown to be capable of establishing 21 steps on a distinctness-of-image scale. The range of this scale may be adjusted to give the best gloss differentiations of any particular type of glossy material. This adjustment is usually accomplished by varying the distances of lamp to test surface and test surface to observer. Glossy surfaces which reflect sharp images should be compared at greater distances from the lamp, while better differentiations are made on the less-glossy surfaces by moving them closer to the lamp. The average, observed,

distinctness-of-image, gloss-step differences, expressed in gloss steps between the l and r panels of each pair at the two distances, tabulated in table 1, are as follows:

Samples	Distances	
	30 cm	90 cm
"a" pair	0.5	2.3
"b" pair	.3	1.0
"c" pair	4.8	3.0

Thus it can be seen that the glossy "a" pair of panels showed an average difference of only one-half step at 30 cm, while at 90 cm this difference was more than two steps. The converse is true for the "c" pair of low-gloss panels; thus, viewed at 30 cm, the average difference was 4.8 steps, but at 90 cm the difference recognized was only 3.0 steps.

The preparation recently of a specification for the gloss of automobile enamels furnishes an example of the practical use of this flexible gloss scale. Representative test samples of such glossy enamels, some weathered and some fresh, were used for trial observations to determine under what conditions the best gloss differentiations could be made. It was found that at a lamp-to-surface distance of 1 meter, a lamp-to-observer distance of 1.5 meters, and an angle of view equal to 30°, practically the complete gloss scale could be used. The test room was dark, the lamp was placed on a bench, the test panels were placed on the floor, and the observers viewed the images of the lamp target reflected in the various surfaces while standing. Tentatively, the distinctness-of-image gloss requirements were chosen as follows:

Fresh surfaces: B fair, or higher.

After 168 hours of accelerated weathering: C good, or higher.

In comparing the superior and inferior enamels, it was found that the better-grade materials retained their gloss more effectively through accelerated weathering.

IV. IDENTIFICATION OF DIFFERENCES IN BLOOM, OBJECTIVE GLOSS, AND TEXTURE

Bloom, objective gloss, and surface texture were three of the types of gloss identified in the earlier publication.[3] It is not possible to arrange, by means of the lamp, these factors along a scale such as used in the case of distinctness-of-image gloss. However, the lamp and target have proved useful in identifying differences in these three types of surface appearance and in furnishing qualitative, rather than quantitative, data on them.

When using the gloss-inspection lamp for the identification of bloom, one inspects the image of the black spot in the center of the target and the other dark areas in the target. Bloom is indicated as a haze in these dark areas of the image. The two glossy olive-green enamel panels compared in figure 3, "a" pair, for distinctness-of-image

[3] See footnote 1.

TABLE 1.—*Tabulation of distinctness-of-image gloss ratings by six observers of the three pairs of panels compared in figure 3*

[Panels were observed at two distances and surface characteristics noted]

Distance from lamp to sample		30 cm						90 cm					
Observers		RSH	DBJ	KSG	GWH	HJK	WNH	RSH	DBJ	KSG	GWH	HJK	WNH
Panel a–l	A_1	*f*	*g*	*f*	*g*	*f*	*g*						
	A_2												
	A							*f*	*f*	*p*	*p*	*p*	*f*
	B												
	C												
	D												
	E												
Mean rating		(*f*+.5)A_1						(*p*+.5)A					
Nonuniformities									x		x		
Waviness			x	x	x	x	x	x	x	x	x	x	x
Specks, scratches		x		x	x	x	x			x			
Panel b–l	A_1	*f*	*p*	*p*	*p*	*f*	*p*						
	A_2												*f*
	A												
	B							*f*	*g*	*p*	*f*	*f*	
	C												
	D												
	E												
Mean rating		(*p*+.3)A_1						(*f*+.5)B					
Nonuniformities		x		x	x								
Waviness								x	x	x	x		
Specks, scratches		x		x	x	x		x			x	x	
Panel c–l	A_1												
	A_2												
	A												
	B												
	C	*f*	*p*	*f*	*f*	*f*	*f*						
	D							*p*	*f*	*p*	*p*	*p*	*g*
	E												
Mean rating		(*f*−.2)C						(*p*+.5)D					
Nonuniformities				x									
Waviness													
Specks, scratches		x	x	x	x	x		x		x	x		x

Distance from lamp to sample		30 cm						90 cm					
Observers		RSH	DBJ	KSG	GWH	HJK	WNH	RSH	DBJ	KSG	GWH	HJK	WNH
Panel a–r	A_1	*g*	*g*	*g*	*g*	*g*	*g*						
	A_2								*g*	*f*			*p*
	A							*g*			*f*	*g*	
	B												
	C												
	D												
	E												
Mean rating		*g*A_1						(*p*−.2)A_2					
Nonuniformities													
Waviness								x					
Specks, scratches		x		x	x	x	x	x	x	x	x		
Panel b–r	A_1	*p*	*p*	*p*	*p*	*p*	*p*						
	A_2												
	A												*p*
	B							*p*	*p*	*p*	*p*	*p*	
	C												
	D												
	E												
Mean rating		*p*A_1						(*p*+.5)B					
Nonuniformities		x	x		x	x	x		x			x	
Waviness		x	x	x	x	x	x	x	x	x	x	x	x
Specks, scratches				x	x	x			x	x	x		
Panel c–r	A_1												
	A_2												
	A												
	B												
	C												
	D	*p*	*p*										
	E			*f*	*g*	*f*	*g*	*f*	*g*	*p*	*p*	*p*	*p*
Mean rating		*g*E						(*p*+.5)E					
Nonuniformities													
Waviness													
Specks, scratches		x	x	x	x	x	x	x		x	x		

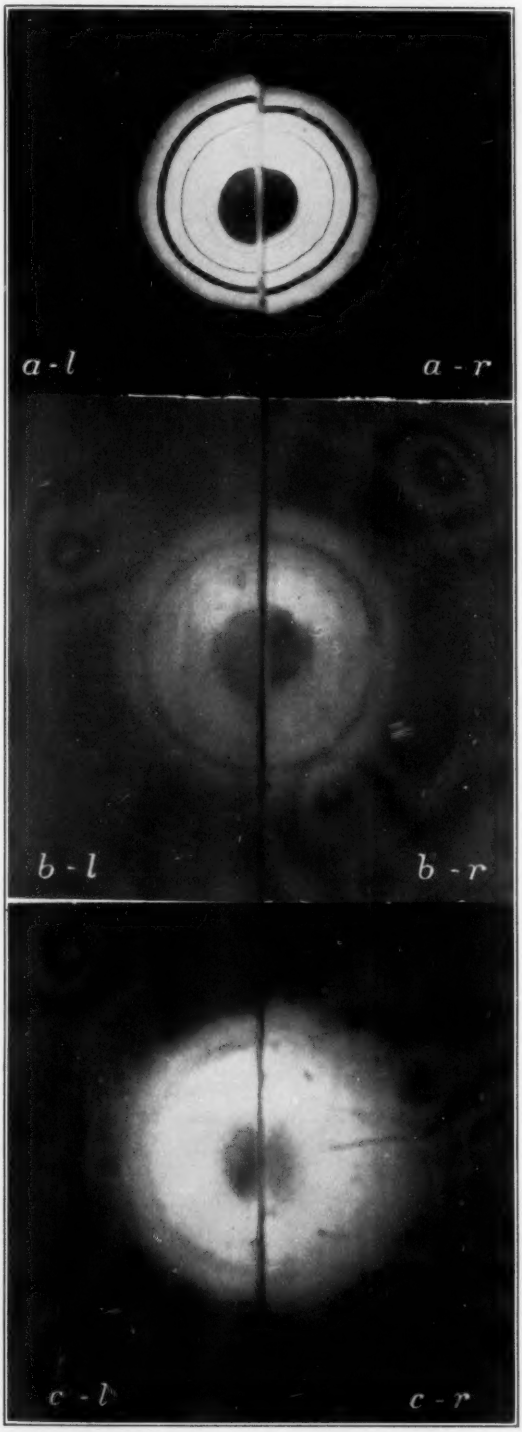

FIGURE 3.—*Comparison of three pairs of panels using the gloss-inspection lamp.*

Panels, a, olive-green enamels; b, white, resinous paints; and c, rubbed furniture finishes. Distances of camera to surface and lamp to surface both about 30 cm; room dark.

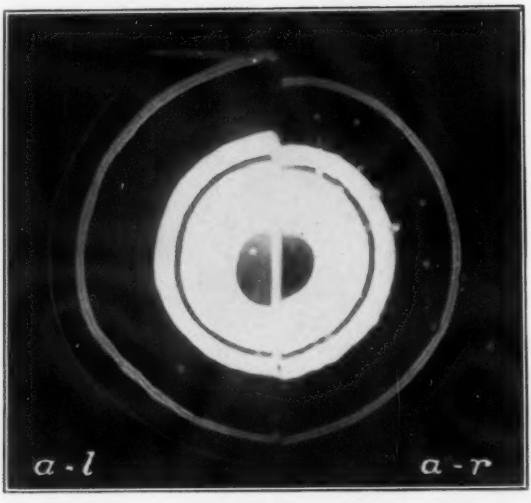

FIGURE 4.—*Comparison of "a" pair of panels shown in figure 3 printed from same negative as in figure 3, but with low density to show effect of bloom on panel* a–l.

gloss, showed also a pronounced difference in bloom. The effect is quite appreciable in the left panel of figure 4, which is another print from the "a" pair negative of figure 3, but less dense. In the "b" pair of white surfaces, figure 3, b–l reflects the sharper images, and also shows more bloom than b–r. Bloom is shown only by surfaces which reflect images.

Objective gloss is more popularly thought of as "shininess." With the gloss lamp and target, it is recognized by the brilliance of reflected images but is not readily measurable. There are a number of other gloss meters, however, which give records of specular reflectance, such as, for instance, the instrument [4] designed by the author in the spring of 1934. References to methods for measuring objective gloss, as well as other gloss factors, are given in the previous circular.[5]

With regard to comparisons of surface texture and the evaluation of irregularities, this lamp is useful as a source of nearly unidirectional light. Nonuniformities, waviness, and specks or scratches were evaluated qualitatively by the observers who compared the six surfaces and obtained the results shown in table 1. Surface irregularities, blemishes, and texture show up distinctly in illumination from a single direction but are less visible in illumination which is well diffused. Texture is most distinct at the angle of specular reflection, and photographs at this angle with the camera focused on the surface tested, give, in our experience, the best records of texture. All the surfaces photographed in figure 3 show irregularities, but they are out of focus because the camera was focused on the image of the target.

V. VALUE OF GLOSS PHOTOGRAPHS

It can be appreciated that photographs such as are shown in figures 3 and 4 are better and more complete records of glossiness and serve better for comparing gloss than do values obtained on any gloss scale. This is because the glossiness of a surface arises from a combination of several factors and these combined factors are seldom expressible as a variation in one dimension. Because of the advantages of the photographic method, the earlier gloss comparator [6] was designed to take a camera directly into the instrument. The camera is always placed in the same position in the instrument; no careful adjusting and focusing are necessary, and the exposures are timed by a prepared table. With the gloss-inspection lamp, on the other hand, it is necessary to set the camera up carefully in the desired position to photograph the effect sought. In spite of the greater care which is necessary, this ability to use the camera in any position is sometimes an advantage because it gives greater latitude for the study of gloss effects.

A 5 by 7 plate camera was used to obtain the photographs shown in figures 3 and 4. This was set up as shown in figure 1, where the camera lens and the lamp target are both about 30 cm from the gloss surfaces. The lens of the camera was stopped-down to about 3 mm so that as much detail as possible would be obtained from the out-of-focus test surfaces.

[4] The Glossmeter, Scientific Section Circular 456 of the NPVLA, Washington, D. C. (April 1934).
[5] See footnote 1.
[6] See footnote 1.

VI. GENERAL TECHNIQUE

As already implied, the observer who wishes to analyze gloss effects must recognize that two distinctly different modes of appearance, as well as several appearance effects, are always possible. One mode results when the observer fixates the glossy surface itself; the other when he fixates the image of some object reflected in that surface. Surface texture, formation, and structure are appreciated when the eye is focused upon the surfaces being studied. On the other hand, form of reflected images, gloss contrasts, and the distribution of light reflected by surfaces are usually appreciated when the observer fixates the images of objects reflected in the glossy surfaces. For this reason, one who wishes to photograph surface features and texture focuses the camera upon the glossy surface, while one who wishes to photograph image reflections, bloom, or contrasts, as in figure 3, focuses the camera upon the image of the target reflected in the test specimens. In this latter case, pimples, irregularities, and grain in the surfaces can be seen, but they are out of focus.

In conclusion, it may be repeated that the gloss-inspection lamp is a convenient source of light for the general study of gloss-appearance effects. The wide variety of ways in which it can be used makes it possible to identify many effects that are not appreciated when using other apparatus. Thus, as described in section II, the distances of the test surface from the lamp and observer and the surrounding lighting can be varied to obtain the conditions which give best discriminations of distinctness-of-image gloss for the particular type of surfaces being studied. Furthermore, unusual gloss effects can often be seen which do not fall directly into one of the classes identified in the previous publication.[7] By using the gloss-inspection lamp to study these effects, and trying different methods of illuminating and viewing the samples, satisfactory conditions for the identification of many effects may be found.

For example, an unusual effect which appeared in comparing the "c" pair of furniture finishes photographed in figure 3 may be described. When these two surfaces were compared from a direction considerably to one side of the direction of image reflection shown, panel c–r, which shows distinctly the lower distinctness-of-image gloss, appeared to have a cleaner and glossier finish than panel c–l. The effect on c–l, which appeared to be similar to bloom or reflection haze, detracted considerably from its glossiness, and yet it was only identified under rather exceptional conditions of illumination.

Directional-distribution measurements of reflection as recommended by McNicholas [8] may eventually lead to a more definite understanding of the conditions under which some of these appearance effects are likely to occur, and such measurements are now in progress; but for the present, empirical methods which are discovered by trial, using devices such as this lamp, offer the best means of identifying and recording the presence of unusual gloss types. Because there is so much latitude in establishing external conditions for the use of this lamp, it is believed that it will prove valuable in examining many types of gloss effects.

WASHINGTON, February 10, 1936.

[7] See footnote 1.
[8] *Absolute methods in reflectometry*, BS J. Research 1, 29 (1928) RP3.

U. S. DEPARTMENT OF COMMERCE NATIONAL BUREAU OF STANDARDS

RESEARCH PAPER RP880

Part of Journal of Research of the National Bureau of Standards, Volume 16, April 1936

AN IMPROVED METHOD FOR PREPARING CAST-IRON TRANSVERSE TEST BARS

By A. I. Krynitsky and C. M. Saeger, Jr.

ABSTRACT

The importance of preparing cast-iron transverse-strength test bars free from "burnt-on" sand and surface defects is discussed. A molding material and casting technique which will produce such test bars in green-sand molds has been developed.

Test bars 0.75, 1.2, 1.5, and 2.2 inches in diameter and 23 inches in length were cast in top-poured and bottom-poured vertical molds, horizontal molds, and horizontally inclined molds. The effect of maximum heating temperature on the transverse breaking strength, hardness, primary structure, and microstructure of test bars made by these methods was investigated. Test bars cast in bottom-poured vertical molds yielded the most consistent results.

The transverse breaking strength of the irons investigated increased with an increase of the maximum heating temperature, regardless of the casting method employed. A finer primary structure and finer graphite and pearlite constituents were found to be associated with higher transverse strength.

CONTENTS

	Page
I. Introduction	367
II. Molding and casting technique	368
1. Types of test bars	369
2. Test-bar molds	369
3. Stock iron	369
4. Melting and casting procedure	369
5. Temperature measurement of molten iron	370
6. Molding material	370
7. Uniformity in dimensions of test bars	372
III. Comparison of test bars produced by four methods	373
1. Four methods of preparing test bars	373
(a) Top- and bottom-poured vertical mold	374
(b) Horizontal mold	374
(c) Horizontally inclined mold	374
2. Surface condition and dimensional uniformity of test bars	374
3. Physical properties of test bars	374
(a) Transverse breaking test	374
(b) Brinell numbers	380
4. Structure	380
(a) Microstructure	380
(b) Primary structure	382
IV. Summary	383
V. References	383

I. INTRODUCTION

In an investigation of the effect of maximum heating temperatures on the physical properties of different types of cast irons [1] [1] a method was developed at the National Bureau of Standards for making trans-

[1] Figures in brackets here and throughout the text indicate literature references given at the end of this paper.

verse-strength test bars in dry-sand molds. The Committees on Cast Iron of both the American Society for Testing Materials and the American Foundrymen's Association have expressed their interest in this subject and pointed out the desirability of extending the investigation to include a study of transverse-strength test bars made in green-sand molds.

It is well known that bars used for the determination of transverse strengths hould not only be free from "burnt-on" sand but should also have a smooth surface, since the breaking strength of a test piece may be seriously affected by the character of its surface. The removal of burnt-on sand by sand blasting or tumbling may leave the surface pitted or roughened, which condition may cause the bars to break under a relatively low load by the so-called "notch effect".

Many investigators are of the opinion that the surface layer on test bars should be removed by machining before the bars are tested. This point was strongly emphasized in the discussion of the paper entitled Relationship in Cast Iron Test Results [2]. It is believed by many investigators that the surface layer or so-called "surface skin" is the strongest part of the bar and, therefore, one should expect its removal to lower the transverse strength. It has been found [1] experimentally that the removal of the surface layer lowers the strength under transverse loading, although the results of some other investigators are not in agreement with this. However, surface defects, such as those mentioned earlier, might account for these results, which indicate the transverse strength of a bar with the surface skin removed to be stronger than a similar bar without the skin removed.

In this investigation an attempt was made to prepare test bars in green-sand molds having smooth surfaces free from burnt-on sand. Factors such as the horizontal or vertical position of the mold, the location and size of the gates and risers, the molding and facing materials, the permeability, strength and degree of ramming of the mold, and the temperature of the metal and rate at which it is poured into the molds, are important and should be considered in producing satisfactory test bars.

The investigation is naturally divided into two parts, the first, to develop a molding procedure which will yield satisfactory test bars when green-sand molds are used, and the second, to compare the results obtained on test bars produced by pouring (1) by the method developed at this Bureau and (2) by the three tentative methods specified by the American Society for Testing Materials [3].

II. MOLDING AND CASTING TECHNIQUE

A molding material to be suitable for this purpose must be such that it is possible to make satisfactory bars of various diameters with irons of various chemical compositions. It was felt that the molding material would be satisfactory if it yielded satisfactory test bars free from burnt-on sand and surface defects, when the following types of irons, and the following melting and casting procedure is used to produce bars of the following sizes.

FIGURE 1.—*Casting showing the method of pouring bars for transverse tests.*

A, Pouring basin; B, down gate; C, feeding ring; D, 2.2-inch bar; E, 1.2-inch bar; F, 1.5-inch bar; G, 0.75-inch diameter bar.

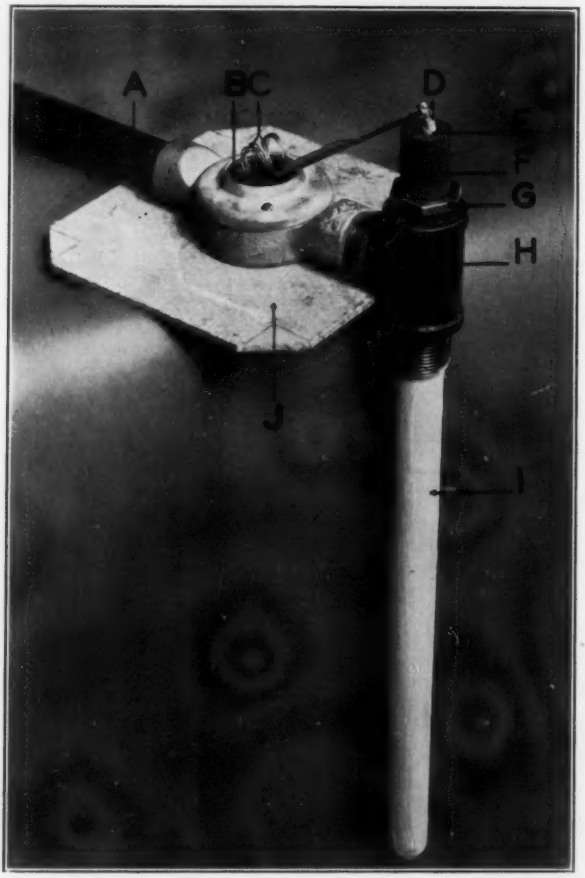

FIGURE 3.—*Thermocouple assembly used in measuring temperatures of molten cast iron.*

A, Thermocouple-handle enclosing extension leads; B, thermocouple junction with extension leads; C, platinum-platinum rhodium thermocouple wires; D, 2-hole porcelain insulating tube; E, porcelain tube; F, graphite tube; G, split lock nut; H, pipe tee; I, refractory coating applied to graphite tube; J, heat insulating plate.

1. TYPES OF TEST BARS

The test bars prepared and studied in this investigation were 23 inches in length and 0.75, 1.2, and 2.2 inches in diameter, respectively. Similar bars, 1.5 inches in diameter, were also used to a limited extent.

2. TEST-BAR MOLDS

The bottom-poured vertical mold, which was developed for casting test bars in dry sand [1], was used in this phase of the investigation. In this method a set of cylindrical test bars, consisting of four pairs molded in a three-part cylindrical flask, with the cheek extending the full length of the bar, were made in green sand (fig. 1). The diameters of the various bars were 0.75, 1.2, 1.5, and 2.2 inches, respectively. The bars were arranged so as to minimize the heating effect of the large bars on the small ones during cooling after casting.

3. STOCK IRON

The types of irons used are shown in table 1.

TABLE 1.—*Results of chemical analyses of stock irons used*

Iron	Total carbon	Silicon	Manganese	Phosphorus	Sulphur	Copper	Nickel	Chromium
	%	%	%	%	%	%	%	%
A	3.99	1.70	0.70	0.59	0.045	0.51	----------	----------
B	3.41	1.63	.49	.44	.073	----------	0.10	0.13
C	3.79	1.32	.73	.12	.06	----------	----------	----------
D	2.86	2.06	.18	.65	.028	----------	----------	----------
E	3.55	2.73	.24	.82	.021	----------	----------	----------
F[1]	2.13	1.64	.14	.49	.013	----------	----------	----------

[1] Chemical analysis calculated.

Irons A, C, and E were sand-cast pig irons. Iron B was a specially selected scrap iron; D, a mixture of E and 20 percent of commercial open-hearth ingot iron; and F, a mixture of E and 40 percent of commercial open-hearth ingot iron.

4. MELTING AND CASTING PROCEDURE

The irons were melted in a crucible of commercial magnesia in a high-frequency induction furnace of the tilting type. Charges of 200 pounds of metal were heated to maximum heating temperatures of 1,400° C (2,550° F); 1,500° C (2,730° F); 1,600° C (2,910° F); and 1,700° C (3,090° F), respectively, and held at the maximum heating temperature for approximately 1 minute before being allowed to cool to the desired pouring temperature.

The metal was allowed to cool from the maximum heating temperature to approximately 150° C (270° F) above the liquidus temperature of the stock pig iron or mixture used in that particular charge. It was then poured directly from the furnace into the test-bar molds, and the bars allowed to remain in the mold for a period of not less than 18 hours. The liquidus temperature was obtained from the diagram in figure 2, which shows the relation [4] between the liquidus temperature of cast iron and the total impurities.

5. TEMPERATURE MEASUREMENT OF MOLTEN IRON

Temperatures up to 1,550° C (2,820° F) were measured by a platinum-to-platinum 10-percent rhodium thermocouple. The thermocouple wires were separated by means of a two-hole porcelain insulator and protected by a closed-end, glazed, porcelain tube inserted into a closed-end graphite tube. The portion of the graphite tube, which came in contact with the molten iron, was coated with a layer of aluminum oxide over which a layer of a mixture of 95 percent of zircon (zirconium silicate) and 5 percent of bentonite was applied. The thermocouple assembly is shown in figure 3. An optical pyrometer was used for measuring temperatures above 1,550° C (2,820° F). In order to determine the corrections to be applied to the readings of the optical pyrometer under these particular conditions, observations were taken simultaneously with both the thermocouple and the optical pyrometer in the temperature range 1,400 to 1,550° C (2,550 to 2,820° F). These corrections were then plotted as a function of the temperature, and the curve extended up to 1,700° C (3,090° F).

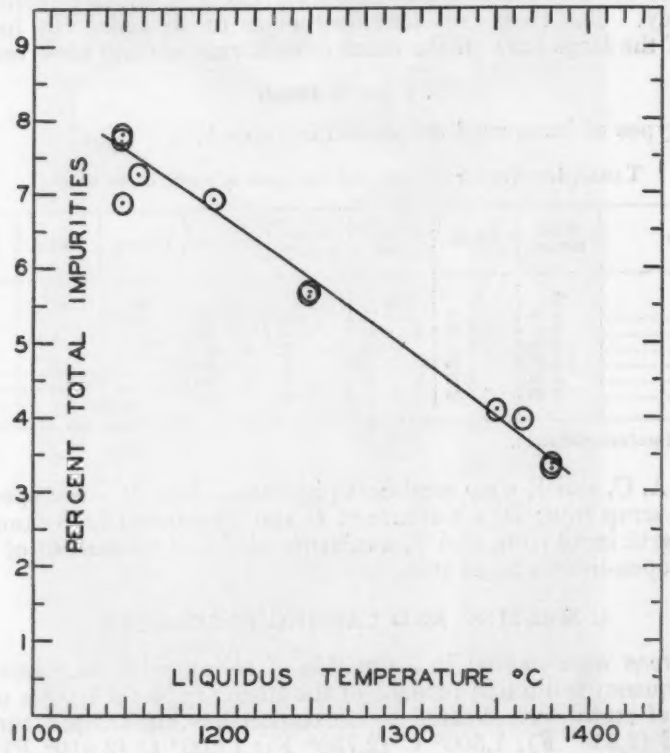

FIGURE 2.—*Relation of liquidus temperature to total impurities in cast iron.*

6. MOLDING MATERIAL

Considerable preliminary work was necessary with green-sand molds to develop a suitable molding material which would yield test bars free from surface defects or "burnt-on" sand. A number of bars

were cast in green-sand molds of various moisture contents made from an iron molding sand commercially known as Lumberton molding sand (American Foundrymen's Association grade 3–C). An excessive amount of burnt-on sand in each case was noted.

Further tests were made with molds of the same molding material in which the cavities were coated with a facing material such as ceylon graphite, as well as a nongraphitic carbonaceous material.[2] Mixtures of the nongraphitic carbonaceous material with bentonite, silica flour, aluminum-oxide cement, or portland cement were also tried as facing material. These were applied by dusting, by brushing with a camel hair brush, and by swabbing with a hemp swab. In each case the facing material was applied in dry form. None of the bars made in molds so treated was satisfactory on account of burnt-on sand.

Mixtures of sand and sea-coal were tried with some degree of success. A mixture of 8 parts of molding sand to 1 part of sea-coal, tempered to approximately 7 percent of moisture, was used in making molds. However, the test bars made in these molds were not entirely satisfactory because of the roughened surface and, to some extent, burnt-on sand. By facing the mold cavities with a fine ceylon graphite, bars were obtained that were free from burnt-on sand, although the surfaces of the bars were still very rough. However, by swabbing the mold surfaces with a nongraphitic carbonaceous material, bars which were free from burnt-on sand and which possessed a very smooth surface were obtained.

This molding mixture composed of 8 parts of molding sand to 1 part of sea-coal, tempered to approximately 7 percent of moisture, with the mold cavities faced with a nongraphitic carbonaceous facing material, was used in the remainder of the experiments and will be referred to as the "selected molding material."

Two experiments were conducted to determine the temperature of the sand between different sizes of test bars immediately after casting. The purpose of these experiments was to determine if the molding sand reached a temperature high enough to produce appreciable annealing effects in the bars. This is particularly of interest in those cases where a small diameter bar is cast in the same mold with larger bars. In both experiments a casting similar to that shown in figure 1 was made. In the first mold, two thermocouples were inserted, one midway between the 0.75- and 2.2-inch bars, and another, between the 0.75- and 1.50-inch bars. The metal was poured into the mold at 1,400° C (2,550° F), and the temperatures at these two points were recorded as the mold cooled to room temperature. At the end of 50 minutes the temperature between the 0.75, and 2.2-inch bars was 300° C (570° F), the maximum observed, while the maximum temperature observed between the 0.75- and 1.5-inch bars was 170° C (340° F). The metal was poured into the second mold at 1,380° C (2,515° F) a thermocouple being placed midway between the 1.5- and 0.75-inch bars and one between the 1.2- and 2.2-inch bars. The maximum temperature observed between the 1.5- and the 0.75-inch bars was 165° C (330° F) and between the 1.2- and the 2.2- inch bars, 400° C (750° F), at the end of 40 minutes.

[2] Approximate analysis:

Volatile matter	4.0%
Fixed carbon	74.0%
Ash	22.0%

On the basis of these results, it is doubtful whether the molding material reached a temperature sufficiently high to have a marked influence on the physical properties of the test bars.

7. UNIFORMITY IN DIMENSIONS OF TEST BARS

Measurements were made to determine the variation in diameter of the bars of different sizes using the selected molding material described earlier. The diameter of each bar was measured at the midsection in four radial directions. The difference between the maximum and minimum diameters is expressed (table 2) in percentage of the average diameter. The 2.2-, 1.2,- and 0.75-inch bars were tested under transverse loading in an Amsler universal testing machine of 50,000-pound capacity, the load being applied to give approximately 0.02-inch deflection in 10 seconds. The span used for the 1.2- and 2.2-inch bars was 18 inches, and for the 0.75-inch bars, 15 inches. The breaking load for each bar was calculated to the nominal diameter and the difference between the breaking loads of the two bars of the same size was calculated as the percentage of the highest breaking load for the pair (table 2). It will be noted from table 2 that the maximum variation in all the bars tested was 0.77 percent in the diameter and 6.2 percent in the breaking load. Complete data on the results of the transverse tests of these bars will be considered later in this paper.

TABLE 2.—*Variations in diameters of cylindrical test bars cast in bottom-poured vertical green-sand molds and in transverse breaking strength of companion bars*

IRON A

Temperature				Average diameter	Difference between maximum and minimum diameter	Difference in breaking load
Maximum heating		Pouring				
°C	°F	°C	°F	*Inches*	*Percent*	*Percent*
1,400	2,550	1,300	2,370	2.26	0.18	3.8
1,400	2,550	1,300	2,370	2.24	.36	
1,400	2,550	1,300	2,370	1.55	.45	(1)
1,400	2,550	1,300	2,370	1.55	.32	
1,400	2,550	1,300	2,370	1.24	.50	2.2
1,400	2,550	1,300	2,370	1.24	.31	
1,400	2,550	1,300	2,370	.79	.63	1.4
1,400	2,550	1,300	2,370	.79	.39	

IRON B

1,400	2,550	1,380	2,515	2.24	0.13	0.6
1,400	2,550	1,380	2,515	2.24	.18	
1,400	2,550	1,380	2,515	1.54	.32	(1)
1,400	2,550	1,380	2,515	1.55	.18	
1,400	2,550	1,380	2,515	1.24	.32	.4
1,400	2,550	1,380	2,515	1.24	.33	
1,400	2,550	1,380	2,515	.80	.37	2.2
1,400	2,550	1,380	2,515	.80	.41	
1,600	2,910	1,380	2,515	2.23	.18	.9
1,600	2,910	1,380	2,515	2.23	.27	
1,600	2,910	1,380	2,515	1.54	.40	(1)
1,600	2,910	1,380	2,515	1.54	.39	
1,600	2,910	1,380	2,515	1.23	.40	4.4
1,600	2,910	1,380	2,515	1.23	.32	

[1] Bars cast for machining to 1.2-in. diameter, not tested for transverse strength.

TABLE 2.—*Variations in diameters of cylindrical test bars cast in bottom-poured vertical green-sand molds and in transverse breaking strength of companion bars*—Continued

IRON C

Temperature				Average diameter	Difference between maximum and minimum diameter	Difference in breaking load
Maximum heating		Pouring				
°C	°F	°C	°F	*Inches*	*Percent*	*Percent*
1,400	2,550	1,300	2,370	2.24	0.40	3.2
1,400	2,550	1,300	2,370	2.25	.40	
1,400	2,550	1,300	2,370	1.54	.70	(1)
1,400	2,550	1,300	2,370	1.54	.26	
1,400	2,550	1,300	2,370	.78	.77	3.2
1,400	2,550	1,300	2,370	.78	.63	
1,500	2,730	1,380	2,515	2.25	.40	3.5
1,500	2,730	1,380	2,515	2.25	.35	
1,500	2,730	1,380	2,515	1.55	.45	(1)
1,500	2,730	1,380	2,515	1.54	.71	
1,500	2,730	1,380	2,515	1.23	.50	2.3
1,500	2,730	1,380	2,515	1.23	.32	
1,500	2,730	1,380	2,515	.80	.38	6.2
1,500	2,730	1,380	2,515	.80	.50	
1,600	2,910	1,380	2,515	2.24	.27	4.2
1,600	2,910	1,380	2,515	2.24	.27	
1,600	2,910	1,380	2,515	1.54	.19	(1)
1,600	2,910	1,380	2,515	1.54	.32	
1,600	2,910	1,380	2,515	1.23	.33	3.1
1,600	2,910	1,380	2,515	1.23	.24	
1,600	2,910	1,380	2,515	.79	.51	.5
1,600	2,910	1,380	2,515	.78	.37	
1,700	3,090	1,380	2,515	2.24	.50	.2
1,700	3,090	1,380	2,515	2.25	.31	
1,700	3,090	1,380	2,515	1.55	.32	(1)
1,700	3,090	1,380	2,515	1.55	.38	
1,700	3,090	1,380	2,515	1.23	.48	3.2
1,700	3,090	1,380	2,515	1.23	.40	

[1] Bars cast for machining to 1.2-in. diameter, not tested for transverse strength.

III. COMPARISON OF TEST BARS PRODUCED BY FOUR METHODS

1. FOUR METHODS OF PREPARING TEST BARS

In the second phase of this investigation, a comparison was made of the physical properties of transverse-strength test bars made by the method developed at this Bureau and by the methods tentatively adopted by the American Society for Testing Materials. These methods differ only in the position in which the bar is cast and the method of pouring. In the method developed at this Bureau, the bars are cast in a vertical position and poured from the bottom. Bars produced in this manner are referred to as bottom-poured vertical mold. The American Society for Testing Materials has tentatively adopted three methods of casting transverse-strength test bars. In one method, the bars are cast in a vertical position and poured from the top (top-poured vertical mold). In another, the bars are cast in a horizontal position (horizontal mold) and in the third, they are cast in a position inclined about 8 degrees with the horizontal (horizontally inclined mold). In the latter case, the bars are poured from

the lower end. Test bars 0.75, 1.2, and 2.2 inches in diameter were produced by each of the above-mentioned methods.

In view of the satisfactory results obtained in the earlier work with the mixture of 8 parts of molding sand to 1 part of sea-coal, tempered to approximately 7 percent of moisture and faced with a nongraphitic carbonaceous refractory material, these materials were used to make the molds for casting transverse-strength test bars by each of four methods.

(a) TOP- AND BOTTOM-POURED VERTICAL MOLD

The mold used, in making these bars shown in figure 4, was a modification of the one used for making the bars shown in figure 1. Bars of the same diameter were cast in pairs simultaneously in a vertical mold, 2 bars being bottom-poured, and 2 bars being top-poured. The molds were made in a three-part cylindrical flask, with the cheek extending the full length of the bars, and the mold cavities were spaced 7 inches between centers.

(b) HORIZONTAL MOLD

Two bars of the same diameter were cast simultaneously through filter cores, with the ends of the bars provided with risers (fig. 5). The distance between the center line of the 2 bars was 6 inches. The patterns used in making these bars were removed by withdrawing them from one end of the flask, thereby eliminating parting-line defects in the mold cavities such as may be encountered when the cope is removed from the drag and the pattern is lifted out from the mold.

(c) HORIZONTALLY INCLINED MOLD

The mold used in making the bars shown in figure 6 was similar to the horizontal mold, with the exception that the risers were connected to an overflow basin, which served as a reservoir to retain the excess of metal poured through the test bar mold during casting. The mold was inclined at an angle of 8 degrees while it was being poured.

2. SURFACE CONDITION AND DIMENSIONAL UNIFORMITY OF TEST BARS

The surfaces of all bars were smooth and free from burnt-on sand, this being true even when a pouring temperature of 1,470° C (2,680° F) was employed. The diameter of each test bar was measured at midsection of the bar in four radial directions, and the differences between the maximum and minimum diameters expressed as the percentage of the average diameter. The results (summarized in table 3) on 64 bars cast by the four methods show that the vertically cast bars, particularly those which were bottom-poured, were much more uniform in their diameter than the bars cast in the horizontal or the horizontally inclined molds.

3. PHYSICAL PROPERTIES OF TEST BARS

(a) TRANSVERSE BREAKING TEST

The results of the transverse breaking tests are shown in tables 4 and 5, and the chemical analyses of the different bars in table 6. The results determined on bars cast as shown in figure 1 in the bottom-

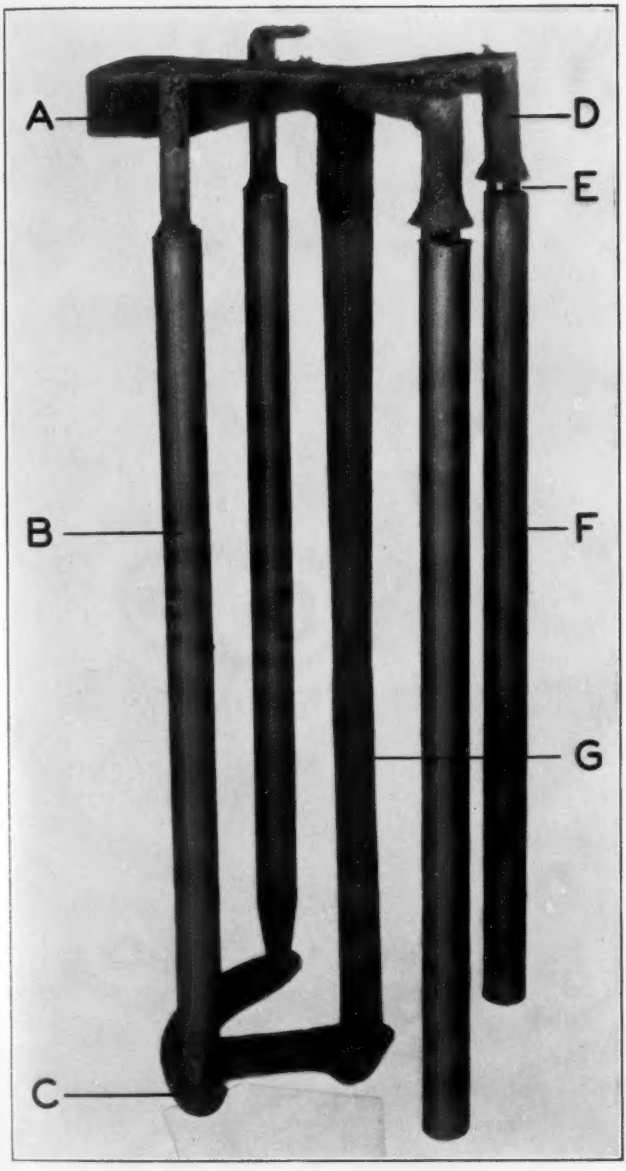

FIGURE 4.—*Transverse-strength test bars cast in a vertical mold by top-pouring and bottom-pouring.*

A, Pouring basin; B, vertically cast bars, bottom-poured; C, feeding semi-ring for bottom-pouring; D, top-pouring gates; E, pencil gates of 0.25-inch diameter made in oil-sand cores; 5 pencil gates for 2.2-inch diameter bars; 3 pencil gates for 1.2-inch diameter bars; 1 pencil gate for 0.75-inch diameter bars; F, vertically cast bars, top-poured; G, down gate.

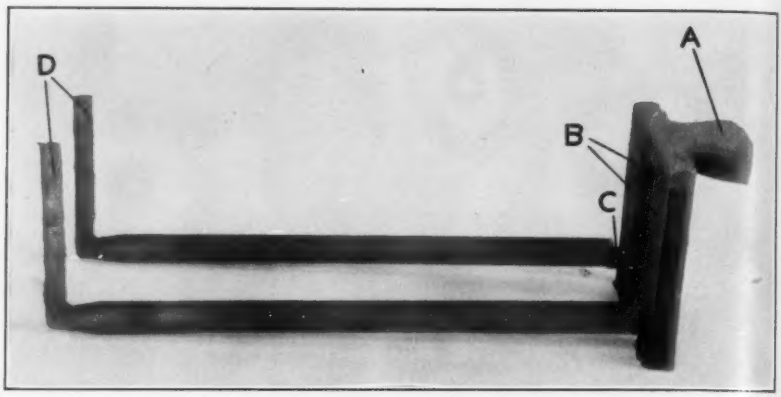

FIGURE 5.—*Transverse test bars cast horizontally.*

A, Pouring gate; B, down gates 1×2.25×10 inches; C, pencil gates of 0.25-inch diameter, 5 gates for 2.2-inch diameter bars, 3 gates for 1.2-inch diameter bars, 1 gate for 0.75-inch diameter bars; D, risers.

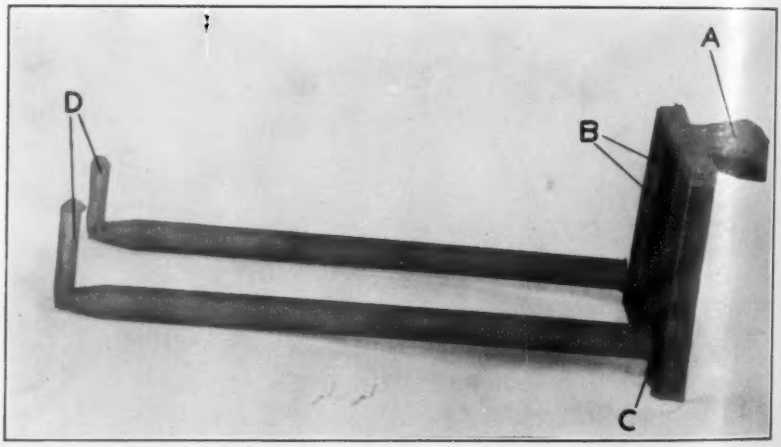

FIGURE 6.—*Transverse test bars cast in a horizontally inclined mold.*

A, Pouring gate; B, down gate 1×2.25×10 inches; C, feeding gate; gates of 1-inch diameter for 2.2-inch diameter bars, gates of 0.75-inch diameter for 1.2-inch diameter bars, gates of 0.5-inch diameter for 0.75-inch diameter bars; D, risers to overflow basin.

poured vertical mold are also included. In view of the fact that higher breaking strengths have been reported for transverse-strength test bars cast in horizontal position when tested with the "cope side" up [5, 6], the test bars cast in the horizontal and the horizontally inclined molds were placed on the testing machine so that their position corresponded to their position in the mold.

TABLE 3.—*Variations in diameter* [1] *of test bars cast by four methods*

Iron	Temperature				Vertical mold				Horizontally inclined mold		Horizontal mold	
	Maximum heating		Pouring		Top poured		Bottom poured		Average	Maximum variation	Average diameter	Maximum variation
	Average diameter	Maximum variation	Average diameter	Maximum variation								
	°C	°F	°C	°F	in.	%	in.	%	in.	%	in.	%
A	1,500	2,730	1,300	2,370	1.25	0.64	1.24	0.48	1.24	2.02	1.25	2.16
	1,500	2,730	1,300	2,370	1.25	.48	1.24	.24	1.24	1.21	1.25	2.00
A	1,600	2,910	1,300	2,370	.80	.62	.80	.50	.82	7.80	.80	2.12
	1,600	2,910	1,300	2,370	.80	1.62	.80	.75	.81	4.57	.80	1.12
A	1,600	2,910	1,300	2,370	1.25	.48	1.24	.08	1.24	.81	1.24	.81
	1,600	2,910	1,300	2,370	1.25	.32	1.24	.40	1.24	.73	1.25	1.36
A	1,600	2,910	1,300	2,370	2.25	.27	2.24	.31	2.26	1.37	2.27	1.10
	1,600	2,910	1,300	2,370	2.25	.62	2.25	.44	2.25	1.51	2.27	1.23
A	1,700	3,090	1,300	2,370	1.25	.88	1.24	.56	1.25	2.72	1.26	1.50
	1,700	3,090	1,300	2,370	1.25	.64	1.24	.32	1.25	1.60	1.25	1.36
C	1,400	2,550	1,380	2,515	1.26	.08	1.24	.32	1.25	2.16	1.26	2.14
	1,400	2,550	1,380	2,515	1.26	.71	1.24	.80	1.25	.64	1.26	2.00
D	1,700	3,090	1,380	2,515	1.25	.64	1.24	.56	1.25	2.24	1.25	1.84
	1,700	3,090	1,380	2,515	1.25	.56	1.24	.56	1.25	1.52	1.25	2.32
F	1,700	3,090	1,470	2,680	1.23	.57	1.22	.08	1.23	.89	1.23	.73
	1,700	3,090	1,470	2,680	1.23	.24	1.22	.24	1.23	.65	1.23	.80

[1] Diameters measured at midsection of test bars, in four radial directions.

TABLE 4.—*Physical properties of test bars cast in bottom-poured vertical molds*

[Brinell-hardness values determined with 3,000-kg load, using 10-mm ball]

Diameter	Maximum heating temperature		IRON A.—POURING TEMPERATURE 1,300° C (2,370° F)					IRON B.—POURING TEMPERATURE 1,380° C (2,515° F)					IRON C.—POURING TEMPERATURE 1,380° C (2,515° F)					IRON C.—POURING TEMPERATURE 1,300° C (2,370° F)				
			Breaking load	Difference	Modulus of rupture, avg	Deflection	Brinell number, avg	Breaking load	Difference	Modulus of rupture, avg	Deflection	Brinell number, avg	Breaking load	Difference	Modulus of rupture, avg	Deflection	Brinell number, avg	Breaking load	Difference	Modulus of rupture, avg	Deflection	Brinell number, avg
in	°C	°F	lb	%	lb/in²	in		lb	%	lb/in²	in		lb	%	lb/in²	in		lb	%	lb/in²	in²	
2.2	1,400	2,550	8,487	3.8	37,200	0.16	------	13,825	0.6	59,700	0.18	------	------	------	------	------	------	10,037	3.2	44,000	0.20	------
2.2	1,400	2,550	8,807					13,920					------	------	------	------	------	10,373				
1.2	1,400	2,550	1,632	2.2	42,700	.24	166	2,312	.4	61,300	.25	210	1,854	0.2	49,000	0.25	172	------	------	------	------	173
			1,596					2,321					1,850					2,103	------	55,700	.25	
.75	1,400	2,550	608	1.4	56,000	.23	------	701	2.2	64,400	.23	------	------	------	------	------	------	524	3.2	47,100	.13	------
------	1,400	2,550	599					717					------	------	------	------	------	507				
2.2	1,500	2,730	------	------	------	------	------	------	------	------	------	------	10,654	3.5	45,100	.22	------	------	------	------	------	------
2.2	1,500	2,730	------	------	------	------	------	------	------	------	------	------	10,280					------	------	------	------	------
1.2	1,500	2,730	1,827	4.7	47,200	.17	183	------	------	------	------	------	1,913	2.3	51,400	.28	173	------	------	------	------	------
1.2	1,500	2,730	1,741					------	------	------	------	------	1,959					------	------	------	------	------
.75	1,500	2,730	------	------	------	------	------	------	------	------	------	------	791	6.2	69,700	.28	------	------	------	------	------	------
.75	1,500	2,730	------	------	------	------	------	------	------	------	------	------	742					------	------	------	------	------
2.2	1,600	2,910	10,985	6.0	48,800	.14	------	15,226	.9	65,100	.18	------	10,700	4.2	47,100	.22	------	------	------	------	------	------
2.2	1,600	2,910	11,682					15,082					11,174					------	------	------	------	------
1.2	1,600	2,910	1,931	1.8	51,600	.21	189	2,721	4.4	70,600	.26	214	2,117	3.1	55,300	.27	190	------	------	------	------	------
1.2	1,600	2,910	1,961					2,600					2,052					------	------	------	------	------
.75	1,600	2,910	585	4.1	54,300	.19	------	765	------	69,900	.19	------	796	.5	72,800	.23	------	------	------	------	------	------
.75	1,600	2,910	610										800					------	------	------	------	------
2.2	1,700	3,090	------	------	------	------	------	------	------	------	------	------	12,027	.2	51,900	.21	------	IRON D.—POURING TEMPERATURE, 1,380° C (2,515 ° F)				
2.2	1,700	3,090	------										12,056									
1.2	1,700	3,090	1,976	5.2	53,800	.18	201	------	------	------	------	------	2,284	3.2	59,600	.25	187	2,475	4.8	64,000	0.19	244
1.2	1,700	3,090	2,085										2,210					2,357				
.75	1,700	3,090	------	------	------	------	------	------	------	------	------	------	805	------	73,300	.18	------	------	------	------	------	------
.75	1.700	3,090	------																			

TABLE 5.—*Physical properties of test bars cast by different methods*

[Brinell hardness values determined with a 3,000-kg load, using 10-mm ball]

IRON A

Diameter	Temperature				Horizontal mold					Horizontally inclined mold					Vertical mold, top-poured					Vertical mold, bottom-poured				
	Maximum heating		Pouring		Breaking load	Difference	Modulus of rupture avg.	Deflection	Brinell number avg.	Breaking load	Difference	Modulus of rupture avg.	Deflection	Brinell number avg.	Breaking load	Difference	Modulus of rupture avg.	Deflection	Brinell number avg.	Breaking load	Difference	Modulus of rupture avg.	Deflection	Brinell number avg.
in	°C	°F	°C	°F	lb	%	lb/in²	in		lb.	%	lb/in²	in		lb	%	lb/in²	in		lb	%	lb/in²	in	
1.2	1,500	2,730	1,300	2,370	1,619	1.6	43,400	0.18	176	1,949	0.5	51,700	0.21	182	1,850	17.7	44,800	0.19	184	1,827	4.7	47,200	0.17	183
1.2	1,500	2,730	1,300	2,370	1,646					1,958					1,522					1,741				
2.2	1,600	2,910	1,300	2,370	10,738	6.3	47,800	.15	------	11,070	2.9	48,400	.15	------	11,400	4.1	48,600	.14	------	10,985	6.0	48,800	.14	------
2.2	1,600	2,910	1,300	2,370	11,465					11,400					10,934					11,682				
1.2	1,600	2,910	1,300	2,370	1,931	3.3	50,400	.22	178	1,894	3.7	51,100	.22	178	1,664	12.5	47,400	.19	187	1,931	1.8	51,600	.21	189
1.2	1,600	2,910	1,300	2,370	1,867					1,967					1,903					1,967				
.75	1,600	2,910	1,300	2,370	644	4.6	59,900	.23	------	597	10.8	51,300	.22	------	486	4.9	45,300	.16	------	585	4.1	54,300	.19	------
.75	1,600	2,910	1,300	2,370	676					533					511					610				
1.2	1,700	3,090	1,300	2,370	2,072	1.8	54,600	.20	187	1,902	11.2	53,700	.19	187	2,132	13.3	52,900	.18	202	1,976	5.2	53,800	.18	201
1.2	1,700	3,090	1,300	2,370	2,035					2,141					1,849					2,085				

IRON C

1.2	1,400	2,550	1,380	2,515	1,641	0.5	43,400	0.25	165	1,805	0.5	48,000	0.23	176	1,770	0.2	46,900	0.22	173	1,854	0.2	49,000	0.25	172
1.2	1,400	2,550	1,380	2,515	1,632					1,814					1,766					1,850				

IRON D

1.2	1,700	3,090	1,380	2,515	2,274	6.2	62,400	0.17	236	2,061	4.1	56,000	0.15	239	2,469	3.2	64,600	0.18	242	2,475	4.8	64,000	0.19	244
1.2	1,700	3,090	1,380	2,515	2,424					2,150					2,389					2,357				

TABLE 6.—*Chemical composition of test bars*

IRON A

Diameter	Temperature				Chemical composition [1] (percent)									
	Maximum heating		Pouring		Total carbon	Graphitic carbon	Combined carbon	Si	P	Mn	S	Cu	Ni	Cr
in.	°C	°F	°C	°F										
2.2	1,400	2,550	1,300	2,370	3.86	3.10	0.76	1.43	0.45	0.52	0.027	0.33	------	------
1.2	1,400	2,550	1,300	2,370	3.91	3.05	.86	1.43	.45	.52	.027	.33	------	------
.75	1,400	2,550	1,300	2,370	3.91	3.03	.88	1.43	.45	.52	.027	.33	------	------
1.2	1,500	2,730	1,300	2,370	3.84	3.11	.73	1.50	.62	.52	.033	.40	------	------
2.2	1,600	2,910	1,300	2,370	3.74	3.14	.60	1.55	.53	.56	.046	.48	------	------
1.2	1,600	2,910	1,300	2,370	3.83	3.28	.56	1.78	.58	.60	.030	.41	------	------
.75	1,600	2,910	1,300	2,370	3.77	3.08	.69	1.60	.55	.59	.045	.48	------	------
1.2	1,700	3,090	1,300	2,370	3.82	3.19	.63	1.58	.57	.63	.043	.51	------	------

IRON B

2.2	1,400	2,550	1,380	2,515	3.24	2.45	0.79	1.46	0.45	0.35	0.068	------	0.07	0.12
1.2	1,400	2,550	1,380	2,515	3.30	2.45	.85	1.46	.45	.35	.068	------	.07	.12
.75	1,400	2,550	1,380	2,515	3.30	2.35	.95	1.46	.45	.35	.068	------	.07	.12
2.2	1,600	2,910	1,380	2,515	3.16	2.37	.79	1.40	.44	.35	.076	------	.07	.12
1.2	1,600	2,910	1,380	2,515	3.25	2.41	1.04	1.40	.44	.35	.076	------	.07	.12
.75	1,600	2,910	1,380	2,515	3.27	2.14	1.13	1.40	.44	.35	.076	------	.07	.12

IRON C

2.2	1,400	2,550	1,300	2,370	3.82	3.02	0.80	1.16	0.10	0.51	0.053	------	------	------
1.2	1,400	2,550	1,300	2,370	3.81	3.01	.80	1.16	.10	.51	.053	------	------	------
.75	1,400	2,550	1,300	2,370	3.83	2.61	1.22	1.16	.10	.51	.053	------	------	------
1.2	1,400	2,550	1,380	2,515	3.73	2.95	.78	1.12	.09	.54	.055	------	------	------
2.2	1,500	2,730	1,380	2,515	3.66	2.90	.76	1.10	.11	.51	.052	------	------	------
1.2	1,500	2,730	1,380	2,515	3.74	2.93	.81	1.10	.11	.51	.052	------	------	------
.75	1,500	2,730	1,380	2,515	3.76	2.56	1.20	1.10	.11	.51	.052	------	------	------
2.2	1,600	2,910	1,380	2,515	3.61	2.77	.84	1.12	.10	.56	.054	------	------	------
1.2	1,600	2,910	1,380	2,515	3.71	2.76	.95	1.12	.10	.56	.054	------	------	------
.75	1,600	2,910	1,380	2,515	3.69	2.14	1.55	1.12	.10	.56	.054	------	------	------
2.2	1,700	3,090	1,380	2,515	3.58	2.85	.73	1.08	.10	.51	.053	------	------	------
1.2	1,700	3,090	1,380	2,515	3.60	2.70	.90	1.08	.10	.51	.053	------	------	------
.75	1,700	3,090	1,380	2,515	3.63	.95	2.68	1.08	.10	.51	.053	------	------	------

IRON D

1.2	1,700	3,090	1,380	2,515	2.86	2.06	0.83	2.06	0.65	0.18	0.028	------	------	------

IRON F

1.2	1,700	3,090	1,470	2,680	2.13	------	------	1.64	0.49	0.14	0.013	------	------	------

[1] Analyses made by R. H. Elder and Roy Deas, American Cast Iron Pipe Co., Birmingham, Ala.

It is noteworthy that the difference in breaking loads for the two bars of a pair is, in general, smaller for bars cast either horizontally or in bottom-poured vertical molds than for the bars cast in the horizontally inclined mold or in the top-poured vertical mold.

In comparing the effect of maximum heating temperature on the strength of the 1.2-inch bars made by different methods it will be noticed (fig. 7) that in general the strength increases with an increase of maximum heating temperature, in the range 1,500 to 1,700° C (2,730 to 3,090° F).

The 1.2-inch bars made of iron A by different methods, with maximum heating temperature of 1,700° C (3,090° F), differed only slightly in their transverse breaking loads.

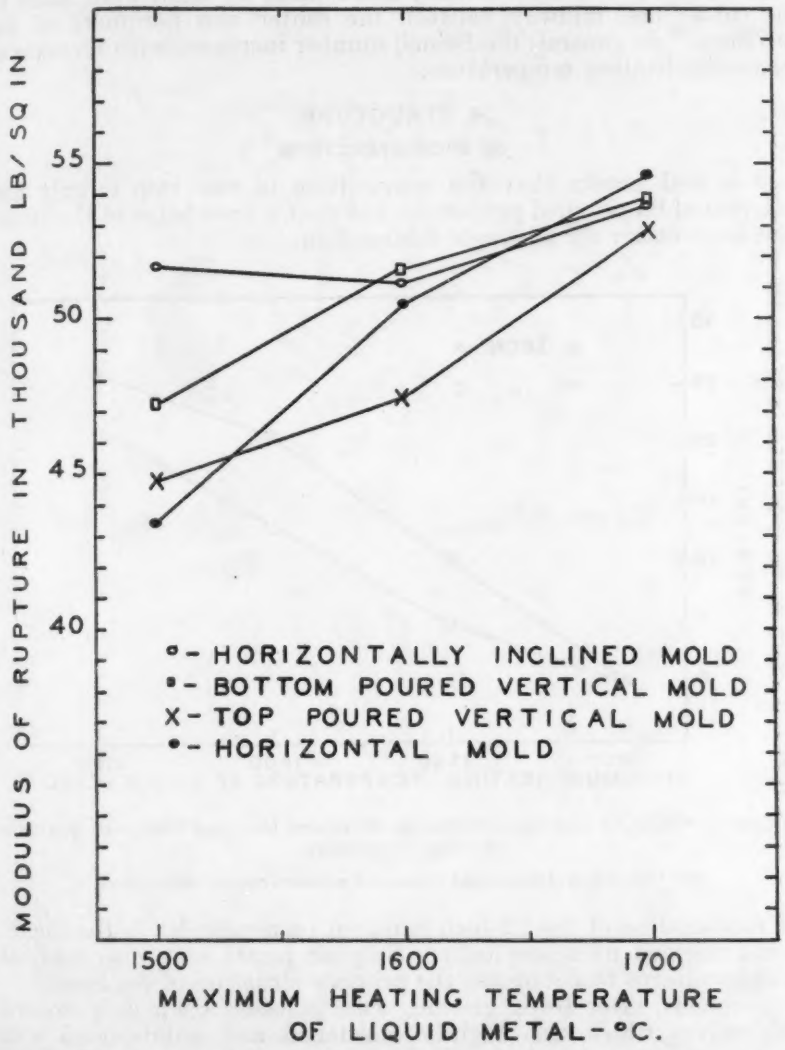

FIGURE 7.—*Relation between modulus of rupture and maximum heating temperature.*

Transverse-strength test bars, 1.2-inch in diameter, of iron A, were cast by four different methods.

On the basis of the breaking strength shown in tables 4 and 5, it appears that iron A was more affected by superheating than iron C (fig. 8), and that the modulus of rupture depended upon the cross-sectional area of the test bars and the amount of superheating (fig. 9).

(b) BRINELL NUMBERS

Brinell determinations were made on disks 0.5 inch in thickness, cut from broken sections of the 1.2-inch bars adjacent to the fracture. Impressions with a 10-mm ball, under 3,000-kg load, were made in the center and midway between the center and periphery of the specimen. In general, the Brinell number increased with increase of maximum heating temperature.

4. STRUCTURE

(a) MICROSTRUCTURE

It is well known that the composition of cast iron is only one criterion of its physical properties, and that a knowledge of the structure is necessary for adequate information.

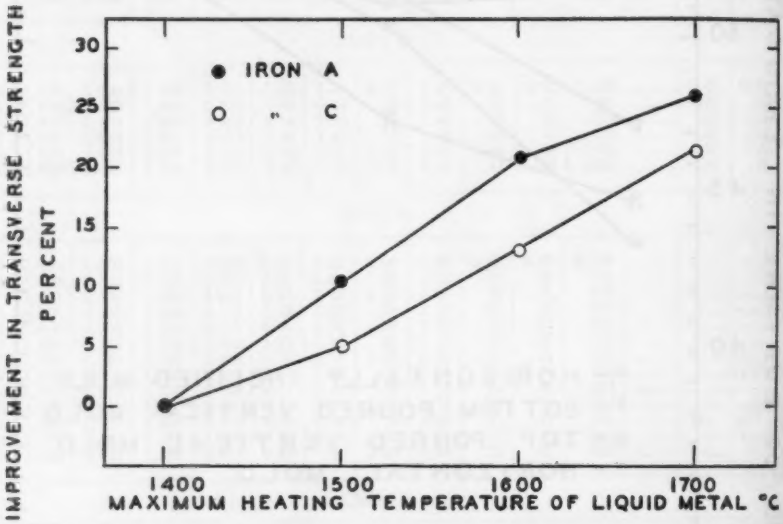

FIGURE 8.—*Relation showing increase in transverse breaking load with maximum heating temperature.*

The 1.2-inch bars of irons A and C were cast in bottom-poured vertical molds.

Cross sections of the 1.2-inch bars, cut perpendicular to the length, were examined microscopically. Sulphur prints were also made of these specimens to determine the primary structure of the irons.

Specimens, after being ground, were polished on a disk covered with velvet which was slightly moistened and impregnated with rouge. Micrographs of the specimens, as polished and after being etched with a 1-percent solution of nitric acid in ethyl alcohol, were made at 100 and 500 diameters near the center and the periphery of the specimen.

No significant difference in microstructure was found in the test bars of the same iron made by different methods. As is to be expected, those irons with the higher strength had finer graphite particles and finer pearlite. Some illustrations of the structure observed are shown in figures 10 to 12, inclusive.

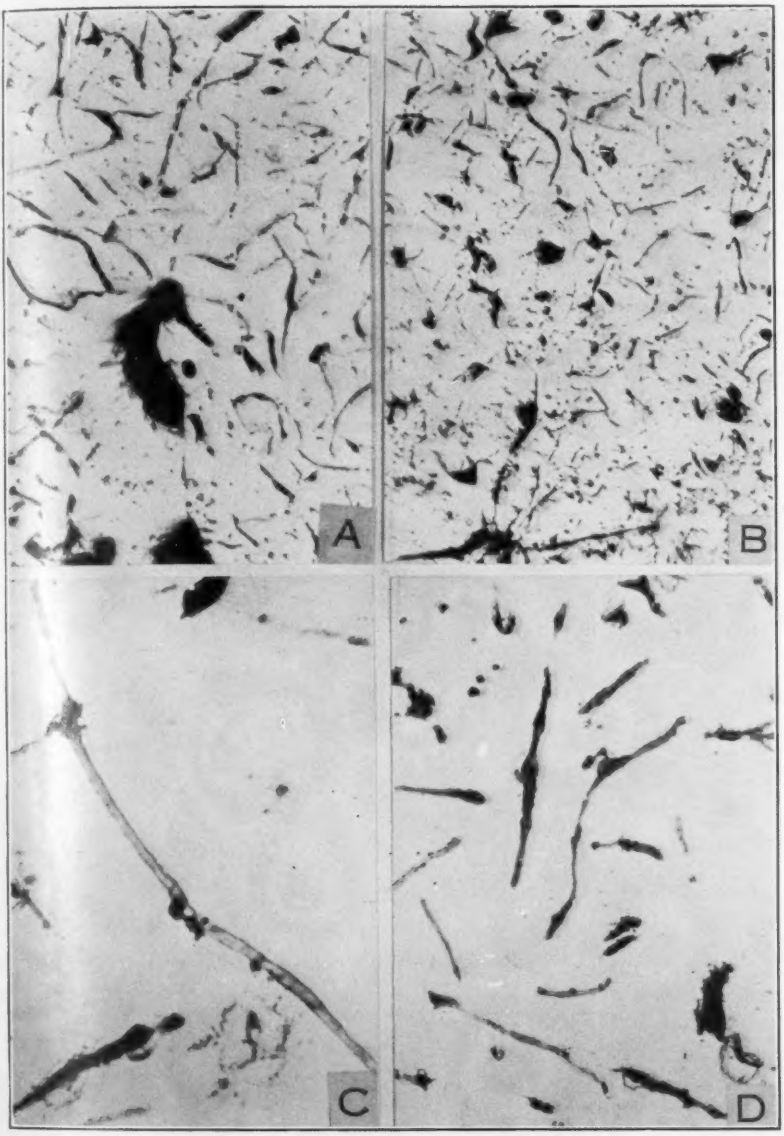

FIGURE 10.—*Microstructure of polished transverse section of 1.2-inch test bar of iron* A *cast in bottom-poured vertical mold.*

Maximum heating temperature 1,400° C (2,550° F); pouring temperature 1,300° C (2,370° F). Modulus of rupture 43,200 lb/in². A, center, × 100; B, periphery, × 100; C, center, × 500; D, periphery, × 500.

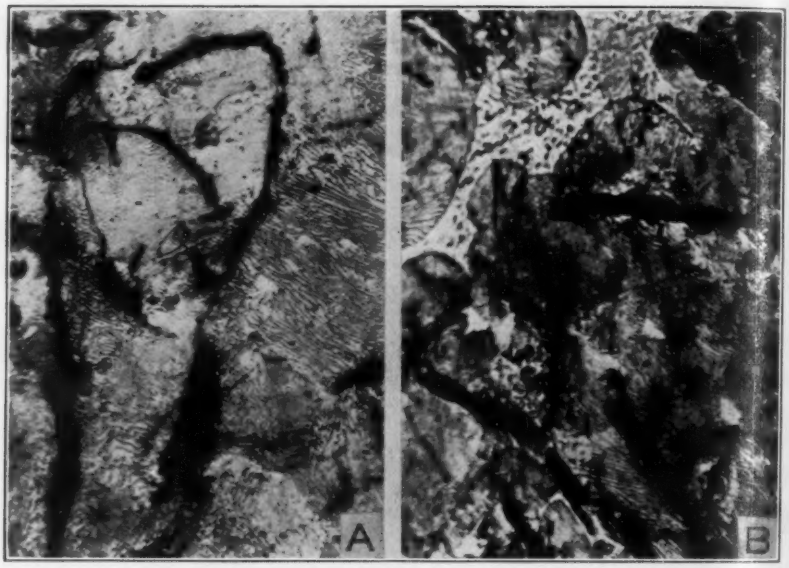

FIGURE 11.—*Microstructure of material of figure 10 after etching.*
Etched with 1-percent solution of nitric acid in ethyl alcohol. A, center × 500; B, periphery × 500.

Figures 10 and 11 represent the structure of the 1.2-inch bars cast in a bottom-poured vertical mold and show the presence of coarse graphite and pearlite, to which the low strength of these test bars may be attributed. Figure 12 shows the structure of similar bars made of

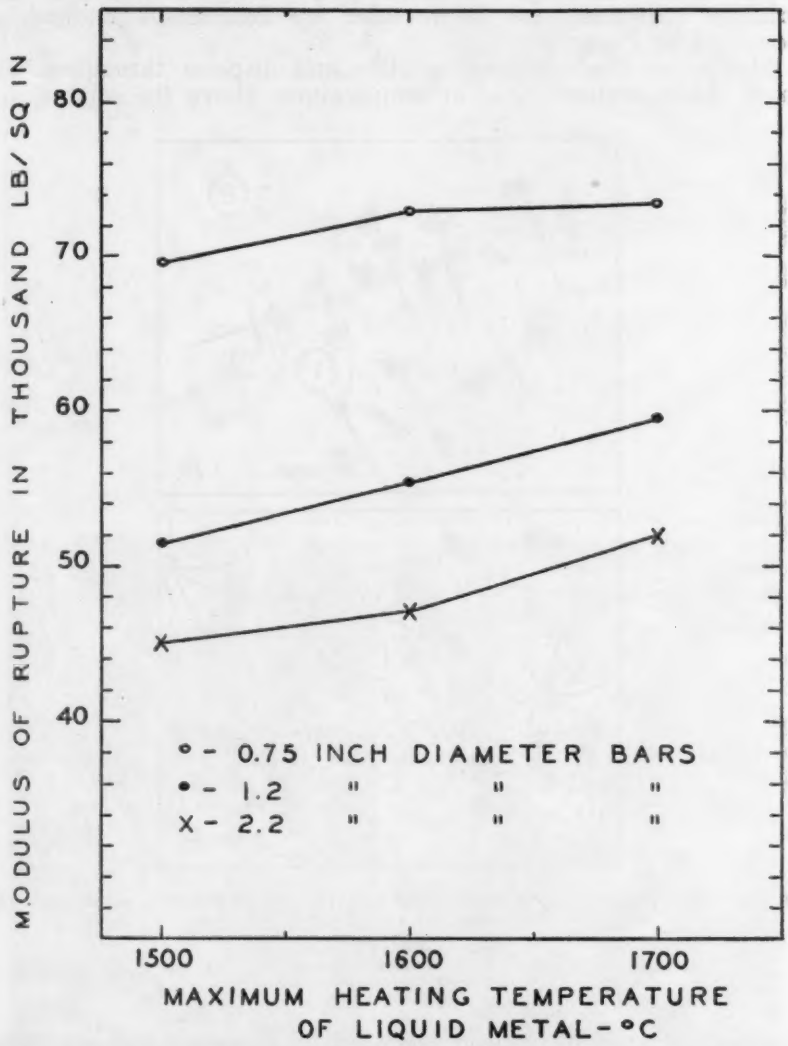

FIGURE 9.—*Relation between modulus of rupture of transverse-strength test bars and maximum heating temperature.*

Iron C was cast in bottom-poured vertical molds.

the same iron but heated to a higher temperature 1,700° C (3,090° F). The decrease in the size of the graphite particles and pearlite, as compared with figures 10 and 11, is believed to be significant.

(b) PRIMARY STRUCTURE

Another factor, which may have an important effect on the physical properties of cast iron, is the primary structure. By the term "primary structure" is meant that structure which is formed during solidification and not the structure revealed by the fracture. The primary structure may be revealed by Baumann's method, as described by Preuss [7].

Manganese-rich sulphides solidify and disperse throughout the mass of the molten metal at temperatures above the solidus, and

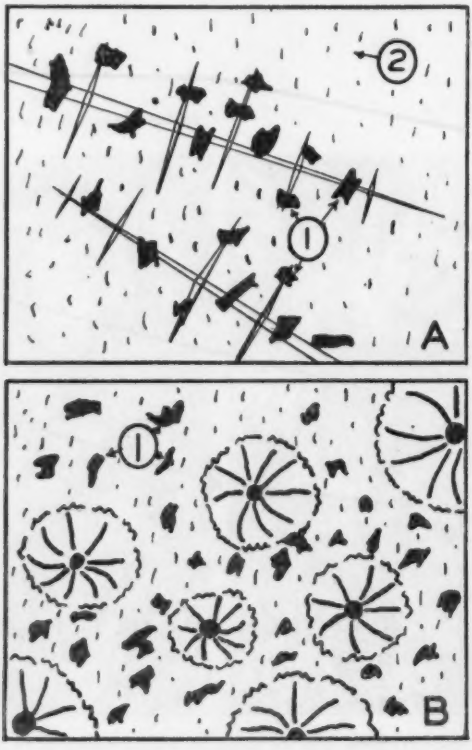

FIGURE 13.—*Arrangement of manganese sulphide particles during solidification of cast iron, according to Roll [8].*

A.—Dendritic solidification.
B.—Globular solidification.
1.—Manganese-rich sulphides.
2.—Mother liquor.

upon solidification of the iron, the particles arrange themselves along the axes and branches of the dendrites or along the grain boundaries, as is illustrated in figure 13.

Sulphur prints were made of the cross sections of all 1.2- and 2.2-inch transverse strength test bars used (fig. 14) and the differences observed in the primary structure of bars cast by different methods were very slight. Sulphur prints of bars of the same iron heated to the maximum temperatures of 1,400° C (2,550° F) and 1,700° C (3,090° F) suggest that the higher strength of the bars is associated with a finer primary structure.

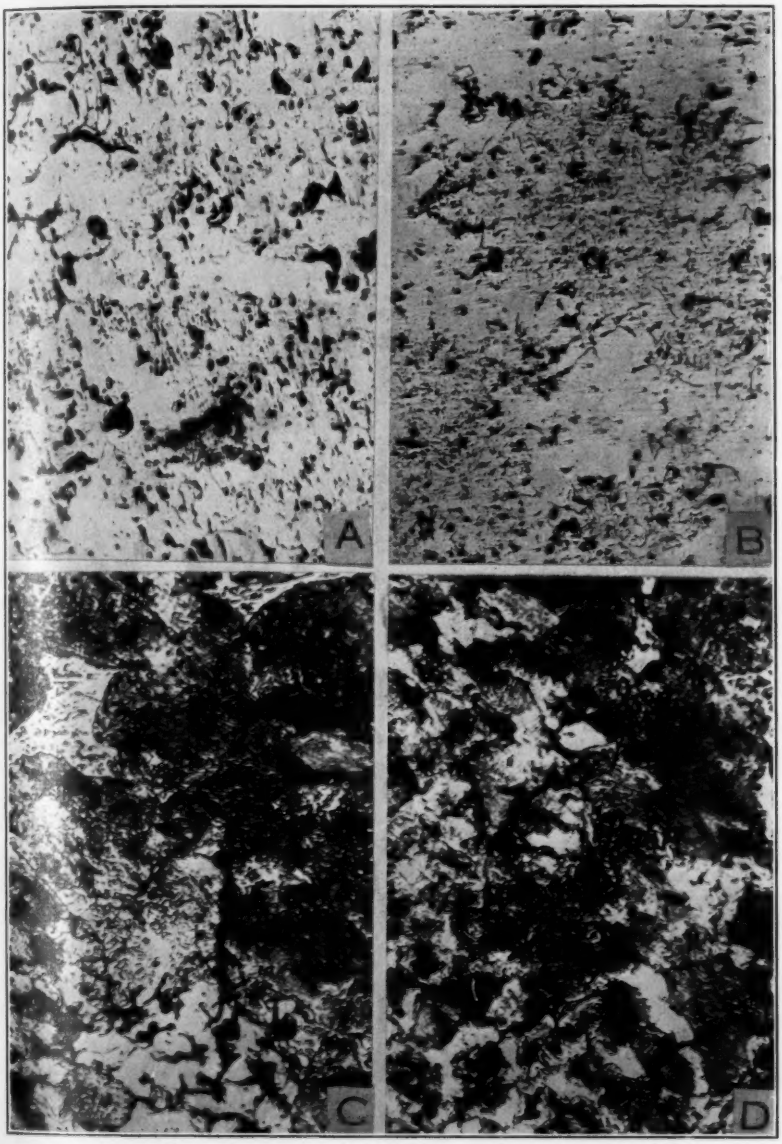

FIGURE 12.—*Microstructure of material of figure 10 after a maximum heating temperature of 1,700° C (3,090° F); other conditions as for figure 10.*

Modulus of rupture 55,200 lb/in². A, center × 100; B, periphery × 100, both polished; C, center × 500; D, periphery × 500, both etched with 1-percent solution of nitric acid in ethyl alcohol.

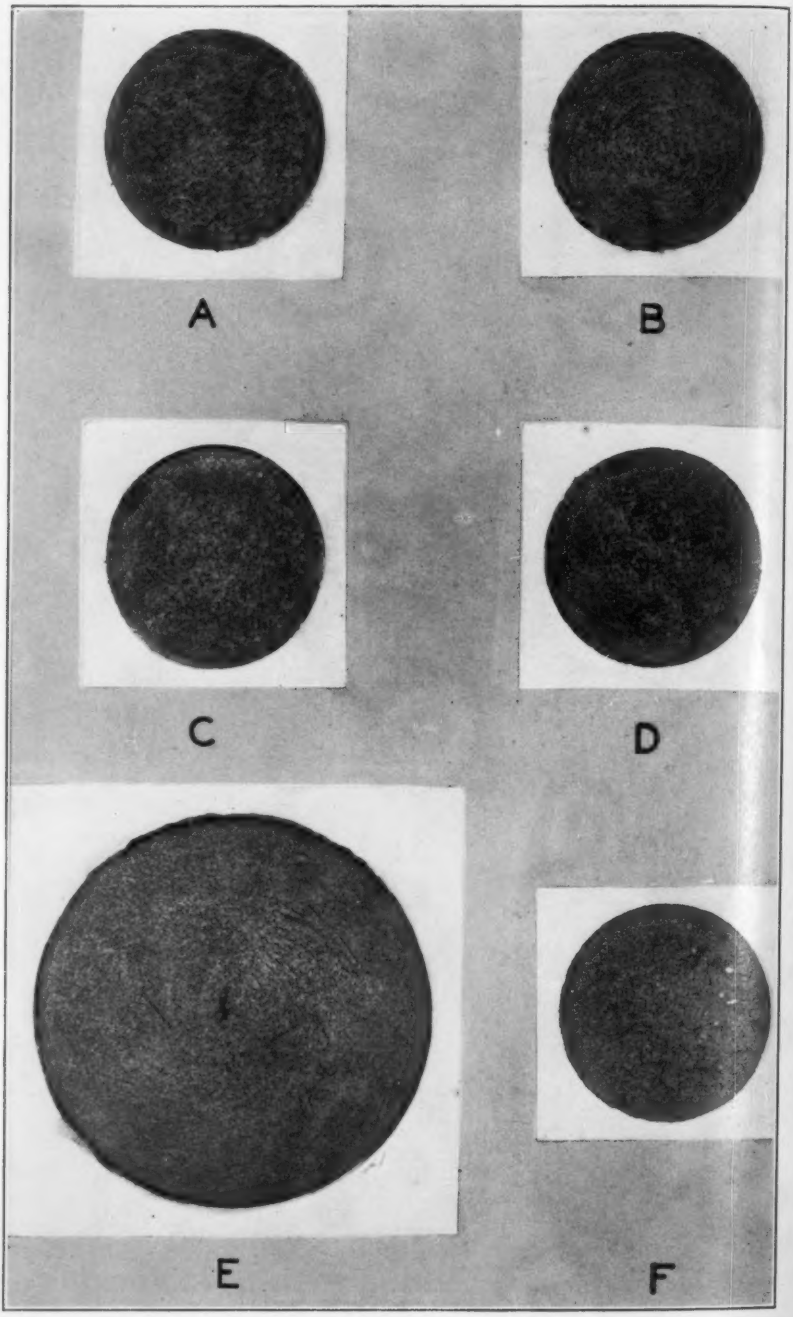

FIGURE 14.—*Sulphur prints of cross section of transverse-strength test bars of iron C, poured at 1,380° C (2,515° F).*

A.—Horizontal mold
B.—Horizontal inclined mold
C.—Top-poured vertical mold
D.—Bottom-poured vertical mold
} 1.2-inch bars. Maximum heating temperature 1,400° C (2,550° F).

E.—2.2-inch bars
F.—1.2-inch bars
} Maximum heating temperature 1,700° C (3,090° F). Bottom-poured vertical mold.

IV. SUMMARY

In preparing transverse-strength test bars of cast iron, freedom from burnt-on sand and other surface defects is very important.

A method of casting transverse-strength test bars in green-sand molds, consisting of a mixture of 8 parts of iron molding sand to 1 part of sea-coal, tempered to approximately 7 percent of moisture, with the surface of the mold cavities swabbed with a carbonaceous nongraphitic material, has been found satisfactory in preparing test bars having superior surface characteristics.

Five types of cast irons heated to maximum heating temperatures of 1,400° C (2,550° F); 1,500° C (2,730° F); 1,600° C (2,910° F); and 1,700° C (3,090° F), respectively, and then cooled to a temperature of 150° C (270° F) above the liquidus temperature were poured directly from the high-frequency induction furnace into transverse-strength test-bar molds.

Four methods of molding test bars of various diameters were employed; bottom-poured vertical mold, top-poured vertical mold, horizontal mold, and horizontally inclined mold.

The temperatures of the molds after casting test bars were measured. The data obtained do not indicate that the temperature attained by the molding material between the different diameter test bars was sufficiently high to influence the physical properties of the bars to any appreciable extent as the maximum temperatures of the mold were well below the critical temperature of the iron.

Vertically cast bars, particularly those which were bottom-poured, were much more uniform in diameter than bars cast in horizontal or horizontally inclined molds. The bars of iron A made by different methods, with a maximum heating temperature of 1,700° C (3,090° F), differed only slightly in the transverse breaking loads.

The effect of maximum heating temperature on the strength and hardness of the transverse-strength test bars made by four methods was studied. In general, the strength and hardness of all the bars investigated increased with increase of maximum heating temperature.

No essential differences in the primary structure or in the microstructure of test bars of the same composition and size, but cast by different methods, were revealed.

A finer primary structure, and finer graphite and pearlite constituents, were found to be associated with higher transverse strength.

The authors express their appreciation and thanks to L. D. Jones, senior molder, for the assistance rendered by him in this investigation.

V. REFERENCES

[1] C. M. Saeger, Jr. and E. J. Ash, *Properties of gray cast iron as affected by casting conditions*, Trans. Am. Foundrymen's Assn. **41,** 449 (1933); NBS J. Research **13,** 573 (1935) RP726.

[2] G. L. Harbach, *Relationship in cast iron test results.* Foundry Trade J. (London) **53,** 61–63 and 72 (1935); *Present position of the cast iron test bars,* discussion on Harbach's paper, Foundry Trade J. (London) **53,** 146–147 (1935).

[3] Tentative specifications for gray iron castings, Proc. ASTM, **32,** I, 630 (1932).

55384—36——7

[4] E. J. Ash and C. M. Saeger, Jr., *Shop method for determining volume changes in cast iron during casting*, Trans. Am. Foundrymen's Assn. **40,** 188–200 (1932).
[5] R. Moldenke, The Principles of Iron Founding, second edition, p. 197 (McGraw-Hill Book Co., New York, 1930).
[6] S. Southcott, *Test bars from the foundrymen's point of view*, Foundry Trade J. (London) **51,** 73–75 (1934).
[7] R. Baumann's method as described in Die praktische Nutzanwendung der Prüfung des Eisens durch Ätzverfahren und mit Hilfe des Mikroskopes, by E. Preuss-Berndt-v. Schwarz, p. 6 (Julius Springer, Berlin, Germany, 1927).
[8] Franz Roll, Das Primärgefüge des grauen Gusseisens, Arch. Eisenhuttenw. **8,** no. 3, 129–130 (Sept. 1934).

WASHINGTON, February 28, 1936.